



National Library  
of Canada

Bibliothèque nationale  
du Canada

Acquisitions and  
Bibliographic Services Branch

Direction des acquisitions et  
des services bibliographiques

395 Wellington Street  
Ottawa, Ontario  
K1A 0N4

395, rue Wellington  
Ottawa (Ontario)  
K1A 0N4

*Your file* *Votre référence*

*Our file* *Notre référence*

## NOTICE

The quality of this microform is heavily dependent upon the quality of the original thesis submitted for microfilming. Every effort has been made to ensure the highest quality of reproduction possible.

If pages are missing, contact the university which granted the degree.

Some pages may have indistinct print especially if the original pages were typed with a poor typewriter ribbon or if the university sent us an inferior photocopy.

Reproduction in full or in part of this microform is governed by the Canadian Copyright Act, R.S.C. 1970, c. C-30, and subsequent amendments.

## AVIS

La qualité de cette microforme dépend grandement de la qualité de la thèse soumise au microfilmage. Nous avons tout fait pour assurer une qualité supérieure de reproduction.

S'il manque des pages, veuillez communiquer avec l'université qui a conféré le grade.

La qualité d'impression de certaines pages peut laisser à désirer, surtout si les pages originales ont été dactylographiées à l'aide d'un ruban usé ou si l'université nous a fait parvenir une photocopie de qualité inférieure.

La reproduction, même partielle, de cette microforme est soumise à la Loi canadienne sur le droit d'auteur, SRC 1970, c. C-30, et ses amendements subséquents.

**Canada**



National Library  
of Canada

Acquisitions and  
Bibliographic Services Branch

395 Wellington Street  
Ottawa, Ontario  
K1A 0N4

Bibliothèque nationale  
du Canada

Direction des acquisitions et  
des services bibliographiques

395, rue Wellington  
Ottawa (Ontario)  
K1A 0N4

*Your file* *Votre référence*

*Our file* *Notre référence*

THE AUTHOR HAS GRANTED AN IRREVOCABLE NON-EXCLUSIVE LICENCE ALLOWING THE NATIONAL LIBRARY OF CANADA TO REPRODUCE, LOAN, DISTRIBUTE OR SELL COPIES OF HIS/HER THESIS BY ANY MEANS AND IN ANY FORM OR FORMAT, MAKING THIS THESIS AVAILABLE TO INTERESTED PERSONS.

L'AUTEUR A ACCORDE UNE LICENCE IRREVOCABLE ET NON EXCLUSIVE PERMETTANT A LA BIBLIOTHEQUE NATIONALE DU CANADA DE REPRODUIRE, PRETER, DISTRIBUER OU VENDRE DES COPIES DE SA THESE DE QUELQUE MANIERE ET SOUS QUELQUE FORME QUE CE SOIT POUR METTRE DES EXEMPLAIRES DE CETTE THESE A LA DISPOSITION DES PERSONNE INTERESSEES.

THE AUTHOR RETAINS OWNERSHIP OF THE COPYRIGHT IN HIS/HER THESIS. NEITHER THE THESIS NOR SUBSTANTIAL EXTRACTS FROM IT MAY BE PRINTED OR OTHERWISE REPRODUCED WITHOUT HIS/HER PERMISSION.

L'AUTEUR CONSERVE LA PROPRIETE DU DROIT D'AUTEUR QUI PROTEGE SA THESE. NI LA THESE NI DES EXTRAITS SUBSTANTIELS DE CELLE-CI NE DOIVENT ETRE IMPRIMES OU AUTREMENT REPRODUITS SANS SON AUTORISATION.

ISBN 0-612-00497-X

Canada



**UNIVERSITÉ D'OTTAWA**  
**UNIVERSITY OF OTTAWA**

## **Slovenská rodná dedina**

**...Aj keď ma osud zavolá do sveta za chlebom,  
ja ostavám vždy a všade verná Ti chotár môj...**

**Venujem mojim rodičom a babičke Cecilii.**

## ABSTRACT

The chemistry of low-valent titanium is poorly developed apart from ubiquitous cyclopentadienyl derivatives.

Among the possible supporting ligands for stabilizing low-valent transition-metal complexes, are alkylamides. By introducing bulky amides such as  $R_2N^-$  ( $R=Me_3Si$ ,  $iPr$ ,  $Cy$ ) in the chemistry of Ti(III), we have opened a new field in the coordination and organometallic chemistry of this early transition metal.

Synthetic methodology is focused on the preparation of novel bis(amido) Ti(III) complexes via transmetallation reaction of  $TiCl_3THF_3$  with  $R_2NLi$ , using different stoichiometric ratios, reaction conditions and in the some cases the presence of chelating ligands, such as TMEDA.

The  $(R_2N)_2Ti(\mu-Cl)_2Li(TMEDA)$  ( $R=iPr$  **4**,  $Cy$  **5**) complexes provide a unique example of reversible reductive coupling of pyridine. The formation of 1,2,3,4-tetraphenyl-1-butene **9**, promoted by diisopropyl derivative **4**, is the result of reductive coupling followed by the transfer of two molecules of hydrogen.

The large steric bulk of the amido ligands and their electronic flexibility allowed us to investigate novel bis(amido) Ti(III) complexes in further ligand replacement reactions with different functions, such as hydrides, borohydrides and alkyls.

## ACKNOWLEDGEMENTS

During my graduate studies I worked with colleagues without whose contribution this thesis would not have been possible.

Therefore I would like to say a special "Thank you" to my research supervisor Dr. Sandro Gambarotta for his understanding, patience, guidance, and moral support.

Thanks also to Dr. Darrin Richeson for his helpful discussions and advice.

My "Comrades in arms" on the chemistry battlefield are thanked for their friendship which made the research more fun.

Thanks is going to the technical staff at the Chemistry Department University of Ottawa.

I am grateful to my parents and family overseas and in Canada. To my husband John, who always encouraged my graduate work goes a special hug and kiss .

## TABLE OF CONTENTS

	Page
DEDICATION	ii
ABSTRACT	iii
ACKNOWLEDGEMENTS	iv
TABLE OF CONTENTS	v
LIST OF FIGURES	viii
LIST OF SCHEMES	ix
LIST OF TABLES	xi
LIST OF ABBREVIATIONS	xii
CHAPTER ONE Introduction	1
1.1 Metal-Promoted Organic Synthesis.	3
1.2 Low-Valent Titanium and Dinitrogen Fixation/Activation.	7
1.3 CO Chemistry of Low-Valent Titanium	15
1.4 Ziegler-Natta Catalysis	18
1.5 Summary	21
CHAPTER TWO Literature Survey of Low-Valent Titanium Amides, Hydrides, Borohydrides and Alkyls	22
2.1 The Steric and Electronic Properties of Amido (NR <sub>2</sub> ) Ligands	22
2.2 Titanium Amides	27
2.3 Titanium Hydrides and Borohydrides	32
2.3 Titanium Alkyls	39
2.5 Scope of Thesis	47

CHAPTER THREE	Results and Discussion	48
3.1	Titanium Amides	48
3.2	Titanium Hydrides and Borohydrides.	70
3.3	Titanium Alkyls	78
CHAPTER FOUR	Summary	97
CHAPTER FIVE	Experimental Section	101
5.1	General Procedures	101
	X-ray Crystal Diffraction Analysis	102
	Preparation of $Cy_2NLi$	103
	Preparation of $(iPr)_2NLi$	104
5.2	Synthesis and Characterization of Titanium Amides	104
	Preparation of $[(Me_3Si)_2N]_2Ti(Cl)(THF)$	1 104
	Preparation of $(Me_3Si)_2NTi(Cl)_2(THF)_2$	2 105
	Preparation of $\{[(Me_3Si)_2N]_2TiCl_2\}[Li(TMEDA)_2]$	3 105
	Preparation of $[(iPr)_2N]_2Ti(\mu-Cl)_2Li(TMEDA)$	4 106
	Preparation of $(Cy_2N)_2Ti(\mu-Cl)_2Li(TMEDA)$	5 106
	Preparation of $\{[(iPr)_2N]_2TiCl_2\}[\mu-(NC_5H_5-C_5H_5N)]$	6 107
	Preparation of $\{(Cy_2N)_2TiCl_2\}[\mu-(NC_5H_5-C_5H_5N)]$	7 108
	Preparation of $(Cy_2N)_2Ti(Cl)(^tBu-py)$	8 108
	Reaction of $[(iPr)_2N]_2Ti(\mu-Cl)_2Li(TMEDA)$ with PhCCPh	9 109
	Preparation of $(Cy_2N)_2Ti(Cl)_2$	10 109
5.3	Synthesis and Characterization of Titanium Hydrides and Borohydrides	110
	Preparation of $[(Me_3Si)_2N]_2Ti(BH_4)(THF)$	11 110
	Preparation of $[(Me_3Si)_2N]Ti(py)_2(BH_4)_2$	12 111
	Preparation of $\{[(Me_3Si)_2N]_2Ti(\mu-S)\}_2$	13 111
	Preparation of $[(Me_3Si)_2N]_2Ti(H)(PMe_3)$	14 112
	Preparation of $Ti(BH_4)_3(THF)_3$	15 112
5.4	Synthesis and Characterization of Titanium Alkyls	113
	Preparation of $[(Cy_2N)_2Ti(Ph)_2]Li(TMEDA)$	16 113
	Preparation of $\{[(iPr)_2N]_2Ti(Ph)_2\}[Li(TMEDA)_2]$	17 113

Preparation of $\{(Cy_2N)_2Ti(\mu-Me)_2\}_2$	18	114
Preparation of $(Cy_2N)_2Ti(\mu-Me)_2Li(TMEDA)$	19	115
Preparation of $(Cy_2N)_2TiMe_2$	20	115
Preparation of $(Cy_2N)_2Ti[CH_2Si(Me)_3]_2$	21	116
Preparation of $(Cy_2N)_2Ti[CH_2C(Me)_3]_2$	22	
method a		117
method b,		117
Polymerization of $CH_2=CH_2$		118
<b>APPENDIX</b>		119
<b>SUGGESTIONS FOR FURTHER RESEARCH</b>		127
<b>REFERENCES</b>		128

## LIST OF FIGURES

Figure	Page
1.1 <i>End-on</i> versus <i>Side-on</i> Dinitrogen Bonding Modes	11
1.2 Specific Dinitrogen Bonding in Titanium Complexes	12
1.3 The Active Center of Polymerization of Propylene at the Edge of a Crystal Lattice	20
2.1 M-N $\sigma$ -Bond Interaction	23
2.2 M-N $\pi$ -Bond Interaction	23
2.3 Amido as Bridging Moiety	24
2.4 Titanium Oxo-Carbene Complex	26
2.5 Titanium-Carbene Complex	28
2.6 Bonding Modes of BH <sub>4</sub> Ligand	36
2.7 Structure of Ti(BH <sub>4</sub> ) <sub>3</sub> (PMe <sub>3</sub> ) <sub>2</sub>	37
2.8 Thermolysis of Cp* <sub>2</sub> TiMe	46
3.1 ORTEP Drawing of [(Me <sub>3</sub> Si) <sub>2</sub> N] <sub>2</sub> Ti(Cl)(THF) 1	51
3.2 ORTEP Drawing of [(Me <sub>3</sub> Si) <sub>2</sub> N]Ti(Cl) <sub>2</sub> (THF) <sub>2</sub> 2	53
3.3 ORTEP Drawing of (Cy <sub>2</sub> N) <sub>2</sub> Ti( $\mu$ -Cl) <sub>2</sub> Li(TMEDA) 5	55
3.4 ORTEP Drawing of [{" <sup>i</sup> Pr) <sub>2</sub> N] <sub>2</sub> TiCl] <sub>2</sub> [ $\mu$ -(NC <sub>5</sub> H <sub>5</sub> -C <sub>5</sub> H <sub>5</sub> N)] 6	59
3.5 Mass Spectrum of 1,2,3,4-tetraphenyl-1-butene	63
3.6 <sup>1</sup> H-NMR of 1,2,3,4-tetraphenyl-1-butene	64
3.7 <sup>13</sup> C-NMR of 1,2,3,4-tetraphenyl-1-butene	65
3.8 V-metallacyclobutane Species	66

3.9	ORTEP Drawing of $(\text{Cy}_2\text{N})_2\text{Ti}(\text{Cl})_2$ 10	69
3.10	IR Absorbption Bands of $\text{BH}_4$ ligand in 11, 12, 15	71
3.11	ORTEP Drawing of $[(\text{Me}_3\text{Si})_2\text{N}]_2\text{Ti}(\text{BH}_4)(\text{THF})$ 11	73
3.12	ORTEP Drawing of $[(\text{Me}_3\text{Si})_2\text{N}]\text{Ti}(\text{py})_2(\text{BH}_4)_2$ 12	75
3.13	ORTEP Drawing of $\{[(\text{Me}_3\text{Si})_2\text{N}]_2\text{Ti}(\mu\text{-S})\}_2$ 13	77
3.14	ORTEP Drawing of $\{[(i\text{Pr})_2\text{N}]_2\text{Ti}(\text{Ph})_2\}[\text{Li}(\text{TMEDA})_2]$ 17	81
3.15	ORTEP Drawing of $\{(\text{Cy}_2\text{N})_2\text{Ti}(\mu\text{-Me})\}_2$ 18	83
3.16	Plot of the Highest Occupied MO	85
3.17	MO Resulting from Ti-H-Ti Interaction	86
3.18	$d_\pi\text{-}p_\pi$ Interaction of Ti-N	86
3.19	ORTEP Drawing of $(\text{Cy}_2\text{N})_2\text{Ti}(\mu\text{-Me})_2\text{Li}(\text{TMEDA})$ 19	88
3.20	ORTEP Drawing of $\text{Cy}_2\text{N})_2\text{TiMe}_2$ 20	91
3.21	NMR-scale Polymerization of Ethylene	95

## LIST OF SCHEMES

Scheme	Page
1.1 Reductive Dimerization of Cyclohexanone and Cyclo-2-hepten-1-ol	3
1.2 Mechanism of Reductive Coupling Reaction	5
1.3 Reductive Elimination Pathway to Ti(II) Aryloxide	6
1.4 Mechanism of Dinitrogen Reduction	8
1.5 <i>Side-on</i> versus <i>End-on</i> Dinitrogen Low-Valent	14

## Titanium Complexes

1.6	Carbene Mechanism of Ethylene Polymerization	21
2.1	Hydroboration and Oxidation of Styrene	32
2.2	The Insertion of Ph <sub>2</sub> CN <sub>2</sub> into Ti-CH <sub>3</sub> Bond	41
2.3	Reactivity of Cp <sub>2</sub> TiMe	43
3.1	Reactions of TiCl <sub>3</sub> (THF) <sub>3</sub> with R <sub>2</sub> NLi (R=Me <sub>3</sub> Si, Cy, <sup>i</sup> Pr)	49
3.2	Reactivity of (R <sub>2</sub> N) <sub>2</sub> Ti(μ-Cl) <sub>2</sub> Li(TMEDA) with py (R= <sup>i</sup> Pr 4, Cy 5)	57
3.3	Reductive Coupling of Pyridine	61
3.4	Proposed Mechanistic Pathway for the Reaction 3.1	67
3.5	Synthesis of Ti(III) Borohydrides	70
3.6	Reaction of (R <sub>2</sub> N) <sub>2</sub> Ti(μ-Cl) <sub>2</sub> Li(TMEDA) (R=Cy 5, <sup>i</sup> Pr 4) with PhLi	79
3.7	(Cy <sub>2</sub> N) <sub>2</sub> Ti(μ-Cl) <sub>2</sub> Li(TMEDA) 5 and (Cy <sub>2</sub> N) <sub>2</sub> TiCl <sub>2</sub> 10 in the Reaction with MeLi	82
3.8	Schrock-type Carbene Formation via α-Hydrogen Abstraction	92
3.9	Reaction of (Cy <sub>2</sub> N) <sub>2</sub> Ti(μ-Cl) <sub>2</sub> Li(TMEDA) 5 and (Cy <sub>2</sub> N) <sub>2</sub> Ti(Cl) <sub>2</sub> 10 with LiCH <sub>2</sub> Si(Me) <sub>3</sub> and LiCH <sub>2</sub> C(Me) <sub>3</sub>	92
3.10	Disproportionation of Ti(III) Precursor	94

## LIST OF TABLES

Table		Page
1	Crystallographic Parameters for $[(\text{Me}_3\text{Si})_2\text{N}]_2\text{Ti}(\text{Cl})(\text{THF})$ 1 and $[(\text{Me}_3\text{Si})_2\text{N}]\text{Ti}(\text{Cl})_2(\text{THF})_2$ 2	120
2	Crystallographic Parameters for $(\text{Cy}_2\text{N})_2\text{Ti}(\mu\text{-Cl})_2\text{Li}(\text{TMEDA})$ 5 and $(\text{Cy}_2\text{N})_2\text{Ti}(\text{Cl})_2$ 10	121
3	Crystallographic Parameters for $\{[(i\text{Pr}_2\text{N})_2\text{TiCl}]_2(\mu\text{-}(\text{NC}_5\text{H}_5\text{-C}_5\text{H}_5\text{N}))\}$ 6	122
4	Crystallographic Parameters for $[(\text{Me}_3\text{Si})_2\text{N}]_2\text{Ti}(\text{BH}_4)(\text{THF})$ 11 and $[(\text{Me}_3\text{Si})_2\text{N}]\text{Ti}(\text{py})_2(\text{BH}_4)_2$ 12	123
5	Crystallographic Parameters for $\{[(\text{Me}_3\text{Si})_2\text{N}]_2\text{Ti}(\mu\text{-S})\}_2$ 13	124
6	Crystallographic Parameters for $\{[(i\text{Pr}_2\text{N})_2\text{Ti}(\text{Ph})_2][\text{Li}(\text{TMEDA})_2]\}$ 17 and $(\text{Cy}_2\text{N})_2\text{TiMe}_2$ 20	125
7	Crystallographic Parameters for $\{(\text{Cy}_2\text{N})_2\text{Ti}(\mu\text{-Me})\}_2$ 18 and $(\text{Cy}_2\text{N})_2\text{Ti}(\mu\text{-Me})_2\text{Li}(\text{TMEDA})$ 19	126

## LIST OF ABBREVIATIONS

bipy	- 2,2'-bipyridyl
Bz	- benzyl
Cp	- cyclopentadienyl anion
Cp*	- pentamethylcyclopentadienyl anion
1,5-COD	- 1,5-cyclooctadiene
15-C-5-	- 1,4,7,13-pentaoxacyclopentadecane
cryptand 2.2.2	- 4,7,13,16,21,24-hexaoxa-1,10-diazabicyclo [8.8.8] hexacosane
dmpe	- dimethylphosphinoethane
DME	- 1,2-dimethoxyethane
diglyme	- bis(2-methoxyethyl) ether
DEPT	- Distortionless Enhancement of Polarization Transfer
EPR	- Electron Paramagnetic Resonance Spectroscopy
eq	- equivalent
Fv	- fulvene
Ind	- indenyl anion
iPr	- isopropyl
L/Ln	- sum of ligands
M	- metal
Me	- methyl
Me <sub>3</sub> tacn	- 1,4,7-trimethyl-1,4,7-triazacyclononane
MP2	- perturbational algorithm

m.p.	- melting point
MS	- Mass Spectrometry
Np	- neopentyl
Nf	- neophyl
ORTEP	- Oak Ridge Thermal Ellipsoid Program
Ph	- phenyl
py	- pyridine
RT	- room temperature
Red-Al	- 3.4 M toluene solution of bis(2-ethoxy methoxy) aluminum sodium hydride
<sup>t</sup> Bupy	- 4-( <i>tert</i> -butyl)pyridine
TMEDA	- N,N,N',N'-tetramethylethylenediamine
THF	- tetrahydrofuran
UHF	- unrestricted Hartree-Fock calculation
ZINDO/Hückel	- Molecular Orbital calculation

## CHAPTER I

### INTRODUCTION

With reports of several remarkable chemical transformations and applications, the research and development of titanium metal complexes has become an ever growing field. The reactions encompass a broad range of reactivity such as metal promoted organic synthesis,<sup>1</sup> dinitrogen activation/fixation,<sup>2</sup> CO chemistry,<sup>3</sup> and Ziegler-Natta catalysis.<sup>4</sup>

As a result of both the availability of Ti(IV) starting materials, and the fairly high stability of +IV oxidation state, the chemistry of this oxidation state has been largely established with a variety of supporting ligands. Highly reactive functions including alkyls, hydrides, imides, and carbenes have been thoroughly identified and their chemical reactivity widely investigated. Lower oxidation states complexes have been less thoroughly studied. Zero- and negative- valent titanium complexes are virtually unknown or limited to less than a handful of carbonyl derivatives. In addition, little information is available for Ti(II) and Ti(III) complexes. One dominating characteristic of the chemistry of Ti(II) and Ti(III) lies in the fact that the most significant part of their chemistry has been developed almost exclusively with cyclopentadienyl anions and derivatives as supporting ligands. Apart from these systems, the chemistry of these two oxidation states remains

poorly explored (especially for Ti(II)) and limited to a few diverse examples.<sup>5</sup>

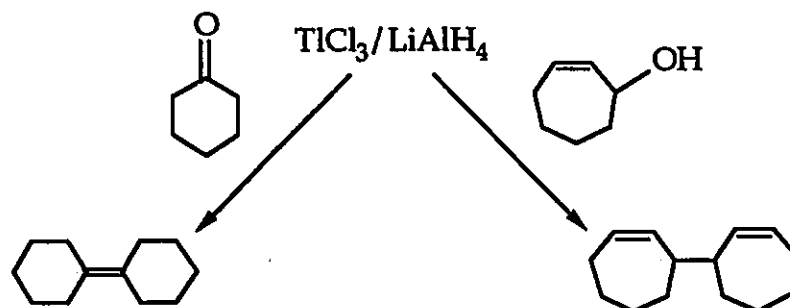
However, there are several features which make the chemistry of these two oxidation states particularly attractive for closer investigation. The  $d^2$  electronic configuration of the +II oxidation state of titanium gives rise to a series of interesting properties. For example, the carbenoid behavior of this metal, associated with a very strong reducing power ( $E^0 = -1.63$  V), makes this system ideal for oxidative addition reactions, reductive couplings, dinitrogen and CO coordination, metal promoted organic synthesis, preparation of hydrides, and the trapping and stabilization of highly reactive functionalities (nitrenes and carbenes). In the case of Ti(III), the  $d^1$  electronic configuration provides a radical-like reactivity to the metal center which is useful for one-electron transfer reactions, reductive couplings, hydrogen abstraction reactions, and to a certain extent, for polymerization reactions.<sup>6</sup>

The aim of this section is to review the reactivity and application of low-valent titanium compounds in metal promoted organic synthesis, dinitrogen activation-fixation, CO chemistry and Ziegler-Natta catalysis. These useful transformations provide a continuous stimulus for synthetic studies and characterizations of novel Ti(III) complexes.

## 1.1 Metal-Promoted Organic Synthesis.

Transition metal complexes are very important tools in both organic synthesis and catalysis. The major goal of these two procedures is the formation of pure products in higher yield and with increased chemo-, regio- and enantioselectivity.<sup>7</sup>

Over the past 15 years low-valent titanium reagents, prepared by treatment of  $\text{TiCl}_3$  or  $\text{TiCl}_4$  with strong reducing agents, have been widely used to induce carbonyl coupling reactions. An elegant application of low-valent titanium is the  $\text{TiCl}_3/\text{LiAlH}_4$  catalyzed reductive dimerization of ketones, aldehydes and benzylic alcohol in high yield (80%) (Scheme 1.1).<sup>8</sup>

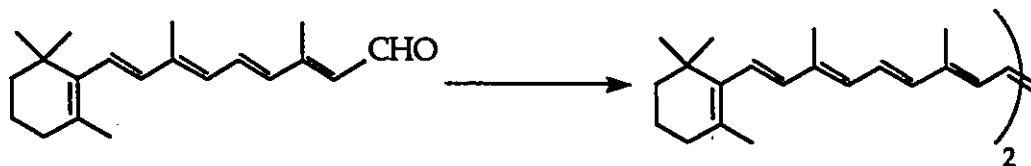


**SCHEME 1.1** Reductive Dimerization of Cyclohexanone and Cyclo-2-hepten-1-ol

Following this procedure, reductive coupling reactions have been successfully used for a number of: i) unsaturated and saturated aliphatic carbonyls, and ii) aromatic ketones and aldehydes.<sup>9</sup>

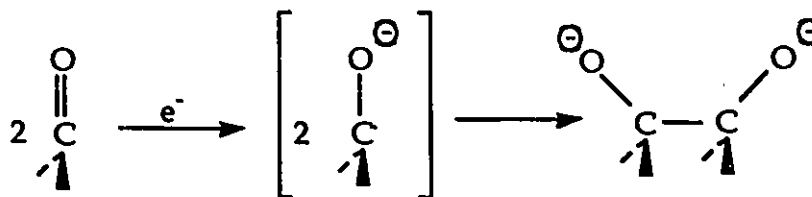
One of the most useful applications of this methodology is the coupling reaction of retinal to yield  $\beta$ -carotene (Eq. 1.1), a substance

used as a yellow food-coloring agent and source of vitamin A. This high-yield titanium-based synthesis is now patented for use in the industrial production of  $\beta$ -carotene.<sup>9</sup>



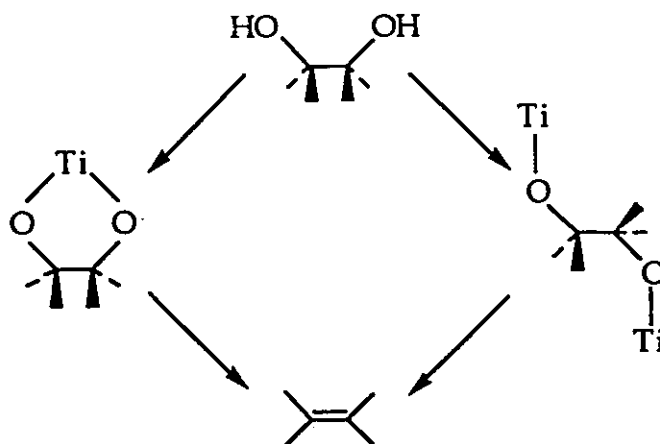
1.1

A detailed mechanistic study has demonstrated that the coupling reaction takes place in two steps (Eq. 1.2).<sup>9</sup>



1.2

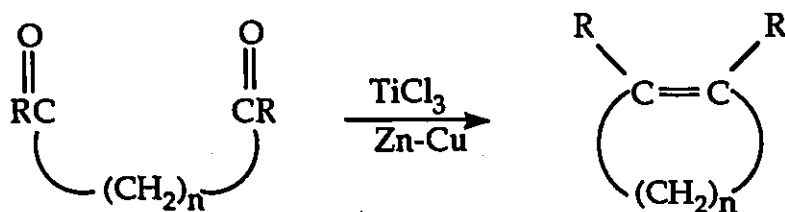
In the first stage the tri-valent titanium-metal center performs one-electron reduction of the ketone to generate a ketyl radical which dimerizes, yielding the pinacol. In the second step, a deoxygenation reaction forms a C=C double bond. The deoxygenation may either occur: i) via formation and decomposition of the five-membered titanium-containing ring and consequent elimination of oxo-titanium species, or ii) through an intermediate in which two diol oxygens are bound to different titanium atoms (Scheme 1.2).<sup>9</sup>



**SCHEME 1.2** Mechanism of Reductive Coupling Reaction

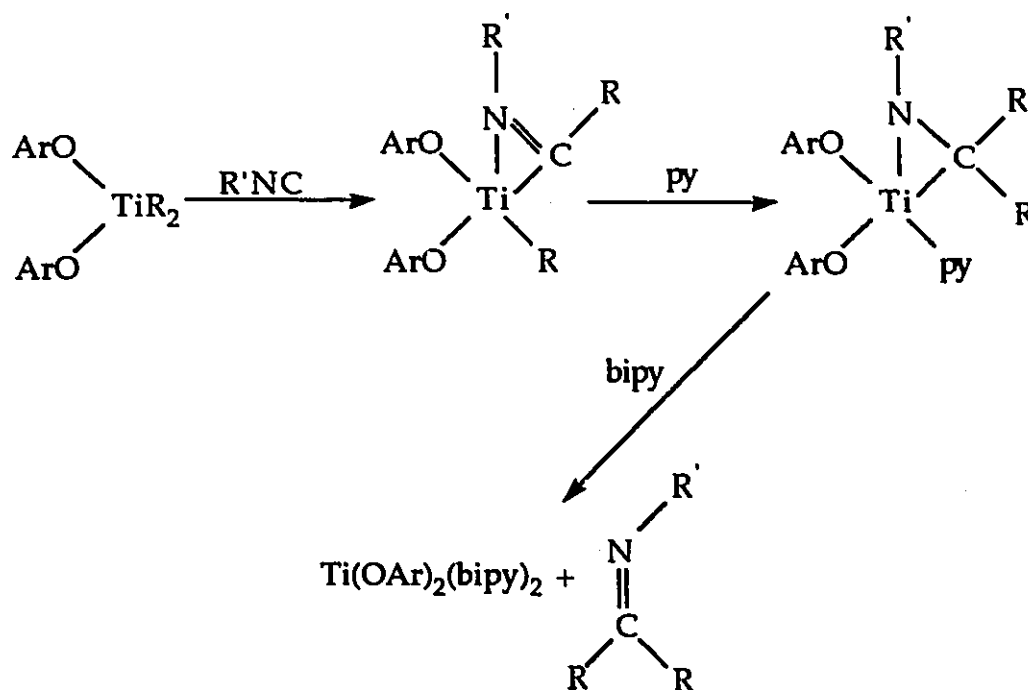
The ability of titanium complexes to promote reductive coupling reactions provides a versatile preparative route for the synthesis of organic macrocyclic rings. These reactions afford macrocyclic compounds in very good yields and have been successful in the preparation of macrocycles as large as 22 membered rings (Eq. 1.3).<sup>10</sup>

The general feasibility of this method has also encouraged the employment of Ti(III) reagents for the synthesis of natural products such as flexibilene (a 15-membered-ring diterpene), and various twisted cycloalkenes.<sup>9</sup>



1.3

In recent years, the chemistry of Ti(II) complexes has become more attractive, because this oxidation state has become accessible with non-Cp systems, such as bulky aryloxides. An unprecedented Ti(II) bisaryloxy derivative was obtained through ligand induced reductive-elimination of imine from a Ti(IV) iminoacyl complex (Scheme 1.3).<sup>11,12</sup>



**SCHEME 1.3** Reductive Elimination Pathway to Ti(II) Aryloxy

(Ar=2,6-diisopropylphenoxide,  $\text{R}'=\text{}^t\text{Bu}$ ,  $\text{R}=\text{CH}_2\text{Ph}$ )

The mono- $\eta^2$ -iminoacyl alkyl Ti compound,  $\text{Ti}(\text{OAr-2,6-}^i\text{Pr}_2)_2(\eta^2\text{}^t\text{BuNCCH}_2\text{Ph})(\text{CH}_2\text{Ph})$ , obtained from the insertion of  ${}^t\text{BuNC}$  into the Ti- $\text{CH}_2\text{-Ph}$  bond, undergoes alkyl migration upon reaction with  $\text{py}$ , forming the  $\eta^2$ -imine compound  $\text{Ti}(\text{OAr-2,6-}^i\text{Pr}_2)_2[\eta^2\text{}^t\text{BuNC}(\text{CH}_2\text{Ph})_2](\text{py})$ . The use of 2,2'-bipyridyl ligand, enforced the elimination

of imine and allowed the isolation of  $\text{Ti}(\text{OAr-2,6-}^i\text{Pr}_2)_2(\text{bipy})_2$ . The +II oxidation state has been confirmed by cyclovoltammetric studies showing two one-electron oxidation waves at -0.95 and -0.07 V, and a one-electron reduction wave at -1.51 V were observed.<sup>11</sup>

A similar synthetic procedure has been employed for the preparation of a Ti(II) ethylene complex.<sup>12</sup> The addition of  $\text{PMe}_3$  to a solution of titanacyclopentane species of  $[(\text{Ar}''\text{O})_2\text{Ti}(\text{CH}_2)_4]$  ( $\text{Ar}''\text{O}$ =2,6-diphenylphenoxide), afforded dark red crystals of the ethylene complex  $[(\text{Ar}''\text{O})_2\text{Ti}(\eta^2\text{-C}_2\text{H}_4)(\text{PMe}_3)]$ . The assignment of the formal oxidation state (+II or +IV) in this complex is not conclusive. However, further treatment of this complex with  $\text{Ph}_2\text{CO}$  led to the insertion of two molecules of  $\text{Ph}_2\text{CO}$  into the Ti-C bond of ethylene, forming a 2,7-dioxatitanacycloheptane ring, which is the characteristic behavior of tetravalent titanium.

## 1.2 Low-Valent Titanium and Dinitrogen Fixation/Activation.

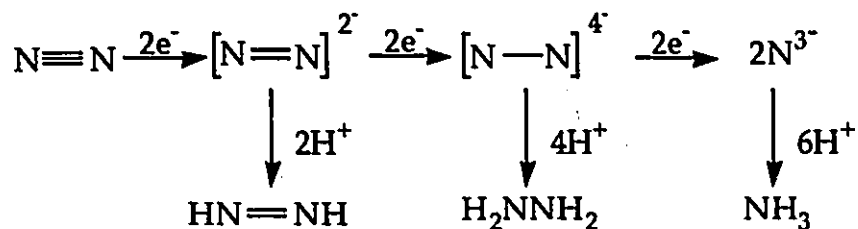
The very high reactivity of low-valent early transition metals and their strong reducing power are the key for understanding their ability to react with exceptionally stable molecules, such as dinitrogen. The activation of dinitrogen performed by these systems is one of the most interesting aspects of their reactivity.<sup>13</sup>

After more than 30 years since the discovery of the first dinitrogen complex, the chemistry of coordinated dinitrogen remains limited to elemental transformations, such as coordination to a metal center, and the reduction to ammonia and hydrazine. The limitation of

the dinitrogen systems to perform useful incorporation of N<sub>2</sub> into organic substrates, is in sharp contrast to the performance of naturally occurring systems, where nitrogen is the starting material for the biosynthesis of several organic products.<sup>14</sup>

The first and unique example of metal-promoted incorporation of dinitrogen into an organic substrates was described by Volpin, who found that aromatic organolithium compounds react at room temperature with dinitrogen in the presence of titanium compounds (TiCl<sub>4</sub>, Cp<sub>2</sub>TiCl<sub>2</sub>, etc.), to yield aromatic amines and ammonia after hydrolysis.<sup>15</sup>

In general, the reduction of dinitrogen occurs in three steps and requires six electrons. This process can be schematically represented by the following steps (Scheme 1.4). In the first step, a diazene intermediate is formed, followed by further reduction to a hydrazine intermediate, and finally cleavage of the N-N bond yields a nitride which forms ammonia upon hydrolysis.<sup>16</sup>



**SCHEME 1.4** Mechanism of Dinitrogen Reduction

Activation of nitrogen via coordination to a metal is thought to be gauged by the change in N-N bond length upon ligation. The bond lengths in metal dinitrogen complexes typically ranges between 1.0-

1.16Å for mononuclear and 1.12-1.36Å for dinuclear or higher clusters, while in free N<sub>2</sub> the bond length is 1.098Å.<sup>17</sup>

Dinitrogen has been demonstrated to coordinate to transition metals by using four types of bonding (Fig. 1.1).<sup>17</sup> *End-on* complexes (type I in Fig. 1.1) have been widely documented for large family of low-valent mononuclear Mo, Re and W species.<sup>13</sup> Depending on the nature and the oxidation states of the transition metals, these complexes may be surprisingly robust. This type of bonding has never been shown to be the starting point for any useful transformation of dinitrogen.<sup>13</sup>

The bridged *end-on* coordination II (Fig. 1.1) where an N<sub>2</sub> unit is coaxial with a M-M vector is more interesting and promising in terms of reactivity. This type of complex is well documented for middle transition elements, and has proven to be the first step towards further reduction to hydrazine. Dinitrogen has also been used as a labile ligand for the stabilization of highly reactive and coordinatively unsaturated organometallic fragments.<sup>13</sup>

The existence of complexes where N<sub>2</sub> adopts the *side-on* bonding mode of type III (Fig. 1.1) has never been crystallographically demonstrated for a mononuclear system. In only one case, Cp<sub>2</sub>Zr(CH<sub>2</sub>SiMe<sub>3</sub>)N<sub>2</sub>, has the *side-on* bonding fashion of dinitrogen been claimed on the basis of EPR and IR data.<sup>18</sup> The infrared spectrum showed no absorption bands in the range of 2400-1500 cm<sup>-1</sup>, which is diagnostic of *end-on* ligated dinitrogen. Computer simulation of the EPR spectra showed that the observed 1/2/3/2/1 quintet is satisfactorily modeled by the interaction of one Zr(III) nucleus with two

magnetically equivalent  $^{14}\text{N}$  nuclei. Treatment of this compound with HCl or HBr yielded hydrazine.

Type IV *side-on* bridged dinitrogen complexes (Fig. 1.1) are documented for low-valent early transition metals.<sup>17</sup> These complexes are of particular interest, since the crystallographic data indicates that the N-N distance has been significantly elongated, thus suggesting a considerable extent of N-N multiple bond reduction. The first example of a *side-on* coordination of dinitrogen with structure IV was achieved with the preparation and characterization of a dinuclear samarium complex  $\{\text{Cp}'_2\text{Sm}\}_2(\mu\text{-}\eta^2\text{:}\eta^2\text{-N}_2)$  containing N-N bond length of 1.088 Å.<sup>19</sup> The fact that the N-N distance in this complex is not significantly different from that of free  $\text{N}_2$ , suggests that no reduction has occurred in spite of the *side-on* fashion of bonding.

However, in the case of Zr(II) a very interesting example of *side-on* bonded dinitrogen of type IV has been determined in  $\{[(\text{R}_2\text{PCH}_2\text{SiMe}_2)_2\text{N}]\text{ZrCl}\}_2(\mu\text{-}\eta^2\text{:}\eta^2\text{-N}_2)$  ( $\text{R}=\text{iPr}, \text{tBu}$ ) complexes.<sup>17</sup> In these species a remarkable lengthening of the N-N bond distance (1.548(7) Å), even longer than the N-N single bond of hydrazine (1.46 Å), has been observed. By contrast, the *end-on* bonding mode observed for  $\{[(\text{iPr}_2\text{PCH}_2\text{SiMe}_2)_2\text{N}]\text{Zr}(\eta^5\text{-C}_5\text{H}_5)\}_2(\mu\text{-}\eta^1\text{:}\eta^1\text{-N}_2)$  showed significantly shorter N-N distance (1.3 Å).<sup>17</sup> Both complexes generated, upon acidification, 1 eq of hydrazine. Simplified MO calculations carried out for both bonding modes showed that the interaction of the three available *d* orbitals ( $d_{xy}$ ,  $d_{xz}$ ,  $d_{yz}$ ) on each metal fragment with the dinitrogen ligand, determines the bonding fashion. Analysis of the *side-on* bonding mode showed that the two  $d_{xy}$  and  $d_{yz}$  orbitals which have  $\delta$ - and  $\pi$ - symmetry, are antibonding with respect to the  $\text{N}_2$  unit.

For the *end-on* bonding fashion  $d_{xz}$  and  $d_{yz}$  orbitals which are of  $\pi$ -symmetry are also antibonding with the  $N_2$  fragment. The main difference between these two bonding models is that the  $\delta$ -molecular orbital of the *side-on* form is not stabilized as much as the  $\pi$ -molecular orbital, thus resulting in a more energetically favorable bridging *end-on* bonding mode. An extended Hückel ZINDO calculation carried out on  $\{(H_3P)_2Cl(H_2N)Zr\}(\mu-\eta^2:\eta^2N_2)$  as a simplified model, suggests that on each Zr fragment there are only two  $d$  orbitals available for bonding dinitrogen while the third  $d$  orbital is involved in  $\pi$ -bonding with the amide lone pair. Therefore, the orientation of amide ligand is responsible for the formation of the *side-on* form of  $N_2$  in the first complex, due to the  $d_{\pi-p\pi}$  overlap between the Zr and amide nitrogen. This inhibits the  $\pi$ -bond formation required for *end-on*  $N_2$ .

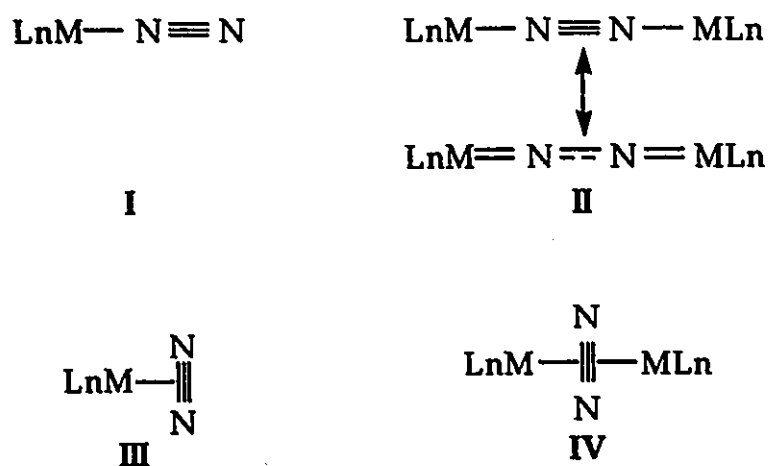


FIG. 1.1 *End-on* versus *Side-on* Dinitrogen Bonding Modes

The great ability of a titanocene system to give dinitrogen fixation is an expected result of the high reactivity of divalent titanium. An unique example of dinitrogen activation promoted by titanocene

was achieved by Pez in 1982 with the characterization of the Ti cluster  $(\mu^3\text{-N}_2)[(\eta^5\text{:}\eta^5\text{-C}_{10}\text{H}_8)(\eta\text{-C}_5\text{H}_5)_2\text{Ti}_2]-[(\eta^1\text{:}\eta^5\text{-C}_5\text{H}_4)(\text{C}_5\text{H}_5)_3\text{Ti}_2].$   
 $[(\eta\text{-C}_5\text{H}_5)_2(\text{C}_6\text{H}_{14}\text{O}_3)\text{Ti}].\text{diglyme}.$  The bonding mode is illustrated in (Fig. 1.2 V).<sup>2</sup> As a result of this multiple coordination, the N-N length (1.301Å) is considerably longer than in free dinitrogen and is intermediate between those observed in azo- and hydrazo-compounds. Hydrolysis of this complex gave ammonia exclusively.

An example of multiple *side-on* coordination of dinitrogen (type VI in Fig. 1.2) is provided by the mixed-valence  $\{[(\text{Me}_3\text{Si})_2\text{N}]_2\text{Ti}\}_2(\mu\text{-}\eta^2\text{:}\eta^2\text{-N}_2)_2[\text{Li}(\text{TMEDA})_2].$ <sup>20</sup>

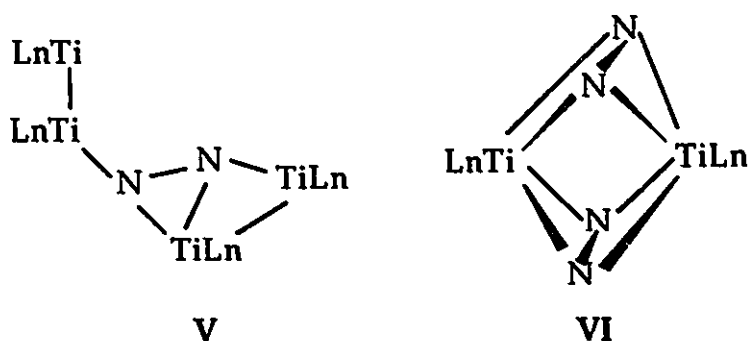
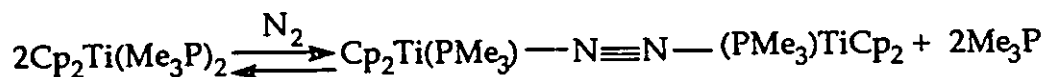


FIG. 1.2 Specific Dinitrogen Bonding in Titanium Complexes  
 (Ln=sum of ligands)

A phosphine-stabilized titanocene  $\text{Cp}_2\text{Ti}(\text{PMe}_3)_2$  is a convenient precursor to low valent titanocene complexes.<sup>21</sup> Exposure of this species to nitrogen (Eq. 1.4) results in the complexation of dinitrogen with an *end-on* bonding fashion (N-N=1.191Å).



1.4

Complexes formulated as  $[\text{Cp}^*_2\text{Ti}]_2(\mu\text{-N}_2)$ ,  $\{[\text{Ti}(\text{Cp}^*)_2]_2(\text{N}_2)\}_2(\text{N}_2)\}$ ,  $[(\text{Cp})_2\text{Ti}](\mu\text{-N}_2)$ , and  $[\text{Cp}_2\text{Ti}(\text{N}_2).\text{MgCl}]$  have also been claimed.<sup>22</sup> Unfortunately, these compounds were not obtained in crystalline form and therefore their structures remain questionable. However, the presence of nitrogen in these compounds has been demonstrated by the fact that all species formed ammonia upon hydrolysis.

Reduction of  $\text{Ti}(\text{Cl})_3(\text{THF})_3$  with metallic magnesium in THF under  $\text{N}_2$  forms the  $\text{TiNMg}_2\text{Cl}_2\text{THF}$  complex.<sup>23</sup> This complex liberated nitrogen upon oxidation, and ammonia upon hydrolysis. It also reacts under mild conditions with  $\text{CO}_2$  or  $\text{CS}_2$  to form the corresponding isocyanate or thioisocyanate titanium derivatives (Eq. 1.5).

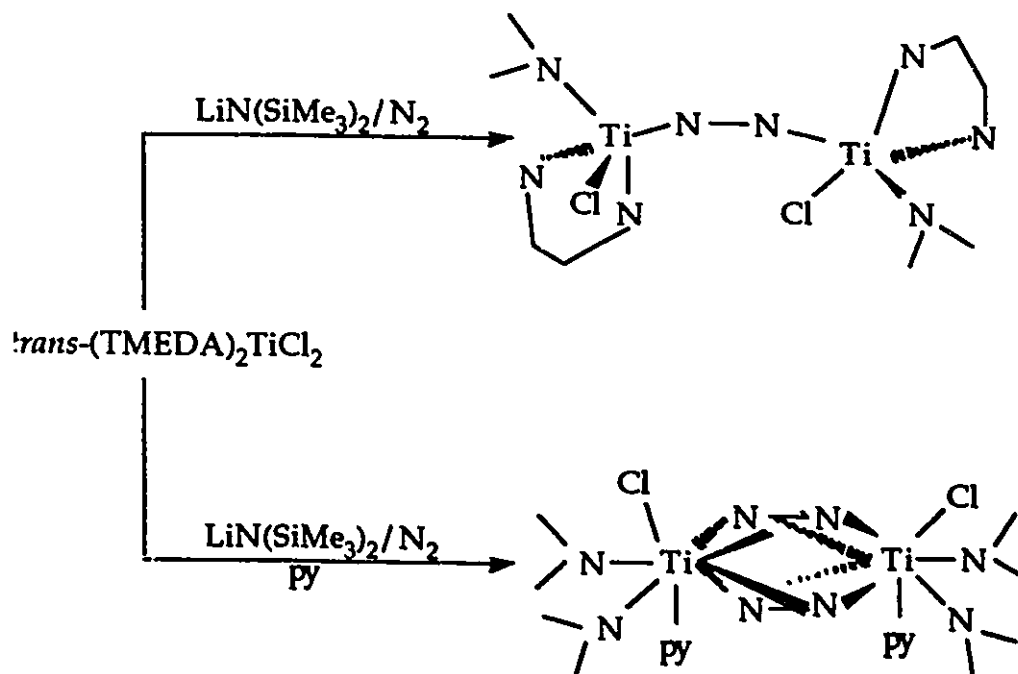


X=O or S

1.5

A surprisingly robust Ti/dinitrogen complex has been obtained by reaction of *trans*-(TMEDA)<sub>2</sub>TiCl<sub>2</sub> with (Me<sub>3</sub>Si)<sub>2</sub>NLi in a 1:1 ratio. The reaction led to the formation of an *end-on* bridged N<sub>2</sub>  $\{[(\text{Me}_3\text{Si})_2\text{N}]\text{TiCl}(\text{TMEDA})\}_2(\mu\text{-N}_2)$  complex.<sup>20</sup> The unusually short Ti-N distance of 1.762Å, the almost linear arrangement of the Ti-(μ-N<sub>2</sub>)-Ti moiety, and the rather long N-N distance of 1.289Å are consistent with the presence of considerable electronic delocalization over the Ti-(μ-N<sub>2</sub>)-Ti moiety. Surprisingly reaction with pyridine did not release

dinitrogen, but rather replaced TMEDA leaving the  $\text{TiN}_2\text{Ti}$  moiety intact (Scheme 1.5).<sup>24</sup>

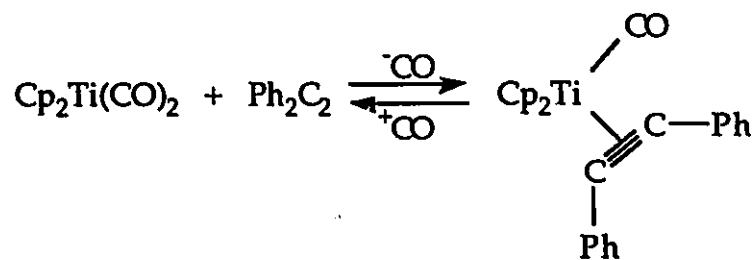


**SCHEME 1.5** *Side-On* versus *End-On* Low-Valent Titanium Complexes

There is only one example of dinitrogen fixation promoted by a Ti(III) system.<sup>25</sup> An X-ray diffraction study of  $\mu$ -dinitrogen bis[*p*-tolylidicyclopentadienyl titanium (III)],  $[\text{Cp}_2\text{Ti}(\textit{p}\text{-CH}_3\text{C}_6\text{H}_4)]_2\text{N}_2$  showed two titanium atoms bridged by an *end-on* dinitrogen molecule ( $\text{N}-\text{N}=1.162(12)\text{\AA}$ ). This diamagnetic complex yielded a mixture of hydrazine and ammonia upon hydrolysis.

### 1.3 CO Chemistry of Low-Valent Titanium

Metal carbonyls have played an important role in the development of modern transition-metal chemistry. The majority of titanium carbonyl complexes reported in the literature contain titanium in the +II oxidation state.<sup>5</sup> Until 1985, the only available low-valent precursor for the preparation of titanocene derivatives was  $\text{Cp}_2\text{Ti}(\text{CO})_2$ , obtained by reduction of  $\text{Cp}_2\text{TiCl}_2$  with Al under a CO atmosphere.<sup>3</sup> An alternative method for the synthesis of  $\text{Cp}_2\text{Ti}(\text{CO})_2$  involves the carbonylation of  $\text{Cp}_2\text{Ti}(\text{BH}_4)$ .<sup>26</sup> Treatment of  $\text{Cp}_2\text{Ti}(\text{BH}_4)$  with CO in  $\text{Et}_3\text{N}$  for four days resulted in the formation of  $\text{Cp}_2\text{Ti}(\text{CO})_2$  with an 80% yield. Further treatment of  $\text{Cp}_2\text{Ti}(\text{CO})_2$  with  $\text{Ph}_2\text{C}_2$  (Eq. 1.6)<sup>27</sup> afforded  $\text{Cp}_2\text{Ti}(\text{CO})(\text{PhCCPh})$ , a highly reactive catalyst for the hydrogenation of styrene, trans-stilbene, oct-1-ene and 1,4-diphenylbutadiene.



#### 1.6

Ti(II) carbonyls stabilized by phosphine ligands have been prepared by reduction of  $\text{Cp}_2\text{TiCl}_2$  with magnesium in THF carried out in the presence of  $\text{Me}_3\text{P}$ .<sup>28</sup> The reaction produced  $\text{Cp}_2\text{Ti}(\text{PMe}_3)_2$  which was isolated in good yield. Further reactions of this complex with several ligands gave a general replacement of one or both phosphines.

In particular, reaction with CO gave a mixture of mono  $\text{Cp}_2\text{Ti}(\text{PMe}_3)(\text{CO})$  and dicarbonyl  $\text{Cp}_2\text{Ti}(\text{CO})_2$  derivatives within a few minutes. Phosphine replacement by HCCH yielded  $\text{Cp}_2\text{Ti}(\text{PMe}_3)(\text{HCCH})$ .<sup>29</sup> Stoichiometric reaction of this complex with alcohols resulted in protonation of the alkyne units and formation of Ti(IV) vinylalkoxide species  $\text{Cp}_2\text{Ti}(\text{OR})(\text{CH}=\text{CH}_2)$ . Reaction with one equivalent of  $\text{H}_2\text{O}$  gave a binuclear vinyl-bridged  $\mu$ -oxo complex  $[\text{Cp}_2\text{Ti}(\text{CH}=\text{CH}_2)]_2(\mu\text{-O})$ .<sup>29</sup>

CO-replacement reaction by  $\text{PMe}_3$  on  $\text{Cp}_2\text{TiCO}_2$ , or reduction of  $\text{Cp}_2\text{TiCl}_2$  carried out in the absence of CO and in the presence of 1 eq of  $\text{PMe}_3$  resulted in the activation of the C-H bond of one Cp ring and formation of the dimeric  $(\eta^1\text{-}\eta^5\text{-C}_5\text{H}_4)$ -bridged complex  $\{\text{Cp}[\mu\text{-}(\eta^1\text{-}\eta^5\text{-C}_5\text{H}_4)]\text{Ti}(\text{PMe}_3)\}_2$ , which was crystallographically characterized.<sup>30</sup>

Other examples of carbonyl titanium species involve the zero- and negative-oxidation states of titanium. The preparation of the first anionic carbonyl complex,  $[\text{CpTi}(\text{CO})_4]^-$ , was reported in 1986 and was achieved by reducing  $\text{CpTiCl}_3$  with sodium naphthalenide in THF at  $-70^\circ\text{C}$  under Ar.<sup>31</sup> Ten minutes after the reaction started, argon was replaced by CO, causing the color of the solution to change rapidly. The resulting carbonyl derivative was isolated in 60% yield and was shown to be thermally stable up to  $175^\circ\text{C}$ .

By employing crown ethers and related alkali metal complexants, some other anionic non-Cp titanium-carbonyl species were successfully synthesized and characterized.<sup>32</sup>  $[\text{Ti}(\text{CO})_6]^{2-}[\text{K}(2,2,2)]_2$  was obtained by the two electron reduction of  $\text{Ti}(\text{CO})_3(\text{dmpe})_2$  with 2 eq of  $\text{KC}_{10}\text{H}_8$  and 2 eq of cryptand (2.2.2) in THF. Carbonylation of  $\text{TiCl}_4(\text{DME})$ , with 6 eq of  $\text{KC}_{10}\text{H}_8$  and 4 eq of 15-C-5 in DME at  $-70^\circ\text{C}$

under CO yielded the isolatable salt of  $[\text{Ti}(\text{CO})_6]^{2-}[\text{K}(15\text{-C-}5)_2]_2$ . Both complexes were fully characterized by multinuclear NMR spectroscopy.

A general synthetic methodology for the preparation of low-valent mono Cp derivatives of transition metals involves the reductive elimination of one of the two cyclopentadienyl ligands by using an alkali metal in the presence of a neutral ligand.<sup>33</sup> In the case of  $\text{Cp}_2\text{Ti}(\text{CO})_2$  this procedure allowed the synthesis of  $[\text{K}(2.2.2)][\text{CpTi}(\text{CO})_2(\text{dmpe})]$  (reaction of  $\text{Cp}_2\text{Ti}(\text{CO})_2$ , dmpe, 2 eq  $\text{KC}_{10}\text{H}_8$ , cryptand (2.2.2), in THF at  $-70^\circ\text{C}$ ). Protonation of  $[\text{K}(2.2.2)][\text{CpTi}(\text{CO})_2(\text{dmpe})]$  in 1,2-dimethoxyethane at  $-60^\circ\text{C}$  with 1 eq of acetic acid instantly produced a red-violet solution, which yielded deep violet crystals of  $\text{CpTi}(\text{CO})_2(\text{dmpe})\text{H}$ . This is the first example of a crystallographically characterized titanium hydrido carbonyl species.<sup>33</sup>

The reduction of  $\text{TiCl}_4(\text{THF})_2$  in the presence of dmpe in THF at  $-78^\circ\text{C}$ , followed by carbonylation, gave  $\text{Ti}(\text{CO})_3(\text{dmpe})_2$  in 80% yield.<sup>34</sup> This species partially converts at room temperature, and under CO, to the hepta-coordinated  $\text{Ti}(\text{CO})_5(\text{dmpe})$ . Treatment of this mixture with  $\text{BH}_3\cdot\text{THF}$  caused the complete conversion of  $\text{Ti}(\text{CO})_3(\text{dmpe})_2$  into  $\text{Ti}(\text{CO})_5(\text{dmpe})$ . A further ligand replacement reaction of  $\text{Ti}(\text{CO})_5(\text{dmpe})$  with  $\text{Me}_3\text{tacn}$ , under mild conditions (THF,  $20^\circ\text{C}$ ) produced  $(\text{Me}_3\text{tacn})\text{Ti}(\text{CO})_4$  which is the first example of an amine carbonyl complex of zero-valent titanium.<sup>35</sup>

The 16-electron  $\text{Ti}(\text{CO})_6$ , is an extremely unstable complex that can only be isolated and characterized at very low temperatures (ca  $-200^\circ\text{C}$ ).<sup>36</sup> This species may be stabilized by using phosphine ligands, resulting in the formation of  $(\text{Me}_3\text{P})_2\text{Ti}(\text{CO})_5$  or  $(\text{Me}_3\text{P})_3\text{Ti}(\text{CO})_4$  species, characterized by NMR spectroscopy. Recently, it was reported that the

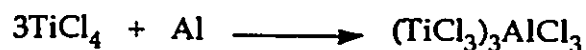
reaction of  $R_3SnCl$  ( $R=Me, Ph, cyclohexyl$ ) with  $[K(15-C-5)_2]_2[Ti(CO)_6]$  in THF produced hexacarbonyltitanium (0) salts of  $[R_3SnTi(CO)_6]^-$ . This complex is an unique example of a crystallographically characterized hexacarbonyltitanium(0) species.<sup>37</sup>

#### 1.4 Ziegler-Natta Catalysis

Many of the roots of modern organometallic chemistry can be traced to the initial discovery by Ziegler and Natta that transition metal complexes in combination with Lewis-acidic aluminum alkyl compounds are efficient catalysts for the polymerization of ethylene and propylene.<sup>4,38</sup> This early work coupled with the development of homogeneous catalysts for olefin metathesis (mainly based on transition metals in high oxidation states) have provided much of the driving force for the rapid development of new areas of coordination and organometallic chemistry.<sup>39</sup>

Although the area of Ziegler-Natta catalysis has been extensively reviewed, the identity of the active catalytic species and the polymerization mechanism are still under debate. A typical Ziegler-Natta catalyst consists of a combination of  $Et_3Al$  or  $Et_2AlCl$  with  $TiCl_4$  or with  $TiCl_3$ . The technical difficulties associated with this process (deactivation of catalyst after polymerization, removal of the diluent, quenching of the catalyst residues with HCl and alcohols) and the industrial requirements for production of polymers (stability and the formation of the active center of the catalyst, formation of polymers with high stereospecificity) has prompted research to improve this

catalytic system.<sup>40</sup> A titanium-based Stauffer catalyst prepared via reduction of  $\text{TiCl}_4$  with Al (Eq. 1.7) produced excellent results for the polymerization of ethylene.



1.7

The preparation and characterization of catalytically active species based on the crystalline modifications ( $\alpha$ ,  $\beta$ ,  $\gamma$ ,  $\delta$ ) of  $\text{TiCl}_3$  are very important for Ziegler-Natta polymerization in terms of understanding their catalytic activity and stereospecificity. Early studies of propylene polymerization were carried out with the  $\alpha$ - $\text{TiCl}_3$  modification yielding very low activity and stereospecificity. Later, the catalyst was replaced by more active forms of  $\text{TiCl}_3$ , namely the  $\gamma$  and  $\beta$  forms. The  $\gamma$ - $\text{TiCl}_3$  species with only one coordination site at the active center, promotes the formation of *trans*-1,4-polymers, whereas the  $\beta$ - $\text{TiCl}_3$  species, which provides more reactive sites, favors the formation of a mixture of homo-*cis* and homo-*trans*- polymers. The highly active  $\delta$  modification was obtained by mechanical grinding of the  $\alpha$  modification.<sup>4</sup>

Much work has been done to determine the position of the active centers of polymerization and many different possibilities have been proposed. In general, it is postulated that an active center can be located on the slits or edges of a crystal lattice as shown in Fig. 1.3.<sup>4</sup>

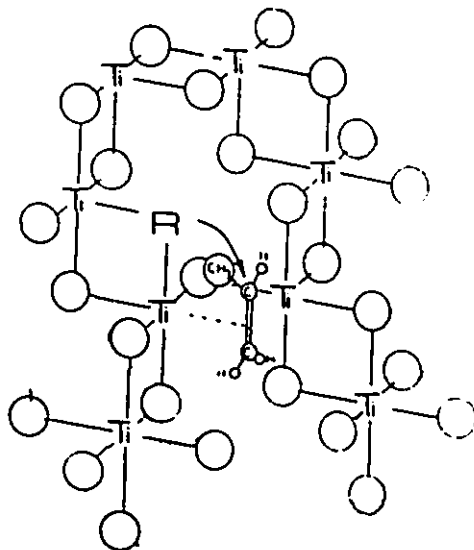
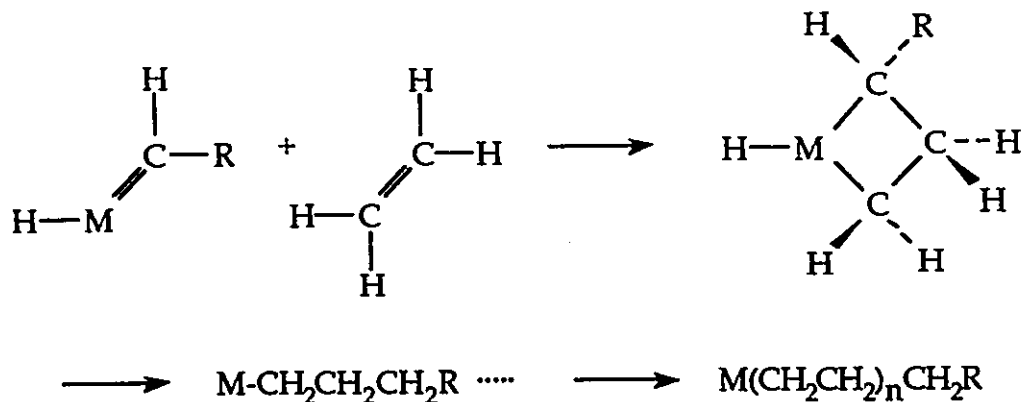


FIG. 1.3 The Active Center of Polymerization of Propylene at the Edge of a Crystal Lattice (○=Cl)

In order to understand the nature of the active site and the polymerization mechanism itself, homogeneous catalysts have been extensively investigated. Catalysts based on cyclopentadienyl derivatives of Ti(IV) are probably among of the best understood systems. Nearly all experiments and theories agree that polymerization occurs by addition of an olefin to a catalyst center, followed by the insertion of the complexed olefin into metal-carbon bond. Based on the results of kinetic experiments, several possible mechanisms have been proposed to model the growth of the polymer chain in a M-C bond of the active complex. Among the several mechanisms which have been proposed, a mechanism involving formation of a metallacyclobutane intermediates, has been shown to play an important role (Scheme 1.6).<sup>38,39</sup>



**SCHEME 1.6** Carbene Mechanism of Ethylene Polymerization

This mechanism involves the initial formation of alkylidene from a metal alkyl complex, followed by the addition of ethylene to form a metallacyclobutane ring, which insert ethylene into the metal-carbon bond thus starting the polymer growth.

## 1.5 Summary

Low-valent titanium displays a promising and diversified reactivity, which leads to several areas of interest (metal promoted organic synthesis, coordination of small molecules, such as  $\text{N}_2$  and  $\text{CO}$  and catalysis).

In spite of this wide interest, the chemistry of low-valent titanium remains poorly understood. More systematic work is necessary to develop new classes of compounds which may work as starting points for exploring and explaining the chemical reactivity of low-valent titanium complexes.

## CHAPTER II

### LITERATURE SURVEY OF LOW-VALENT TITANIUM AMIDES, HYDRIDES, BOROHYDRIDES AND ALKYL

Much of the early work in the organometallic and coordination chemistry of low valent titanium resulted in the formation of unstable products which were not fully characterized. This paucity may be explained by their instability towards disproportionation, and the lack of suitable starting materials enabling formation of complexes via mild-condition ligand-replacement reactions.<sup>5</sup>

This chapter is an overview of the literature pertaining to the chemistry of low valent titanium amides, hydrides, borohydrides and alkyls.

#### 2.1 The Steric and Electronic Properties of Amido (NR<sub>2</sub>) Ligands

In contrast to the extensive development in the chemistry of the M-C bond, the reactivity of the M-N bond has been far less investigated. However, there is an extensive and important chemistry surrounding transition-metal to nitrogen bonds, involving commonly occurring nitrogen donor ligands such as pyridines, amines, porphyrins, corrins, etc.<sup>41</sup>

Anionic amides  $(R_2N)^-$  are one of the most productive family of ligands possibly due to their electronic and steric properties.<sup>42</sup>

For alkylamido ligands there are three bonding possibilities. The fig. 2.1. shows a metal-nitrogen  $\sigma$  bond with a pyramidal  $sp^3$  nitrogen. This type of coordination is documented in the literature with M-N distances usually ranging from 1.981-2.157Å.<sup>42,43</sup>

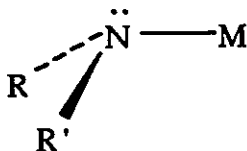


**FIG. 2.1** M-N  $\sigma$  Bond Interaction

The strength of the M-N bond of early transition metal complexes can be generally ascribed to the multiple bond character of the M-N moiety. The  $\pi$ -bond interaction is formed by the overlap of the nitrogen lone pair with an appropriate empty  $d$  orbital of the metal (Fig. 2.2).<sup>43</sup>

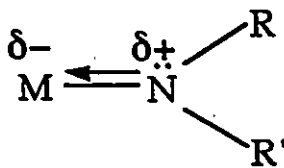


**FIG. 2.2** M-N  $\pi$ -Bond Interaction

The presence of M-N  $\pi$ -bond usually results in shorter M-N distances (typically in the range of 1.85-1.98Å), and in trigonal planar coordination geometry of the N atom.<sup>43,48a</sup> Also theoretical calculation based on the localized orbital ionization method supports  $d\pi-p\pi$  bonding.<sup>44</sup>

Another important characteristic of amide ligands is their ability to form a bridge between two or more metal centers. The electron deficiency of the metal centers and the consequent tendency to achieve a partial saturation by sharing the amido ligands is usually the driving force to adopt this particular bonding mode (Fig. 2.3).<sup>43</sup>

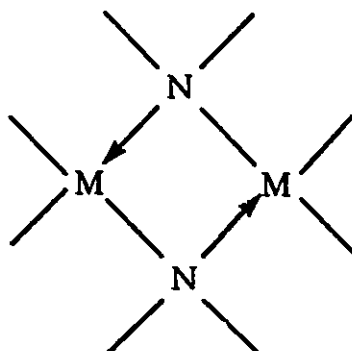
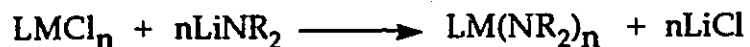


FIG. 2.3 Amido as Bridging Moiety

Transmetallation reactions carried out with Li-amides and metal-halide are one of the most convenient synthetic routes for the preparation of transition metal amides (Eq. 2.1), though other synthetic strategies are also available. The major advantage of the transmetallation is that Li amides are conveniently prepared (reaction of commercially available  $n\text{BuLi}$  with corresponding amine), the reaction byproduct  $\text{LiCl}$  is easily eliminated by filtration, and therefore

does not interfere with the isolation and purification of the transitionmetal derivative.<sup>43</sup>

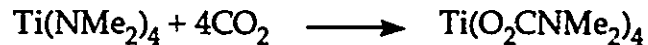


2.1

Another attractive aspect for the employment of amide ligands, is an almost unlimited possibility to adjust the steric hindrance by selecting the appropriate organic substituents. Small dialkylamido ligands such as  $\text{NMe}_2$  and  $\text{NEt}_2$  allow the formation of complexes with high coordination numbers, whereas the use of bulky amido ligands such as  $\text{N}(\text{SiMe}_3)_2$  and  $\text{N}(\text{iPr})_2$ , has allowed the isolation of monomeric metal complexes having unusually low coordination numbers.<sup>41,43</sup>

The reactivity of the M-N functionality has intriguing and promising analogies with the chemistry of the M-C function. One of the most fundamental reactions of both inorganic and organometallic chemistry is the insertion of cumulenes or a variety of unsaturated organic substrates into the M-C bond.<sup>41,43</sup>  $\text{CO}_2$  fixation, for example, is a very challenging problem due to the high stability of this substrate. Given the growth of concern in the past few years for the massive release of  $\text{CO}_2$  into the atmosphere, considerable interest has been focused on this issue.

Titanium tetrakis(dimethylamido)  $\text{Ti}(\text{NMe}_2)_4$  has provided a suitable starting point for the insertion of  $\text{CO}_2$  into M-N bond (Eq. 2.2), forming N,N-dimethylcarbamato compound.<sup>45</sup>



## 2.2

The insertion of CO into M-C bond is a well established process for the preparation of M-acyl functionalities. The high reactivity of the M-N bond enables interaction with several unsaturated systems including CO. However, the result of the carbonylation of the transition metal amides is a poorly understood process. In only one case, the reaction of  $\text{Ti}(\text{NMe}_2)_4$  with 5 eq of  $\text{Fe}(\text{CO})_5$  afforded in a single insertion step Fischer type metallocyclic oxo-carbene complex (Fig.2.4).<sup>46</sup>

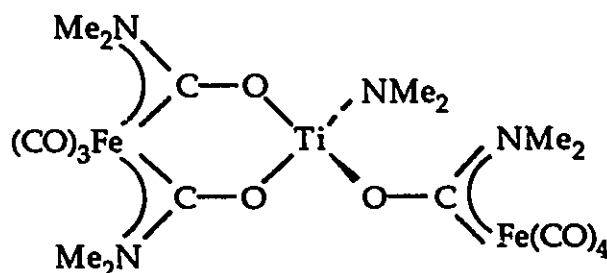


FIG. 2.4 Titanium Oxo-Carbene Complex

Last but not least, the amido group connected to the transition metal displays considerable basicity, and like the M-C bond may be metathasized by several protic substrates such as HCl,  $\text{H}_2\text{O}$ , HOR, HSR (R=alkyl) to eliminate the corresponding amine and offering different classes of derivatives (halides, oxides, alkoxides, thiolates, etc.).<sup>47</sup>

## 2.2 Titanium Amides

Group 4a metal amides are more numerous than those of any other transition metal group. In particular, titanium amides have been studied in the most detail.<sup>48</sup> Homoleptic and heteroleptic Ti(IV) dialkylamido complexes are the most common and readily prepared species. In general, they are thermally stable and show no tendency to polymerize.

Dialkylamido-species  $Ti(NR_2)_4$  ( $R=Me, Et, Pr, iPr, etc.$ )<sup>41,43</sup> can be easily obtained by transmetallation reaction of  $TiCl_4$  with  $LiNR_2$ . However, in the case of the bulky  $(Me_3Si)_2N^-$ , the reaction stops at the level of tri-substitution forming fluxional  $[TiCl\{N(SiMe_3)_2\}_3]$ , whose molecular structure has been determined by single-crystal X-ray diffraction.<sup>49</sup> Fluxional behavior was again observed for the alkyl derivative  $MeTi\{N(SiMe_3)_2\}_3$ , which was prepared via simple alkylation with  $MeLi$ .<sup>50</sup>

The mono-substituted  $Cl_3TiN(SiMe_3)_2$  was successfully prepared by reaction of  $TiCl_4$  with  $NaN(SiMe_3)_2$ .<sup>49</sup> The substitution reaction of  $Cl_2Ti\{N(SiMe_3)_2\}_2$  (prepared as a waxy material from  $TiCl_4$  and  $LiN(SiMe_3)_2$ ) with  $MeMgI$ , produced the dialkyl  $Me_2Ti\{N(SiMe_3)_2\}_2$  complex as a pale yellow solid.<sup>51</sup>

The complexation of the metal center by the bulky bis(trimethylsilyl)amido- $N(SiMe_3)_2$  ligand has two important advantages: i) the possibility to stabilize the low coordination number of the metal, and ii) the tendency to form metallacyclic derivatives performing intramolecular C-H bond activation.<sup>51</sup> For example, the  $MeTi\{N(SiMe_3)_2\}_3$  complex may be easily photolyzed to form a trigonal

planar paramagnetic titanium (III) species  $\text{Ti}[\text{N}(\text{SiMe}_3)_2]_3$ , as confirmed by EPR spectroscopy.<sup>50</sup> A metallacyclic Ti species (Fig. 2.5) was achieved by sodium amalgam reduction of  $\text{TiCl}_2[\text{N}(\text{SiMe}_3)_2]_2$ .<sup>51</sup>

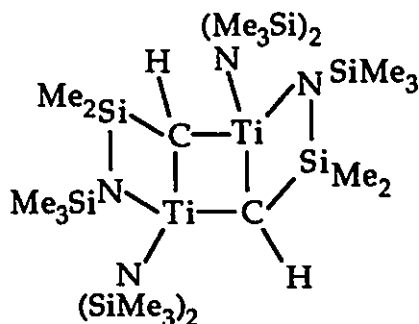
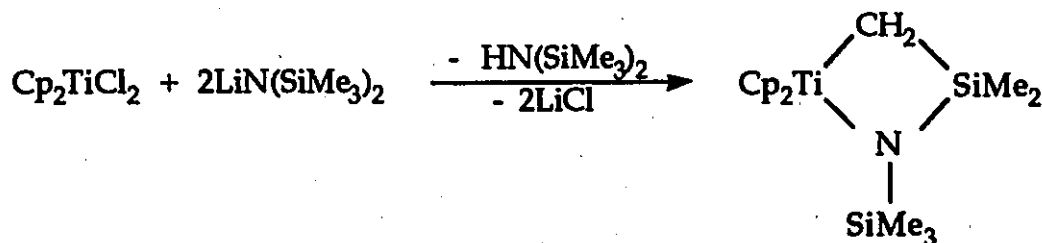
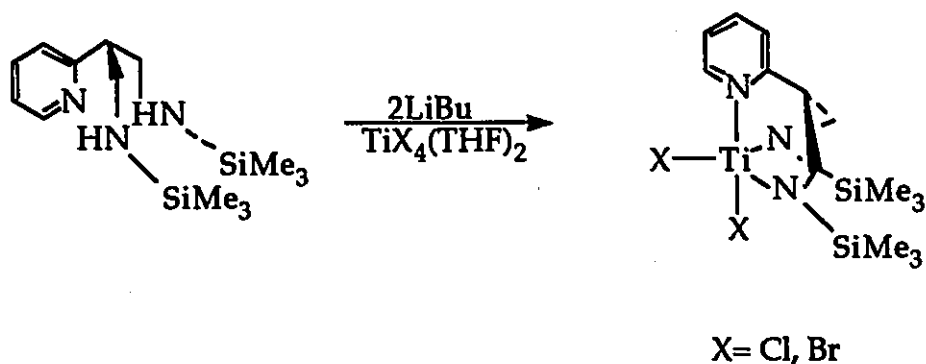


FIG. 2.5 Titanium-Carbene Complex

Another example of intramolecular C-H  $\sigma$  bond metathesis originating from the same amido group has been observed during the reaction of  $\text{Cp}_2\text{TiCl}_2$  with 2 eq of  $\text{LiN}(\text{SiMe}_3)_2$  in pentane (Eq. 2.3).<sup>52</sup> A stable Ti-C  $\sigma$ -bond was formed via deprotonation of the methyl group bound to silicon. The reaction afforded a deep-red solid, whose structure was believed to be a 4-membered titanacyclobutane ring. Evidence supporting this claim has been provided by elemental analysis and mass spectroscopy.



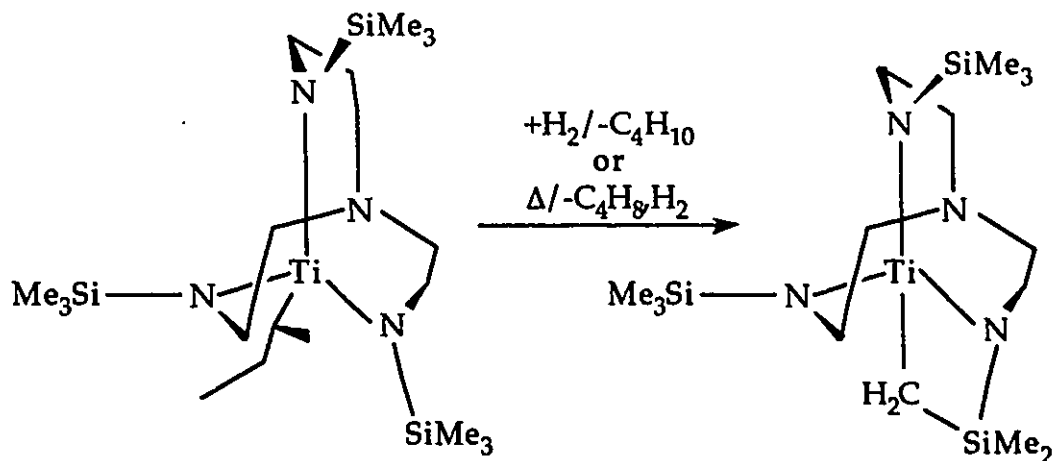
Polyfunctional amido ligands efficiently stabilize complexes through the steric shielding of a large area of the metal coordination sphere.<sup>53</sup> The remaining reactive positions are normally occupied by halide ligands, which can be substituted or removed by reduction. A new series of titanium amido bromides and chlorides has been recently prepared by reaction of  $\text{TiX}_4(\text{THF})_2$  ( $\text{X}=\text{Cl}, \text{Br}$ ) with the tripodal amine of  $\text{CH}(\text{C}_5\text{H}_4\text{N})(\text{CH}_2\text{NHSiMe}_3)_2$  and  ${}^n\text{BuLi}$  in hexane at  $-50^\circ\text{C}$ . Such ligands may serve as potential building blocks for the synthesis of oligonuclear complexes (Eq. 2.4).<sup>53</sup>



## 2.4

In order to explore the chemistry of Ti(IV) amido complexes, the tetradentate ligand  $\text{Li}_3[(\text{Me}_3\text{SiNCH}_2\text{CH}_2)_3\text{N}]$  was reacted with  $\text{TiCl}_4(\text{THF})_2$ .<sup>54</sup> The mono-chloro species  $\text{ClTi}[(\text{Me}_3\text{SiNCH}_2\text{CH}_2)_3\text{N}]$  was isolated from pentane at  $-40^\circ\text{C}$ . The complex was characterized by elemental analysis, NMR, and IR. The chloride group may be easily replaced by alkyls  $\text{LiR}$  ( $\text{R}={}^n\text{Bu}, {}^s\text{Bu}$ ) to afford stable Ti-alkyl derivatives. Upon heating to  $66^\circ\text{C}$ , or upon treating with  $\text{H}_2$ ,  ${}^s\text{BuTi}[(\text{Me}_3\text{SiNCH}_2\text{CH}_2)_3\text{N}]$  complex was converted into a metallacycle (Eq. 2.5). This proceeded via a Ti(IV) monohydride intermediate which

was observed in the NMR and identified by a characteristic resonance at  $\delta$  8.29 ppm.



2.5

The great interest stimulated by the possibility to form N-C bonds from elemental nitrogen has prompted studies on the utilization of amido- and imido-titanium compounds to model the intermediate stage of nitrogen activation.<sup>55</sup> For this purpose, a series of amido complexes  $\text{CpTi}(\text{Cl})_2\text{N}(\text{H})\text{R}$  was synthesized by reacting  $\text{CpTiCl}_3$  with  $\text{Me}_3\text{SiN}(\text{H})\text{R}$  ( $\text{R}=\text{Et}$ ,  $^i\text{Pr}$ ,  $^t\text{Bu}$ ,  $\text{Ph}$ ) at room temperature in THF. Thermolysis of this species produced the imido complexes  $[\text{Cp}(\text{Cl})\text{Ti}]_2(\mu\text{-RN})_2$  via elimination of HCl.

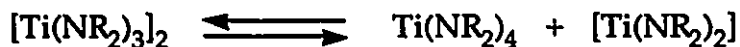
The first Ti(III) titanocene amido complexes  $[\text{Ti}(\text{Cp}^*)_2(\text{NMePh})]$  and  $[\text{Ti}(\text{Cp}^*)_2(\text{NMePh})(\text{CN}^n\text{Bu})]$  with Ti-N bond distances of 2.054 Å, and 2.157 Å, respectively, were recently prepared and crystallographically characterized.<sup>56</sup>

Ti(III) amides formulated as  $\text{Ti}(\text{NR}_2)_3$  ( $\text{R}=\text{Me}$ ,  $\text{Et}$ ,  $\text{SiMe}_3$ ,  $\text{Ph}$ ) have been prepared by a transmetallation reaction ( $\text{TiCl}_3/3\text{LiNR}_2$ ). With the exception of the bulky  $\text{Ti}[\text{N}(\text{SiMe}_3)_2]_3$  monomeric complex, all

of these species are diamagnetic, probably with dinuclear alkylamido-bridged structures, and strong metal-metal interaction.<sup>57</sup> The preparation of [*i*Pr<sub>2</sub>N]<sub>3</sub>Ti was also reported, and a mononuclear structure has been claimed by analogy with [(Me<sub>3</sub>Si)<sub>2</sub>N]<sub>3</sub>Ti. However, the characterization of this compound was carried out only on the basis of its EPR spectrum. The paramagnetism (*g*=1.987) indicated that this complex is monomeric both in solution and solid state.<sup>57</sup>

The synthesis of heteroleptic dialkylamides of Ti(III) was achieved by amine elimination and transamination reactions.<sup>58</sup> For example, amine elimination was obtained during the reaction of [Ti(NMe<sub>2</sub>)<sub>3</sub>]<sub>2</sub> with C<sub>5</sub>H<sub>6</sub> with formation of [( $\pi$ -Cp)Ti(NMe<sub>2</sub>)<sub>2</sub>]<sub>2</sub>. The compound was isolated as a viscous liquid, and its formulation was exclusively proposed on the basis of NMR and EPR data. Transamination of [Ti(NMe<sub>2</sub>)<sub>3</sub>]<sub>2</sub> with HNR<sub>2</sub> produced the mono-substituted product [R<sub>2</sub>NTi(NMe<sub>2</sub>)<sub>2</sub>]<sub>2</sub> (R=Et, *i*Pr). The characterization was limited to the simple comparison of the IR Ti-N absorption bands between starting materials and products.<sup>58</sup>

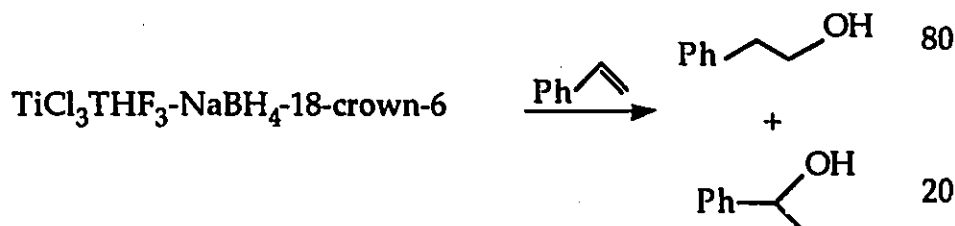
Divalent titanium amides are rare and poorly characterized. One of the best synthetic procedures for their preparation is provided by the disproportionation of the corresponding Ti(III) derivatives. Thus, [Ti(NR<sub>2</sub>)<sub>3</sub>]<sub>2</sub> disproportionated at 55°C to yield Ti(IV) and Ti(II) compound [Ti(NR<sub>2</sub>)<sub>2</sub>] (Eq. 2.6), which was isolated as a black-green crystalline, pyrophoric and probably polymeric solid. Elemental analysis was consistent with the proposed formulation.<sup>58</sup>



### 2.3 Titanium Hydrides and Borohydrides

Transition metal hydrides and borohydrides are important intermediates in many catalytic reactions, such as hydrogenations, hydroformylations, polymerizations.<sup>59</sup> They have been shown to be highly regio- and stereo-selective catalysts in the hydroboration of carbon-carbon double bonds of alkenes, dienes and unsaturated ethers.

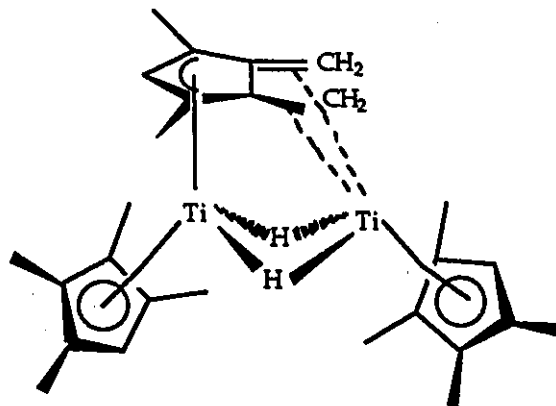
The efficient catalytic system prepared from  $\text{TiCl}_3$  and  $\text{NaBH}_4$  in THF in the presence of 18-crown-6 promotes a highly regio- and stereo-selective catalytic hydroboration of double bonds in a variety of unsaturated compounds.<sup>60</sup> In the case of styrene (Scheme 2.1), the reaction yielded 1- and 2-phenylethanols in 90% total yield (80/20 with each other).



**SCHEME 2.1** Hydroboration and Oxidation of Styrene

Despite the importance of these species, in both synthesis and reactivity, the amount of effort paid to the preparation and characterization of first row early transition metal hydrides and borohydrides derivatives has been relatively small. This stems from their high reactivity, which makes their manipulation difficult and limits the choices of appropriate ancillary ligands.<sup>5</sup>

Terminal hydrides in particular are relatively rare. In the case of titanium, there is only one example of a non-Cp hydride derivative, reported in a US patent and formulated as  $\{\text{TiH}_3[\text{Me}_2\text{P}(\text{CH}_2)_2\text{PMe}_2]\}$ .<sup>5c</sup> On the other hand, hydride ligands are often involved in the bridging interactions.<sup>5</sup> For example, a mixed-valence Ti(III)/Ti(II)  $\mu$ -hydride complex has been obtained via reduction of  $(\text{C}_5\text{HMe}_4)_2\text{TiCl}_2$  with  $\text{LiAlH}_4$  in boiling mesitylene (Eq. 2.7).<sup>61</sup> The reaction gave hydrogen abstraction from one  $\text{C}_5\text{HMe}_4$  ligand forming the dinuclear complex where two  $\text{CpHMe}_4\text{Ti}$  moieties are bridged by two hydrides and one dimethyldimethylenecyclopentadienyl ligand with a Ti-Ti distance (2.732Å).



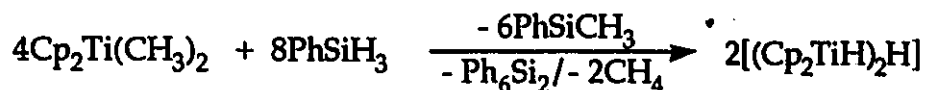
2.7

A similar reduction of  $\text{Cp}_2\text{TiCl}_2$  with  $\text{LiAlH}_4$  in boiling mesitylene produced the dimeric derivative  $\mu$ -( $\eta^5$ : $\eta^5$ -fulvene)-( $\mu$ -H)<sub>2</sub>-( $\eta^5$ -CpTi)<sub>1.5</sub> benzene.<sup>62</sup> The X-ray structure determination shows that

the Ti-H distances are in the range of 1.67-1.76Å, and Ti-Ti distance in the bonding range (2.989Å).

A  $\mu$ -dihydrido mixed-valence Ti(III)/Ti(II) compound  $\mu$ -( $\eta^5$ - $\eta^6$ -Ind)( $\mu$ -H)<sub>2</sub>[Ti( $\eta^5$ Ind)]<sub>2</sub> with a very short Ti-Ti distance (2.745Å) was obtained from the reaction of bis(indenyl)dimethyltitanium with phenylsilane.<sup>63</sup> The presence of bridging hydrogens which could not be conclusively demonstrated from the crystal structure, was confirmed by the comparison of the EPR and IR spectra of the hydride and deuteride analogous. The IR band at 1300 cm<sup>-1</sup> is shifted to 945 cm<sup>-1</sup> upon deuteration. The EPR spectrum consists of a well-resolved 1:2:1 triplet with  $g=1.9885$ , resulting from the coupling of the two hydrides.

The reaction of Cp<sub>2</sub>Ti(CH<sub>3</sub>)<sub>2</sub> with organosilanes led to the formation of an unusual titanocene complex (Eq. 2.8) characterized by EPR and IR measurements.<sup>64</sup>



2.8

A high catalytic activity of titanium-aluminum systems in Ziegler-Natta polymerization and olefin hydrogenation has stimulated considerable efforts for the preparation and characterization of heterobimetallic Ti-Al complexes.<sup>65,66</sup> The reaction of Cp<sub>2</sub>TiH<sub>2</sub>AlH<sub>2</sub> with ethanol or diethylamine in ether produced a new series of titanium-aluminum bimetallic hydride complexes, [CpTi( $\mu_2$ -H)<sub>2</sub>Al(H)( $\mu_2$ -OC<sub>2</sub>H<sub>5</sub>)], [(Cp)<sub>2</sub>Ti( $\mu_2$ -H)<sub>2</sub>Al(H)( $\mu_2$ -N(C<sub>2</sub>H<sub>5</sub>)<sub>2</sub>)]<sub>2</sub>. The reaction of Cp<sub>2</sub>TiH<sub>2</sub>AlR (R=HCl, Cl<sub>2</sub>) or Cp<sub>2</sub>TiAlH<sub>4</sub>Cl with LiAlH<sub>4</sub> yielded a tetra-nuclear complex [(Cp)<sub>2</sub>Ti( $\mu_2$ -H)<sub>2</sub>]<sub>2</sub>Al( $\eta^2$ -H<sub>2</sub>BH<sub>2</sub>). The structures of

all of these complexes have been elucidated by crystallographic determination, showing Ti-H distance of 1.72Å and identical Ti-Al interactions of 2.79Å.<sup>65, 66</sup>

Treatment of bimetallic titanium-magnesium complexes with aluminum alkyls gave materials which showed high catalytic activity for ethylene polymerization.<sup>4,5a</sup> The titanium-magnesium heterobimetallic system  $[(Cp^*)_2TiCl_2]_2iPrMgCl$  (1:2) has been reported as a catalyst for linear head-to-tail dimerization of terminal acetylenes.<sup>67</sup> After 3 days standing at room temperature, this reaction mixture was converted into the trinuclear-hydride complex  $\{[(Cp^*)_2Ti(\mu-H)_2]_2Mg\}$ . The EPR data showed a signal at  $g=1.9896$ , which corresponds to a titanium  $d^1$  electronic configuration. The crystal structure has shown the presence of two perpendicular  $(Cp^*)_2Ti(\mu-H)_2$  fragments attached to one central Mg atom through four equivalent Ti-H-Mg bridges. The Ti-H distances in the planar  $Ti(\mu-H)_2Mg$  bridges are in the range of 1.66-1.79Å.

Borohydride complexes have been successfully used as a precursors for the synthesis of the transition metal-hydrides species.<sup>68</sup>

One of the most significant structural questions for metal borohydrides concerns the mode by which the  $BH_4$  group is attached to the metal.<sup>69</sup> The  $BH_4^-$  ligand can bind to the transition metal by using one, two, or three H bridges (Fig. 2.6). Vibrational spectroscopy allows a reasonable unambiguous distinction to be made between monodentate ( $\eta^1$ ), bidentate ( $\eta^2$ ), and tridentate ( $\eta^3$ ) hydrogen-bridged metal- $BH_4$  interactions.<sup>70</sup>

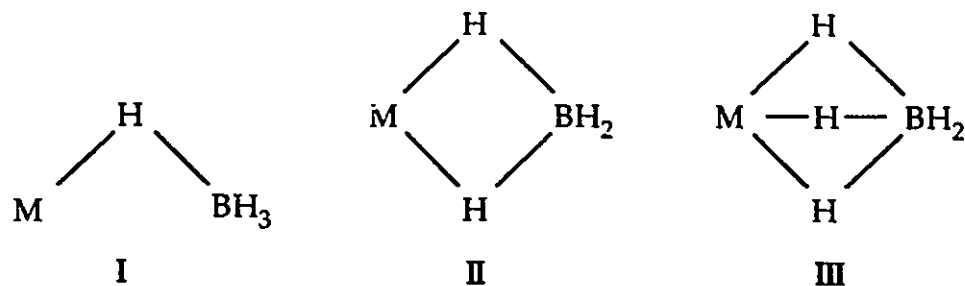
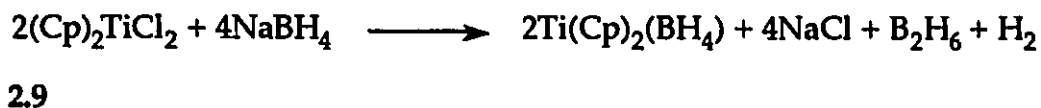


FIG. 2.6 Bonding Modes of  $\text{BH}_4$  Ligand

Besides the sole example of a divalent titanium borohydride  $\text{Ti}(\eta^2\text{-BH}_4)_2(\text{dmpe})_2$  prepared via chloride replacement of  $\text{TiCl}_2(\text{dmpe})_2$  with  $\text{LiBH}_4$ ,<sup>71</sup> borohydride complexes of divalent titanium are to date unexplored. The complex was shown to be paramagnetic with two unpaired electrons. The crystal structure of  $\text{Ti}(\eta^2\text{-BH}_4)_2(\text{dmpe})_2$  indicates that the tetrahedral  $\text{BH}_4$  groups adopt a  $\eta^2$ -bonding mode with titanium, forming Ti-H distances of 2.06Å. Interestingly, the  $\text{BH}_4$  is easily displaced by alkyls and phenoxides.<sup>72</sup>

The first Ti(III) borohydride complex to be isolated and characterized was obtained by replacement/reduction reaction of a Ti(IV) species with  $\text{NaBH}_4$  (Eq. 2.9).<sup>73</sup>



A similar compound could be obtained by chloride replacement of  $\text{Cp}^*_2\text{TiCl}$  with  $\text{LiBH}_4$  in THF affording a monomeric and crystalline  $\text{Cp}^*_2\text{Ti}(\text{BH}_4)$  compound which was stable up to 250°C.<sup>74</sup> The presence of the  $\text{BH}_4$  moiety was confirmed by IR spectroscopy. B-H stretching

vibrations were detected at  $2445\text{ cm}^{-1}$  and  $2410\text{ cm}^{-1}$  and the bridging Ti-H-BH<sub>3</sub> hydride at  $2070\text{ cm}^{-1}$  and  $1950\text{ cm}^{-1}$ . EPR spectra with  $g=1.978$  is in agreement with  $d^1$  electronic configuration of a Ti(III) species.

To date, only two examples of borohydride Ti(III) complexes without Cp ligands have been reported. In 1988, Girolami reported the crystal structure of the  $\text{Ti}(\text{BH}_4)_3(\text{PMe}_3)_2$  (Fig. 2.7), which comprises an approximate trigonal-bipyramidal geometry, with the phosphines in axial positions.<sup>75</sup> One of the three BH<sub>4</sub><sup>-</sup> groups is bidentate, whereas the other two BH<sub>4</sub><sup>-</sup> groups possess unusual geometry, which involves the interaction of the titanium center with one B-H mode in a *side-on* manner. The Ti-H<sub>1</sub> interaction of  $1.73(7)\text{Å}$  was described as "agostic". This bonding mode is of primary interest,<sup>76</sup> because it resembles one of the proposed transition states to be modeled for methane activation studies.

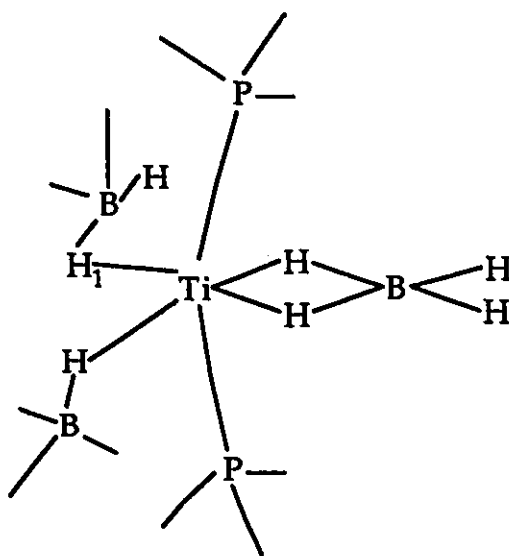


FIG. 2.7 Structure of  $\text{Ti}(\text{BH}_4)_3(\text{PMe}_3)_2$

However, the results of the theoretical calculations carried out for the complex  $\text{Ti}(\text{BH}_4)_3(\text{PMe})_2$  conflict with the structure as determined by X-ray diffraction analysis.<sup>79</sup> The energetical ordering of sixteen different possible structures were analyzed through an electron count. The result indicated that the optimal structure is expected to adopt a  $\eta^2:\eta^2:\eta^3$  coordination mode for the  $\text{BH}_4$  groups. This result is in disagreement with the experimental data, which have shown a  $\eta^1:\eta^1:\eta^2$  coordination. The experimentally determined structure was found to be very high in energy.

The molecular structure of  $\text{Ti}(\text{BH}_4)_3$  and  $\text{Ti}(\text{BD}_4)_3$  was determined in the gas phase by electron diffraction methods, IR and UV photoelectron spectroscopy.<sup>77</sup> The molecule has three tridentate  $\text{BH}_4^-$  groups, giving to the molecule an overall  $\text{C}_{3h}$  symmetry, and exhibiting a planar  $\text{TiB}_3$  skeleton.

The coordination mode of the above complexes was also studied from the theoretical point of view. Twenty different coordination modes of the  $\text{BH}_4^-$  moiety in the  $\text{Ti}(\text{BH}_4)_3$  species were optimized by the analytical gradient method, followed by ab initio UHF calculations and correlation energy at the MP2 level.<sup>78</sup> Results of these theoretical calculations showed that each borohydride group binds the metal in an  $\eta^3$  fashion and that the  $\text{C}_{3h}$  structure is the most stable. This is in agreement with experimental data.

## 2.3 Titanium Alkyls

Since the discovery of  $\text{ZnEt}_2$  in the last century, metal-alkyls have been of considerable interest, and today the chemistry of M-C bond is by far the most important area of both coordination and organometallic chemistry.<sup>5</sup>

Transition metal alkyls are very important for metal-catalyzed polymerization reactions of olefins and acetylenes, hydrogenation, and in some major industrial processes, as for example in the Ziegler-Natta polymerization, and in transition metal-catalyzed metathesis of cyclic olefines.<sup>80</sup> Vitamin B<sub>12</sub> provides a unique example of naturally occurring metal-alkyl .

Dialkyltitanocene compounds  $\text{Cp}_2\text{TiR}_2$  ( $\text{R}=\text{CH}_3, \text{CH}_2\text{C}_6\text{H}_5, \text{C}_6\text{H}_5$ ) have been exploited as efficient photocatalytic systems for the homogenous hydrogenation of olefins under mild conditions (25°C, 1 atm).<sup>81</sup> The active catalytic species, probably a Ti(III) complex, was generated by UV irradiation in the presence of hydrogen gas before the introduction of the substrate. Following this procedure,  $\text{Cp}_2\text{TiMe}_2$  converts hex-1-ene into hex-2-ene, and cycloocta-1,5-diene into cycloocta-1,3-diene within a few minutes. Similarly,  $\text{Cp}_2\text{TiPh}_2$  converts styrene into ethylbenzene in high yield.

The photochemical transformation of terminal olefines into 2-alkenes with E-configuration was promoted by  $[(\text{C}_5\text{Me}_4\text{H})_2\text{Ti}(\text{CH}_3)_2]$ .<sup>82</sup> Rapid transformation was observed in the case of 1-pentene, 1-hexene, 1-octene and 1-decene. Kinetic studies show that the reaction is photoassisted rather than photocatalyzed since it stops as soon as the

irradiation is interrupted. The Ti(III) paramagnetic intermediates formed in this process were monitored by EPR.

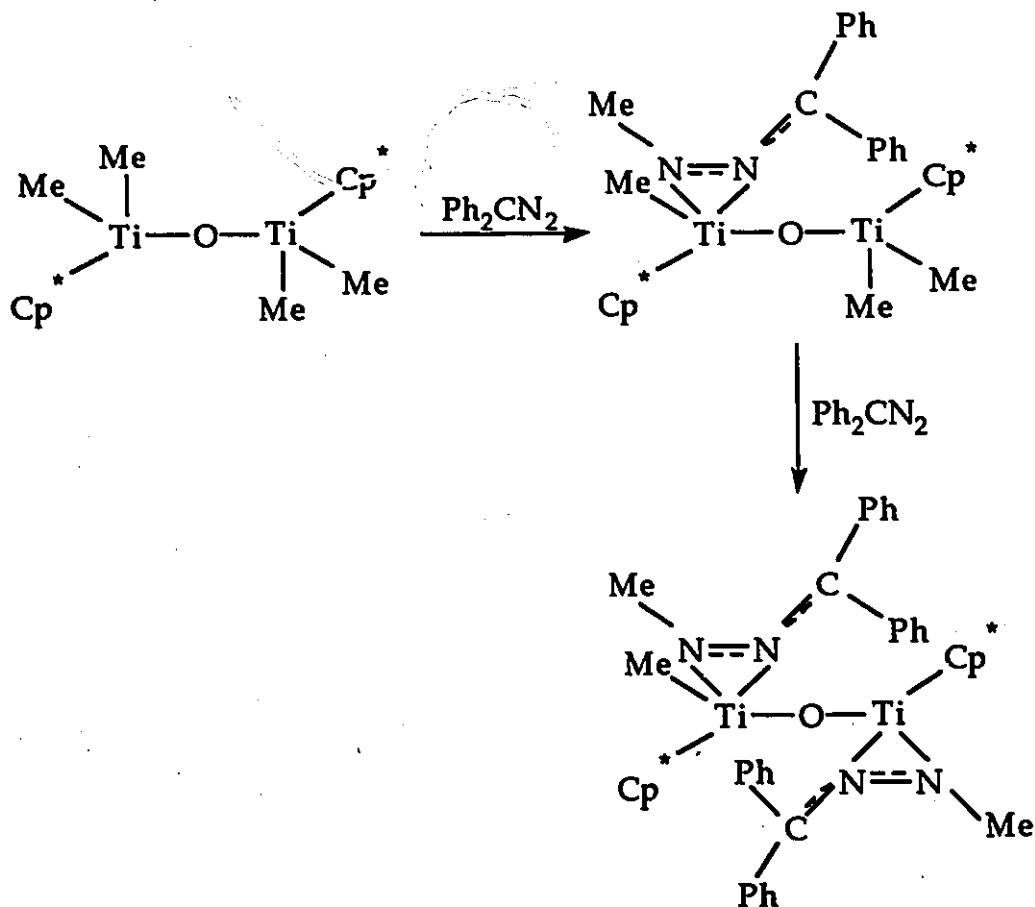
Insertion reactions and metathesis are the most distinctive characteristics of the chemistry of metal-alkyl compounds. The importance of these reactions lies in the fact that they usually lead to the formation of C-C bonds. Among several substrates susceptible to insertion into the M-C bond, CO<sub>2</sub> is of particular interest. For example, photochemical insertion of CO<sub>2</sub> into the titanium-metal bond of (Cp)<sub>2</sub>Ti(CH<sub>3</sub>)<sub>2</sub> formed (Cp)<sub>2</sub>Ti(O<sub>2</sub>CCH<sub>3</sub>)CH<sub>3</sub> in 60% yield through an unusually clean and selective reaction.<sup>83</sup>

The synthesis of Ti(IV) alkyls is very well established and these compounds are on average well characterized. One of the most common routes for their preparation is by chloride replacement using LiR (R=Me, Ph, Bz, Np, etc.) carried out on TiCl<sub>4</sub>, Cp- and Cp\*- Ti(IV) chloride starting materials.<sup>84</sup>

In Ziegler-Natta catalysis the transition state for C-C bond formation involves the migration of an α-hydrogen from the growing polymer chain into the metal-center. Therefore an "agostic" three-center M...H-C interaction is proposed as a preliminary step.<sup>85</sup> The crystal structure of methyltitanium trichloride MeTi(Cl)<sub>3</sub> prepared in the reaction of TiCl<sub>4</sub> with PbMe<sub>4</sub>, showed that the molecule has a dimeric centrosymmetrical structure of Cl<sub>2</sub>MeTi(μ-Cl)<sub>2</sub>TiMeCl<sub>2</sub> where the distorted tetrahedral coordination is caused by a Ti...H-C "agostic" interaction (Ti-C-H=66°; Ti-H=1.92Å). Addition of dmpe to [MeTi(Cl)<sub>3</sub>]<sub>2</sub> resulted in the cleavage of the dimeric structure and formation of monomeric MeTi(Cl)<sub>3</sub>(dmpe). The Ti...H-C "agostic" interaction is

responsible for the distortion of the octahedral geometry of the titanium-metal center ( $\text{Ti-C-H}=70(2)^\circ$ ,  $\text{Ti-H}=2.03\text{\AA}$ ).<sup>86</sup>

Controlled hydrolysis of  $\text{Cp}^*\text{TiMe}_3$  (reaction of  $\text{Cp}^*\text{TiCl}_3/\text{LiMe}$ ) led to the formation of the dimeric  $[\text{Cp}^*\text{TiMe}_2]_2(\mu\text{-O})$ . A slight excess of  $\text{H}_2\text{O}$  yielded trimeric  $[\text{Cp}^*\text{TiMe}(\mu\text{-O})]_3$  containing a  $\text{Ti}_3\text{O}_3$  ring.<sup>87</sup> Alkylation reactions of  $[\text{Cp}^*\text{TiCl}_2](\mu\text{-O})$  with  $\text{RLi}$  ( $\text{R}=\text{Me}$ ,  $\text{CH}_2\text{SiMe}_3$ ,  $\text{CH}_2\text{Ph}$ ) allowed the isolation of the corresponding alkyl/oxo-species.<sup>88</sup> Reaction of 1 eq of  $\text{Ph}_2\text{CN}_2$  with  $[\text{Cp}^*\text{TiMe}_2]_2(\mu\text{-O})$  gave insertion of the diazo moiety into the  $\text{Ti-CH}_3$  bond, forming  $[\text{TiCp}^*\text{Me}(\eta^2\text{-MeNNCPh}_2)]_2(\mu\text{-O})$ . Addition of a second eq gave  $[\text{TiCp}^*\text{Me}(\eta^2\text{-MeNNCPh}_2)]_2(\mu\text{-O})$  (Scheme 2.2).<sup>89</sup>



**SCHEME 2.2** The Insertion of  $\text{Ph}_2\text{CN}_2$  into  $\text{Ti-CH}_3$  Bond

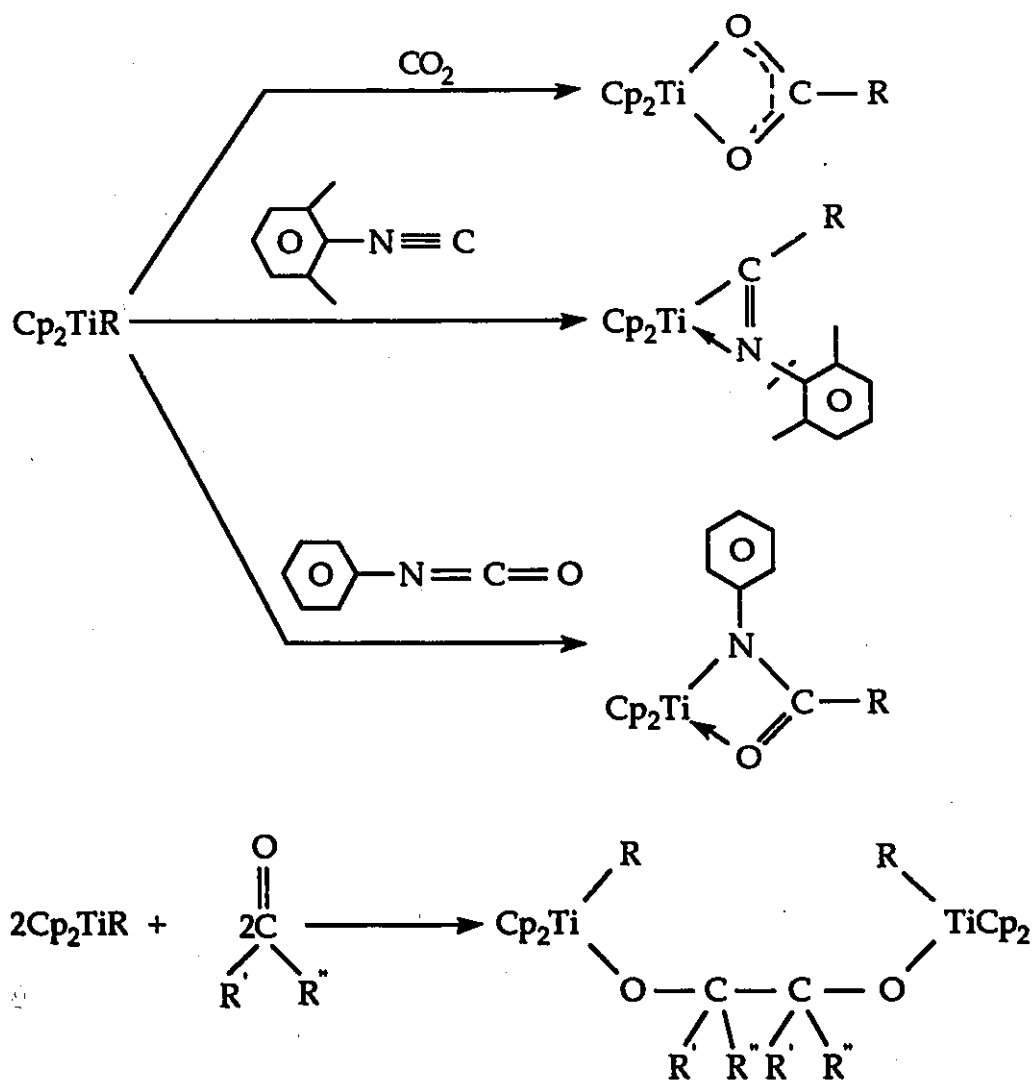
Over the past few years, literature accounts have reviewed the remarkable reactivity of titanacyclobutanes.<sup>5,6,39</sup> The reaction of bis(cyclopentadienyl)titanacyclobutane with  $[\text{ClRh}(\text{COD})]_2$  produced the Ti-Rh  $\mu$ -chloride complex  $\text{Cp}_2\text{Ti}(\mu\text{-CH}_2)(\mu\text{-Cl})\text{Rh}(1,5\text{-COD})$ . Interesting structural features include a short Ti-Rh distance of 2.98Å and the presence of the  $\mu$ -methylene moiety.<sup>90</sup> Metathesis of this complex with aryllithium reagents yielded  $\text{Cp}_2\text{Ti}(\mu\text{-CH}_2)[\mu\text{-}(p\text{-Me}_2\text{N})\text{C}_6\text{H}_4]\text{Rh}(1,5\text{-COD})$  and  $\text{Cp}_2\text{Ti}(\mu\text{-CH}_2)[\mu\text{-}(o\text{-MeO})\text{C}_6\text{H}_4]\text{Rh}(1,5\text{-COD})$ . The structure of  $\text{Cp}_2\text{Ti}(\mu\text{-CH}_2)[\mu\text{-}p\text{-}(\text{Me}_2\text{N})\text{C}_6\text{H}_4]\text{Rh}(1,5\text{-COD})$  was determined by X-ray crystallography. Further shortening of the Ti-Rh distance to 2.827(1)Å indicated a possible metal-metal bond.<sup>91</sup>

In contrast to the tetravalent derivatives, low-valent titanium alkyls are rare, and up to date only a few examples have been reported in the literature.<sup>5</sup>

In 1985, Girolami described the synthesis and structure of a unique example of divalent titanium. Alkylation of  $\text{TiCl}_2(\text{dmpe})_2$  with either  $\text{LiMe}$  or  $\text{MgMe}_2$  led to the formation of a mixture of *trans*- $\text{TiMeCl}(\text{dmpe})_2$  and *trans*- $\text{TiMe}_2(\text{dmpe})_2$ .<sup>92</sup> Preliminary results showed that these species are active as catalysts for olefin polymerization. In contrast to the case of  $\text{TiMe}_2(\text{dmpe})_2$ , the X-ray structure of *trans*- $\text{TiMeCl}(\text{dmpe})_2$  showed that the methyl group was bent towards the metal, indicating possible existence of an "agostic" interaction.

For the organometallic chemistry of Ti(III), major developments have been exclusively obtained with Cp derivatives.<sup>93</sup> Complexes such as  $\text{CpTiR}_2$  ( $\text{R}=\text{CH}_2\text{Ph}$ ,  $\text{CH}_2\text{C}_6\text{H}_4\text{-O-NMe}_2$ ,  $\text{C}_6\text{H}_4\text{-O-CH}_2\text{NMe}$ ) and  $\text{Cp}_2\text{TiR}$  ( $\text{R}=\text{CH}_2\text{SiMe}_3$ ,  $\text{CHPh}_2$ ,  $\text{CH}(\text{SiMe}_3)_2$ ,  $\text{CH}_2\text{CMe}_3$ ,  $\text{CH}_2\text{Ph}$ ) have been prepared and characterized.<sup>93</sup>

Teuben described the synthesis of a series of  $\text{Cp}_2\text{TiR}$  alkyls ( $\text{R}=\text{CH}_3, \text{C}_2\text{H}_5, \text{}^n\text{C}_4\text{H}_9, \text{}^s\text{C}_4\text{H}_9, \text{}^t\text{C}_4\text{H}_9$ ) and their reactions with unsaturated substrates such as cumulenes, isocyanides, and carbon dioxide.<sup>94</sup> The reactions usually proceed by insertion of the substrate into the Ti-C bond, affording iminoacyl, carboxylato and amido derivatives, respectively (Scheme 2.3).



**SCHEME 2.3** Reactivity of  $\text{Cp}_2\text{TiR}$  ( $\text{R}=\text{Me}, \text{R}'=\text{R}''=\text{Me}$ )

All insertion products were obtained in good yields and were fully characterized by elemental analysis, IR and EPR measurements. The pinacol type insertion/dimerization product obtained in the case of ketone results from the coupling of the two Ti(III) species with a  $d^1$  electronic configuration.

Permethylcyclopentadienyl groups are very important and unique ligands in organometallic chemistry. Their large steric bulk relative to the ionic radius of titanium provides a sterically congested unit. Thus, the monomeric and thermally stable complex  $Cp^*_2TiMe$  is an excellent model for investigating the reactivity of the Ti-C bond.<sup>95</sup> Recent examples of  $Cp^*$  alkyl complexes  $Cp^*_2TiR$  ( $R=Me, Et$ ) exhibit a variety of reactions, which can be divided into: insertions, acid-base reactions and adduct formation. Insertion into the Ti-C bond with  $^tBuNC$  resulted in the formation of an iminoacyl complex  $Cp^*_2TiC(Me)=N(^tBu)$ , whereas insertion of CO at  $-60^\circ C$  produced an intensely blue acyl compound  $Cp^*_2TiC(O)Me$ . Reaction with  $CO_2$  yielded the sky-blue methylcarboxylato complex  $Cp_2^*TiO_2CMe$ . When an acidic substrate is used, such as monosubstituted alkynes, C-H  $\sigma$ -bond metathesis reaction takes place with the formation of alkyne derivative followed by elimination of methane. In a reaction with acetone the adduct product of  $Cp^*_2TiMe(O=CMe_2)$  was isolated.<sup>95</sup>

The extensive use of the  $Cp^*$  ligand in early transition metal chemistry, coupled with the current interest in C-H activation, has led to several reports on reactive ring-metallated (fulvene) species.<sup>96</sup> The thermolysis of paramagnetic  $Cp^*_2TiMe$  is a clean, stoichiometric process leading to the fulvene complex  $(\eta^5-C_5Me_5)(\eta^6-C_5Me_4CH_2)Ti$ , with liberation of  $CH_4$  (Fig. 2.8). Kinetic measurements and deuterium

labeling studies indicated that decomposition is catalyzed by  $\text{Cp}^*\text{TiH}$ . Further heating results in the loss of  $\text{H}_2$  and formation of an allyldiene compound,  $(\eta^5\text{-Cp}^*)(\eta^7\text{-C}_5\text{Me}_3(\text{CH}_2)_2)\text{Ti}$ .<sup>7</sup>

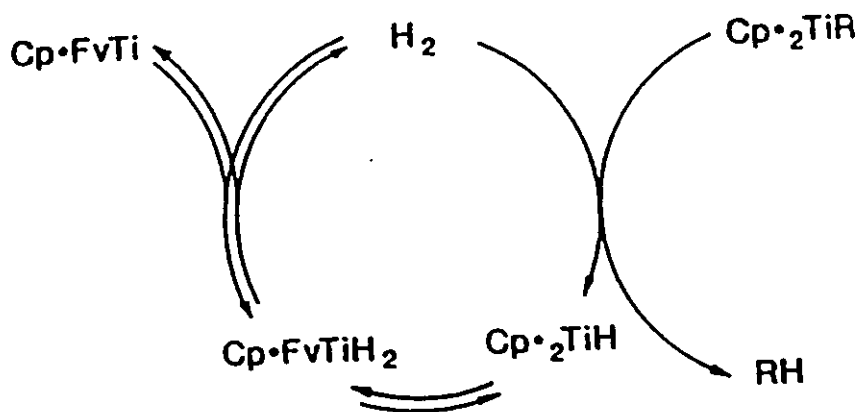
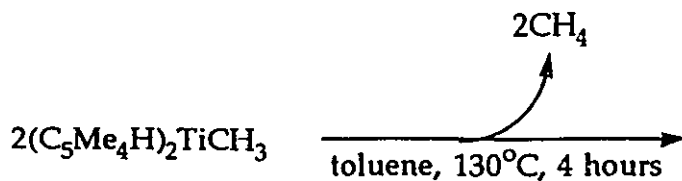
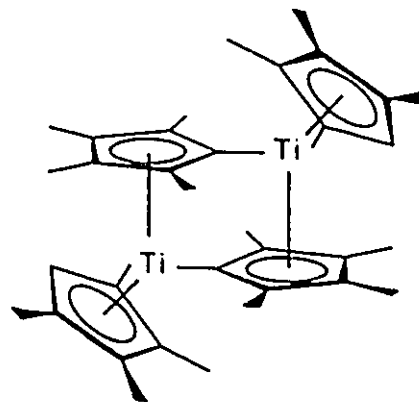


FIG. 2.8 Thermal Decomposition of  $\text{Cp}^*\text{TiR}$  ( $\text{R}=\text{Me}$ )

The replacement of one methyl substituent of the  $\text{Cp}^*$  ligand by a proton remarkably modifies the reactivity.<sup>7</sup> Thermolysis of  $(\eta^5\text{-C}_5\text{Me}_4\text{H})\text{TiMe}$  at  $130^\circ\text{C}$  resulted in the formation of a dinuclear complex  $[\mu\text{-(}\eta^1\text{:}\eta^5\text{-C}_5\text{Me}_4\text{)}(\eta^5\text{-C}_5\text{Me}_4\text{H})\text{Ti}]_2$  and elimination of a stoichiometric amount of methane (Eq. 2.8).



2.8



When the fulvene complex  $(\eta^5\text{-C}_5\text{H}_5)(\eta^6\text{-C}_5\text{Me}_4\text{CH}_2)\text{TiCl}$  was reacted with 2 eq of benzaldehyde  $\text{C}(\text{O})\text{HPh}$ , the yellow microcrystalline air sensitive dialkoxide product  $(\eta^5\text{-C}_5\text{H}_5)\text{Ti}[(\text{OCHPh})_2\text{C}_5\text{Me}_4(\text{CH}_2)]$  was formed via insertion of benzaldehyde into the two Ti-C bonds of the fulvene ligand.<sup>97</sup>

The first examples of titanium alkyl complexes not supported by  $\pi$ -bonded ligands was reported in the late 1960s, with the synthesis and characterization of homoleptic, thermally stable complexes of the general formula  $\text{TiR}_4$  ( $\text{R}=\text{Me}$ ,  $\text{Ph}$ ,  $\text{CH}_2\text{PhCH}_2\text{C}(\text{CH}_3)_3$ ,  $\text{CH}_2\text{Si}(\text{CH}_3)_3$ ). For Ti(III), non-cyclopentadienyl derivatives such as  $[\text{TiCl}_2\text{R}(\text{py})_3]$  ( $\text{R}=\text{Me}$ ,  $\text{Ph}$ ),  $[\text{TiClPh}_2(\text{Et}_2\text{O})_3]$  were also described.<sup>5,84</sup>

Reduction of  $\text{TiR}_4$  ( $\text{R}=\text{CH}_2\text{SiMe}_3$ ,  $\text{CH}_2\text{Ph}$ ), with ethyllithium produced homoleptic Ti(III) alkyls, but in both cases characterization was limited only to chromatography and photocalorimetry.<sup>5</sup>

## 2.5 Scope of Thesis

The literature survey, reported above, clearly indicates that titanium hydrides, borohydrides and alkyls are: i) very important reagents in organic synthesis, ii) may be involved in different catalytic reactions, and iii) display a rich organometallic and coordination chemistry.

Since the synthesis and characterization of Ti(II) and Ti(III) complexes is not very well explored, apart from cyclopentadienyl derivatives, their preparation provides a challenging opportunity for synthetic study.

As part of a large project to investigate the chemistry of titanium in the +III oxidation state, we have focused our attention on the use of bulky bisalkylamides  $R_2NLi$  ( $R=Me_3Si, Cy, iPr$ ) as supporting ligands instead of the ubiquitous cyclopentadienyl ligands.

There are a number reasons for incorporating anionic  $(R_2N)^-$  moieties on to the metal center: i) the electronic flexibility of the N donor atom allows a variety of bonding modes ( $\sigma, \pi, \mu$ ), ii) the differences in steric bulk can modify the coordination environment of the transition metal, and iii) the possibility exists to introduce optical activity by using the chiral amides.

Since highly reactive functions such as, hydrides, borohydrides and alkyls are not very well known for low-valent titanium, their synthesis, characterization and chemical reactivity, utilizing bis(amido) titanium (III) complexes as starting materials, have been preliminary investigated.

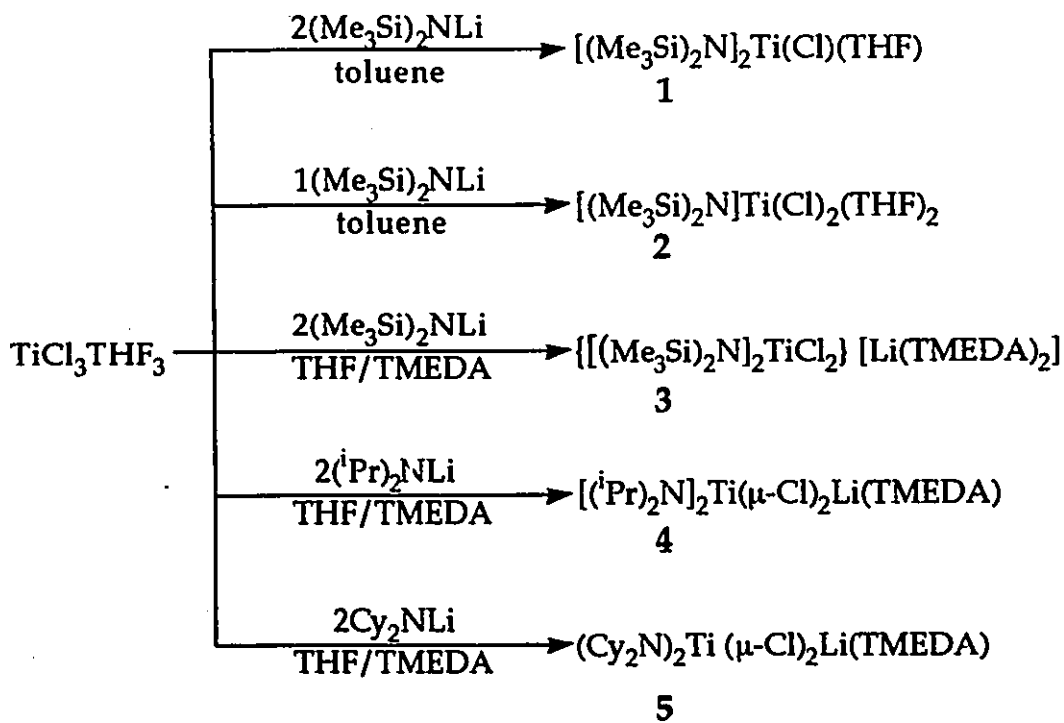
## CHAPTER III

### RESULTS AND DISCUSSION

#### 3.1 Titanium Amides

There are several possible synthetic procedures which, at least in principle, may be useful for the preparation of Ti(III) amides.<sup>43</sup> For example, the reaction of Ti(III) homoleptic alkyls with amines, or the reduction of suitable Ti(IV)  $(R_2N)_{4-x}TiCl_x$  starting materials. The most significant drawback of the first type of reaction lies in both the lack of Ti(III) alkyls and the possibility that the reaction might be uncontrollable, evolving  $H_2$  and forming Ti(IV) species. The second method is also not very favorable, since  $(R_2N)_2TiCl_2$  complexes are unknown or available in very poor yield. Therefore, the most convenient synthetic methodology for the preparation Ti(III) amides remains the transmetallation reaction of  $TiCl_3$  with  $R_2NLi$ .<sup>43</sup> The major advantage of this procedure is that both reagents are readily available.

The reaction of  $TiCl_3 \cdot THF_3$  with  $R_2NLi$  ( $R=Me_3Si, Cy, iPr$ ) produced the corresponding dialkylamido Ti(III) complexes (Scheme 3.1).



**SCHEME 3.1** The Reactions of  $\text{TiCl}_3\text{THF}_3$  with  $\text{R}_2\text{NLi}$   
 ( $\text{R}=\text{Me}_3\text{Si}$ ,  $\text{Cy}$ ,  $\text{iPr}$ )

Complexes 1-5 were characterized by microanalysis, IR, magnetic susceptibility measurements, and single crystal X-ray diffraction analysis. Only in the case of complex 4 the X-ray analysis was not possible due to poor crystal quality. The magnetic susceptibility measurements indicated the presence of one unpaired electron, which corresponds to a  $d^1$  electronic configuration. Typically,  $\mu_{\text{eff}}$  of 1.7-1.8  $\mu\text{B}$  were determined for these Ti(III) species. In some cases the presence of TMEDA was required for stabilizing the final product.

For example, in the case of  $(\text{Me}_3\text{Si})_2\text{NLi}$  different products (1, 2, and 3) were formed depending on both the stoichiometry and the presence of TMEDA.

Addition of 2 eq of  $(\text{Me}_3\text{Si})_2\text{NLi}$  to a green toluene suspension of  $\text{TiCl}_3\text{THF}_3$  gave a dark-green solution. The green monomeric neutral  $[(\text{Me}_3\text{Si})_2\text{N}]_2\text{Ti}(\text{Cl})(\text{THF})$  **1** was obtained after evaporation and recrystallization from hexane at  $-30^\circ\text{C}$ . The presence of  $\text{Me}_3\text{Si}$  moiety in **1** was confirmed by the presence of the characteristic broad band in the infrared spectrum at  $830\text{ cm}^{-1}$ .

The molecular structure of **1** was elucidated by an X-ray crystallographic analysis and is shown in Fig. 3.1 with selected bond distances and angles. The tetrahedral geometry of the titanium metal center is comprised by two trimethylsilylamido ligands, one chloride and a THF molecule ( $\text{Cl1-Ti1-O1}=94.5(1)$ ;  $\text{N1-Ti1-N2}=128.9(2)$ ;  $\text{Cl1-Ti1-N1}=113.9(1)$ ;  $\text{Cl1-Ti1-N2}=104.7(1)^\circ$ ). The Ti-Cl distance ( $\text{Ti1-Cl1}=2.328(2)\text{\AA}$ ) and the Ti-O distance ( $\text{Ti1-O1}=2.089(4)\text{\AA}$ ) are as expected. The fairly short titanium-nitrogen distances ( $\text{Ti1-N1}=1.957(4)$ ;  $\text{Ti1-N2}=1.948(4)\text{\AA}$ ), comparable with those reported in the literature<sup>42,43</sup>, and the trigonal planar geometry of the N atom, suggest the presence of some Ti-N  $\pi$ -bond character. The deviation of the metal center from a regular tetrahedral geometry is probably the result of the large steric hindrance introduced by the two bulky amido group. The planar geometry around the amido nitrogens although slightly distorted ( $\text{Ti1-N1-Si1}=119.1(2)$ ,  $\text{Ti1-N1-Si2}=119.1(2)^\circ$ ), is still in agreement with a  $sp^2$  hybridization of the N atom.<sup>42,43</sup>

In contrast to the formation of **1**, reaction of  $\text{TiCl}_3\text{THF}_3$  with 1 eq of  $(\text{Me}_3\text{Si})_2\text{NLi}$  carried out under the same conditions, formed a mixture of two different products; complex **1** and the blue crystalline  $[(\text{Me}_3\text{Si})_2\text{N}]\text{Ti}(\text{Cl})_2(\text{THF})_2$  **2**.

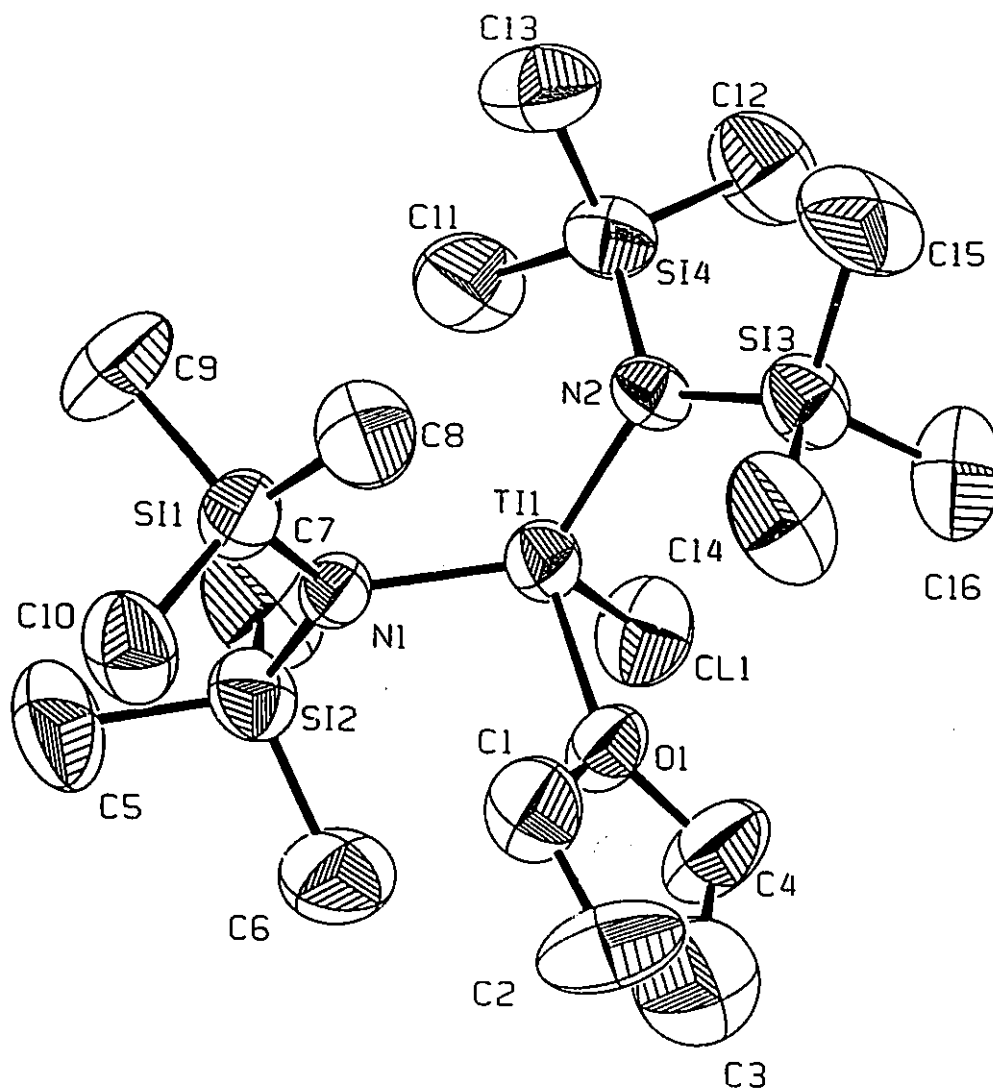


**FIG. 3.1** ORTEP drawing of 1. Bond distances (Å) and angles (deg) are as follows: Ti1-N1=1.957(4), Ti1-N2=1.948(4), Ti1-Cl1=2.328(2), Ti1-O1=2.089(4), Cl1-Ti1-O1=94.5(1), N1-Ti1-N2=128.9(2), Cl1-Ti1-N1=113.9(1), Cl1-Ti1-N2=104.7(1), Ti1-N1-Si1=119.1(2), Ti1-N1-Si2=119.1(2)

Attempts to obtain compound 2 selectively by using different experimental conditions (temperature, reaction time, order of addition of reagents) did not modify the result.

Complex 2 was characterized only by X-ray crystallography (Fig. 3.2). The coordination geometry of the titanium center is distorted trigonal bipyramidal with two molecules of THF occupying the two axial *trans* -position (Cl1-Ti1-Cl2=104.06(4); Cl1-Ti1-O1=88.58(7); Cl1-Ti1-O2=90.45(7); Cl1-Ti1-N1=128.87(9)°). The titanium-chloride distances Ti1-Cl1=2.341(1); Ti1-Cl2=2.333(1)Å are as expected, as well as the Ti-O distances (Ti1-O1=2.135(2); Ti1-O2=2.166(2)Å). The Ti1-N1 distance is slightly shorter (1.941(3)Å) with respect to the bis-amido complex probably due to the release of steric compression. The coordination geometry around the amido nitrogen is regular trigonal planar (Ti1-N1-Si1=119.4(1); Ti1-N1-Si2=121.0(2); Si1-N1-Si2=119.5(2)°).

When carried out in the presence of TMEDA, the reaction of TiCl<sub>3</sub>THF<sub>3</sub> with 2 eq of (Me<sub>3</sub>Si)<sub>2</sub>NLi in THF led to the formation of a light green solution. Colorless crystals of the ionic  $\{[(\text{Me}_3\text{Si})_2\text{N}]_2\text{Ti}(\text{Cl})_2\}[\text{Li}(\text{TMEDA})_2]$  3 separated after evaporation to dryness and recrystallization of the residue from ether at -30°C overnight. Complex 3 is paramagnetic with a magnetic moment of 1.75 μ<sub>B</sub>. The presence of the Me<sub>3</sub>Si moiety was confirmed by the characteristic intense band in the IR spectrum at 835 cm<sup>-1</sup>.

The chemical connectivity of 3 was demonstrated by X-ray diffraction analysis.<sup>24</sup> The titanium-containing anion consists of a distorted tetrahedral Ti(III) atom surrounded by two amido ligands and two chlorine atoms (Cl1-Ti1-Cl2=102.4(1); Cl1-Ti1-N=99.7(3); N1-Ti1-N2=121.9(3)°). Even in this case, the distorted geometry is probably due

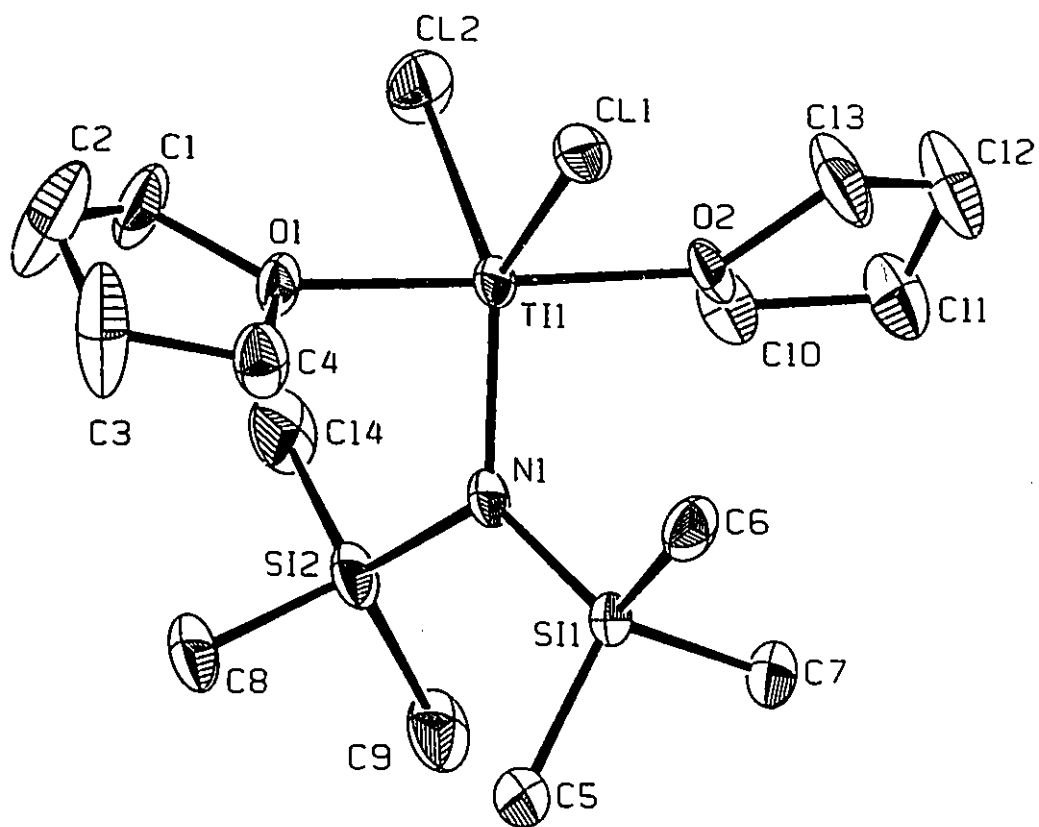


**FIG. 3.2** ORTEP drawing of **2**. Bond distances (Å) and angles (deg) are as follows: Ti1-Cl1=2.347(1), Ti1-Cl2=2.333(1), Ti1-O1=2.135(2), Ti1-O2=2.166(2), Ti1-N=1.941(3), Cl1-Ti1-Cl2=104.06(4), Cl1-Ti1-O1=88.58(7), Cl1-Ti1-O2=90.45(7), Cl1-Ti1-N1=128.87(9), Cl2-Ti1-O1=90.59(7), Cl2-Ti1-O2=88.35(7), Cl2-Ti1-N1=127.05(9), O1-Ti1-O2=178.35(9), O1-Ti1-N1=91.7(1)

to the large steric bulk introduced by the two  $\text{N}(\text{SiMe}_3)_2$  groups. The Ti-N distances ( $\text{Ti1-N1}=1.933(8)$ ,  $\text{Ti1-N2}=1.989(8)\text{\AA}$ ) together with the trigonal planar geometry of the nitrogen atom, indicates that the Ti-N bond possesses some  $\pi$ -bond character. No special features were observed for the tetrahedral  $[\text{Li}(\text{TMEDA})_2]$  cation.

Reactions of  $\text{TiCl}_3\text{THF}_3$  with 2 eq of  $(i\text{Pr})_2\text{NLi}$  and  $\text{Cy}_2\text{NLi}$  at  $-10^\circ\text{C}$  in THF, followed by the addition of 1.5 eq of TMEDA gave complexes  $[(i\text{Pr})_2\text{N}]_2\text{Ti}(\mu\text{-Cl})_2\text{Li}(\text{TMEDA})$  4, and  $(\text{Cy}_2\text{N})_2\text{Ti}(\mu\text{-Cl})_2\text{Li}(\text{TMEDA})$  5. In both cases the products were isolated after evaporation of the solvent to dryness and recrystallization from hexane at  $-30^\circ\text{C}$ . One molecule of TMEDA was found connected to Li suggesting that the role of this chelating amine may only be a minor one. Although, there is no apparent interaction of TMEDA with titanium, its role during the formation of 4 and 5 is crucial for the stabilization of the final complex. In fact, reactions carried out in absence of TMEDA gave only oily products which were not suitable for further characterization. The IR spectrum of both 4 and 5 confirmed the presence of TMEDA by absorption bands in the region  $1064\text{-}934\text{cm}^{-1}$  and at  $790, 770\text{ cm}^{-1}$  (complex 4), and in the region  $1063\text{-}950\text{ cm}^{-1}$  and at  $789, 773\text{ cm}^{-1}$  (complex 5). Complex 4 tested positive for both Li and Cl.

The molecular structure of 5 as demonstrated by X-ray analysis is shown in Fig. 3.3. The tetrahedral geometry of titanium metal center ( $\text{N3-Ti1-N4}=120.5(2)$ ;  $\text{Cl2-Ti1-N4}=116.9(1)$ ;  $\text{Cl1-Ti1-N3}=107.5(1)^\circ$ ) is comprised by two dicyclohexylamido ligands ( $\text{Ti1-N4}=1.917(4)$ ;  $\text{Ti1-N3}=1.906(4)\text{\AA}$ ) and bridging chlorides.

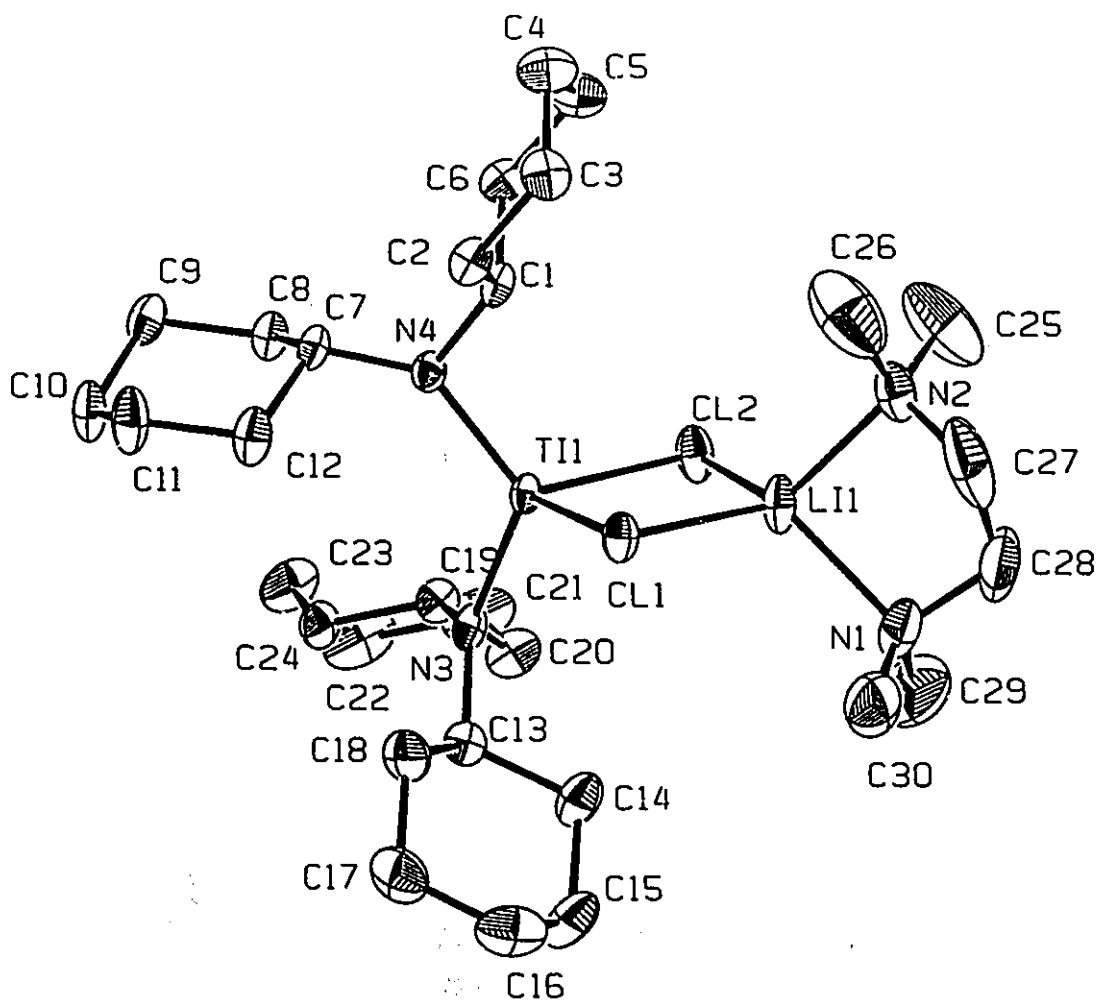
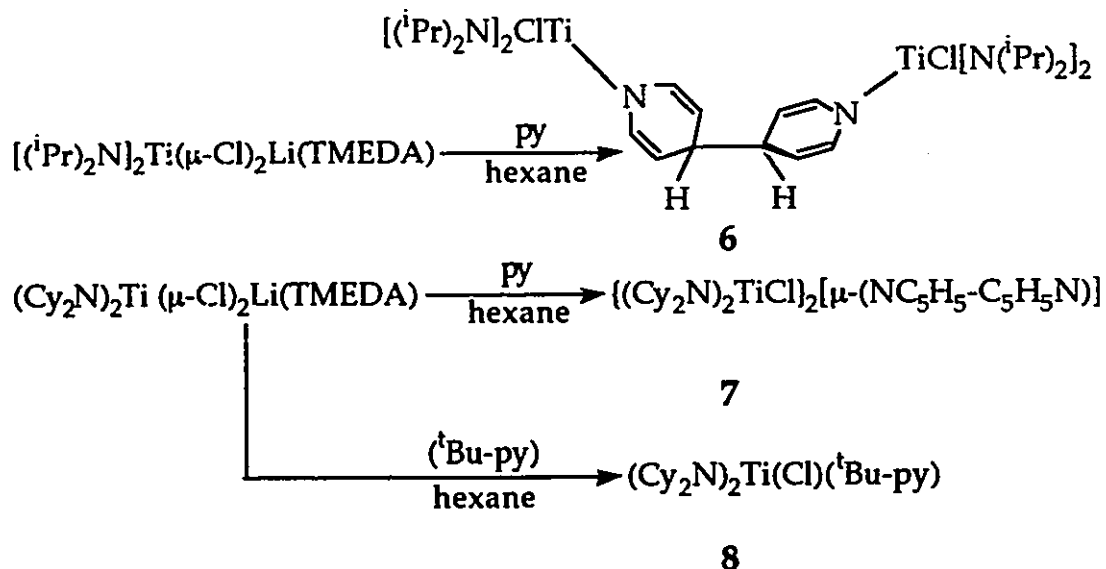


**FIG. 3.3** ORTEP drawing of 5. Bond distances (Å) and angles (deg) are as follows: Ti1-C11=2.436(2), Ti1-C12=2.415(2), Ti1-N3=1.906(4), Ti1-N4=1.917(4), Cl1-Li1=2.35(1), Cl2-Li1=2.31(1), N1-Li1=2.09(1), N3-C13=1.465(7), N4-C1=1.468(6), Cl1-Ti1-C12=93.18(5), Cl1-Ti1-N3=107.5(1), Cl2-Ti1-N3=107.4(1), Cl2-Ti1-N4=116.9(1), N3-Ti1-N4=120.5(2), Ti1-Cl1-Li1=83.5(2), Ti1-N3-C13=137.2(3), Ti1-N4-C1=106.2(3)

The Ti-( $\mu$ -Cl)<sub>2</sub>-Li core is almost planar (Ti1-Cl1-Li1-Cl2=2.5(3)<sup>o</sup>) with the titanium-chloride distances (Ti1-Cl1=2.436(2); Ti1-Cl2=2.145(2)Å). The cyclohexyl groups are in the expected chair conformation.

The structural difference between complexes 3 and 5 is somewhat puzzling. The molecular structure of 3 is composed by two separated  $\{[(\text{Me}_3\text{Si})_2\text{N}]_2\text{TiCl}_2\}^-$  and  $[\text{Li}(\text{TMEDA})_2]^+$  ionic fragments, while the molecular structure of 5 showed that the two fragments are connected into a unique structure of  $(\text{Cy}_2\text{N})_2\text{Ti}(\mu\text{-Cl})_2\text{Li}(\text{TMEDA})$  via Cl-bridges. Although at this stage there is no definitive explanation, we believe that this difference could be ascribed to a further delocalization of the Ti-N  $\pi$ -bond into the Si atom *d* orbitals. Such interaction may result into an overall electron withdrawing effect from the two chlorine atoms toward the amido groups. As a result, the two chlorine atoms become less basic and therefore less competitive with respect to an additional molecule of TMEDA for the coordination of the Li(TMEDA) cation.

The heterobimetallic structure of 3 may be cleaved via coordination of THF or py, forming the corresponding  $[(\text{Me}_3\text{Si})_2\text{N}]_2\text{TiCIL}$  (L=THF, py).<sup>24</sup> With the aim of obtaining similar result in the case of 4 and 5, the reactions of  $(\text{R}_2\text{N})_2\text{Ti}(\mu\text{-Cl})_2\text{Li}(\text{TMEDA})$  (R=<sup>i</sup>Pr 4, Cy 5) with py in hexane were carried out (Scheme 3.2). Unexpectedly, the reaction turned out to be an unprecedented tail-to-tail reversible coupling of pyridine.



**SCHEME 3.2** Reactivity of  $(\text{R}_2\text{N})_2\text{Ti}(\mu\text{-Cl})_2\text{Li}(\text{TMEDA})$  ( $\text{R}=\text{}^i\text{Pr}$  4, Cy 5)

Addition of 1 eq of py to a forest green solution of  $[{}^i\text{Pr}_2\text{N}]_2\text{Ti}(\mu\text{-Cl})_2\text{Li}(\text{TMEDA})$  4 caused the color to change rapidly to ink-blue and within a few minutes to emerald green with formation of white precipitate which was removed by filtration. The emerald green solution slowly turned red-brown upon cooling to  $-30^\circ\text{C}$ . Upon standing two days at low temperature, orange-red crystals of diamagnetic  $\{[{}^i\text{Pr}_2\text{N}]\text{TiCl}\}_2[\mu\text{-(NC}_5\text{H}_5\text{-C}_5\text{H}_5\text{N)}]$  6 were obtained. The presence of quinoid function in complex 6 is confirmed by the absorption bands at  $1655\text{ cm}^{-1}$  and at  $1591\text{ cm}^{-1}$  in the infrared spectrum. Complex 6 is diamagnetic in solid state, but when dissolved in hexane at room temperature, gave a paramagnetic emerald green solution. The process appeared to be reversible, since the green solution again turned red-brown upon cooling and red crystals of 6 separated upon standing at low temperature. EPR spectra of the green

solution of 6 showed the typical band ( $g=1.9660$ ) characteristic for  $d^1$  electronic configuration, without hyperfine structure.

The chemical connectivity of 6 was elucidated by an X-ray analysis (Fig. 3.4). Complex 6 is dimeric with two  $(iPr_2N)_2TiCl$  units connected by a 4,4'-dihydro- $\gamma,\gamma'$ -dipyridyl with each N atom binding one Ti center. The geometry of the two metal centers is almost tetrahedral ( $Cl_2-Ti_1-N_4=108.1(1)$ ;  $Cl_2-Ti_1-N_5=109.8(1)$ ;  $Cl_2-Ti_1-N_6=114.0(1)$ ;  $Cl_1-Ti_2-N_1=114.9(1)$ ;  $Cl_1-Ti_1-N_2=107.0(1)^\circ$ ), and is defined by one chlorine atom, two amido groups and the N atom of the dipyriddy. The titanium-chlorine and titanium-nitrogen distances are rather normal and compare well with those of the other complexes reported in this work ( $Ti_1-Cl_2=2.3069(1)$ ;  $Ti_1-N_5=1.875(4)$ ;  $Ti_1-N_6=1.875(4)\text{\AA}$ ). The dipyriddy molecule connecting the two metal centers is originated by the formal tail-to-tail reductive coupling of two molecules of pyridine. The good quality of the crystal structure allowed us to locate and refine the H atom positions. The pyridine *para*-carbon atoms are tetrahedral. The dipyriddy nitrogen atom is trigonal planar, and forms rather short Ti-N distances ( $Ti_1-N_4=1.946(4)$ ;  $Ti_2-N_3=1.944(4)\text{\AA}$ ) which, similar to the case of amido groups, indicates a significant extent of Ti-N double bond character. The C-C bond between the two pyridine rings ( $C15-C32=1.572(6)\text{\AA}$ ), is as expected for a C-C single bond.

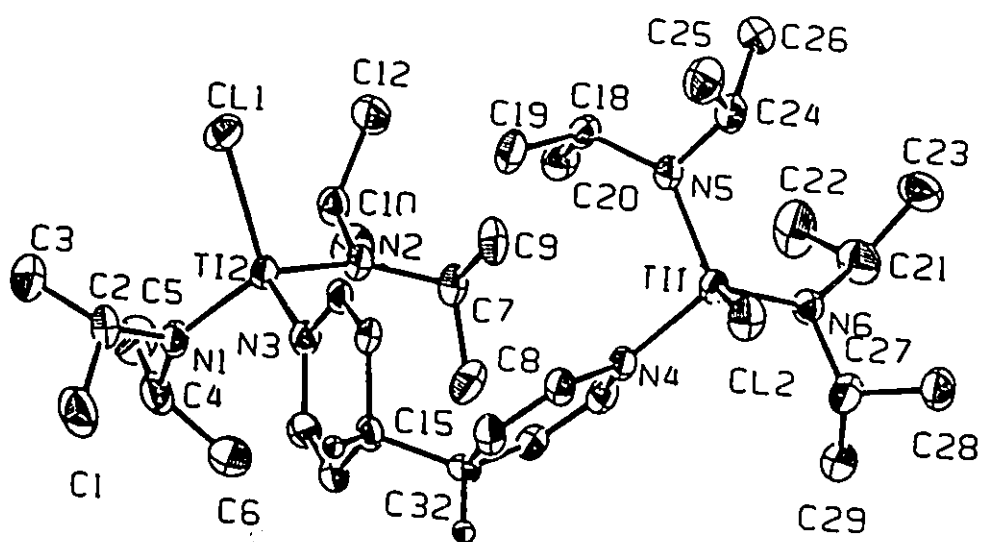
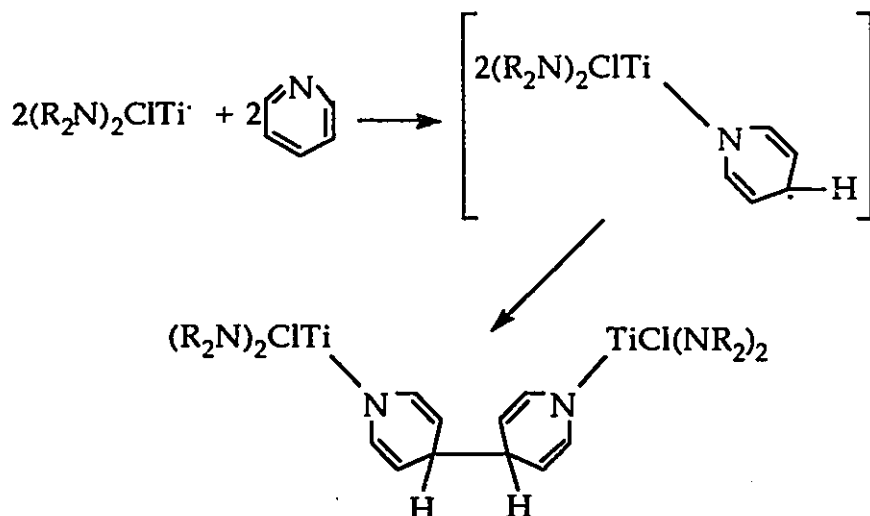


FIG. 3.4 ORTEP drawing of 6. Bond distances (Å) and angles (deg) are as follows: Ti1-Cl2=2.306(1), Ti1-N4=1.946(4), Ti1-N5=1.874(4), Ti1-N6=1.875(4), Ti2-N1=1.883(4), Ti2-N2=1.874(4), Ti1-N3=1.944(4), C15-C32=1.572(6), C15-H31=0.961, C32-H64=0.967, Cl2-Ti1-N4=108.1(1), Cl2-Ti1-N5=109.8(1), N4-Ti1-N5=105.6(2), N5-Ti1-N6=112.9(2), Cl1-Ti2-N1=114.9(1), Cl1-Ti2-N2=107.0(1), N1-Ti2-N2=113.8(2), N1-Ti2-N3=104.4, N2-Ti2-N3=106.2(2)

A very similar reaction was observed in the case of  $(\text{Cy}_2\text{N})_2\text{Ti}(\mu\text{-Cl})_2\text{Li}(\text{TMEDA})$  5. Again, the reaction immediately gave a blue color which subsequently turned green and at low temperature become brown-red. Red-orange crystal of  $\{(\text{Cy}_2\text{N})_2\text{TiCl}\}_2[\mu\text{-(NC}_5\text{H}_5\text{-C}_5\text{H}_5\text{N)}]$  7 separated upon standing one day at this low-temperature. As in the case of complex 6, the change of the color from emerald green at room temperature to brown-red at low-temperature appeared to be reversible. Although, in this case we were not able to grow single crystals of suitable size, compound 7 might reasonably be expected to be isostructural with 6. The infrared spectrum shows in fact the similar absorption bands at  $1695\text{ cm}^{-1}$  and  $1580\text{ cm}^{-1}$  ascribed to the quinoid-like ring. Magnetic susceptibility measurement of 7 in the solid state showed diamagnetic behavior, while the EPR spectrum of a toluene solution confirmed the presence of  $d^1$  Ti(III) species with  $g=1.9677$ .

The  $d^1$  electronic configuration of Ti(III) is responsible for the reductive coupling of the two pyridine molecules, probably involving pyridine radical anions as intermediates. The formation of 6 and 7 clearly indicates that the unpaired electron has been localized on the pyridine *para*-carbon atom, thus forming a radical which achieves the most obvious stabilization through formation of a C-C bond. In this process, Ti(III) is oxidized to Ti(IV) (Scheme 3.3). Although the pyridine molecule loses its aromaticity as a result of the reduction, a further stabilization is probably provided by both the quinoid electronic configuration, and the stabilization energy of the ene-amido function.



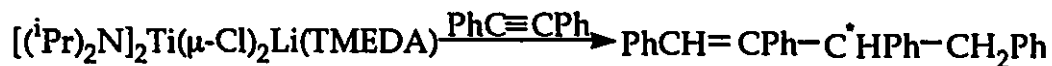
**SCHEME 3.3** Reductive Coupling of Pyridine (R=iPr, Cy)

Although the reductive coupling of pyridine has been presented in the chemistry of hexacarbonylvanadate (-I),<sup>98</sup> the complexes 6 and 7 provides the first example, where the formation of C-C bond between the two rings can actually be reversed. In fact, the reversible color change of 6 and 7 from emerald green at room temperature, to brown-red at  $-30^\circ\text{C}$  suggests the existence of a chemical equilibrium between the diamagnetic dimer in the solid state and the paramagnetic monomeric structure in solution. A suggestion about possible structure of the paramagnetic complex formed by 7 in hexane solution, was provided by the reaction of  $(\text{Cy}_2\text{N})_2\text{Ti}(\mu\text{-Cl})_2\text{Li}(\text{TMEDA})$  5 with *para*-substituted pyridine. The reaction of  $(\text{Cy}_2\text{N})_2\text{Ti}(\mu\text{-Cl})_2\text{Li}(\text{TMEDA})$  with 4-(<sup>t</sup>Bu)py gave the blue crystalline complex  $(\text{Cy}_2\text{N})_2\text{Ti}(\text{Cl})(^t\text{Bu-py})$  8 in good yield. The magnetic moment of 8 ( $1.82\mu_B$ ), measured in solid state, is in agreement with the  $d^1$  electronic configuration of monomeric Ti(III). The characteristic bands observed at  $1606\text{ cm}^{-1}$ ,  $1532\text{ cm}^{-1}$  in the IR spectrum are diagnostic for the presence of an aromatic ring. The

IR spectrum are diagnostic for the presence of an aromatic ring. The magnetic and spectroscopic data of 8, together with the elemental analysis formulated the compound as  $(\text{Cy}_2\text{N})_2\text{Ti}(\text{Cl})(^t\text{Bu-py})$ .

This unexpected performance of Ti(III) diisopropyl and dicyclohexyl amido complexes, prompted us to investigate similar reactions with other substrates, which may possibly act as one electron acceptors. The use of low-valent titanium derivatives in metal-promoted organic synthesis, discussed in the introduction, mainly relies on the ability of these systems to promote C-C bond formation.<sup>1,8,9</sup> For example, the reaction of alkynes with group IV  $d^2$  transition metal complexes gives reductive coupling of a wide variety of alkynes forming metallacyclopentadiene species.<sup>1</sup> However, to the best of our knowledge, there are no reports describing reactivity of  $d^1$  Ti(III) systems with alkynes. Therefore, given the performance of 4 and 5 with py, we have probed the reactivity of these Ti(III) systems with alkynes.

Reaction of  $[(^i\text{Pr})_2\text{N}]_2\text{Ti}(\mu\text{-Cl})_2\text{Li}(\text{TMEDA})$  4 with  $\text{PhCCPh}$  in hexane afforded a colorless diamagnetic product which crystallized out in good yield upon standing overnight at room temperature (Eq. 3.1).



9

## 3.1

The color, solubility properties and air- and thermal stability (m.p.  $146^\circ\text{C}$ ) suggested that this compound might be an organic product. The identity of the compound was revealed by full spectroscopic characterization. The IR spectrum showed an absorption band at  $1596$

$\text{cm}^{-1}$  and a shoulder at  $1486 \text{ cm}^{-1}$ , suggesting the presence of aromatic  $\text{C}=\text{C}$  bonds. Mass spectrometry of compound 9 (Fig. 3.5), showed the parent peak at 360. The fragmentation pattern showed loss of benzylic (M-91) and benzene fragments (M-78). These data suggest that the organic product could be formed by the reductive coupling of two molecules of  $\text{PhCCPh}$ .

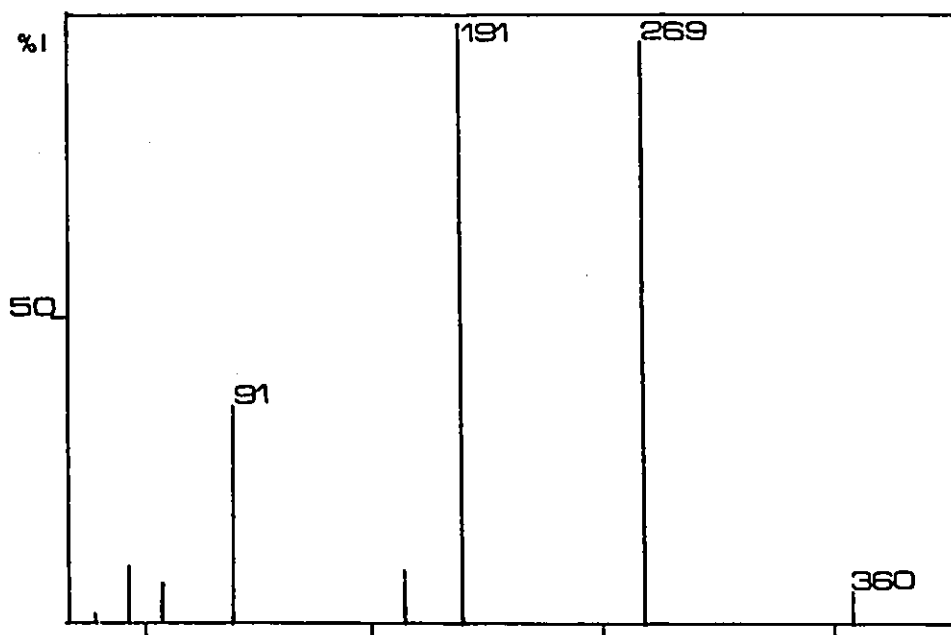


FIG. 3.5 Mass Spectrum of 1,2,3,4-tetraphenyl-1-butene

The  $^1\text{H}$ - and  $^{13}\text{C}$ -NMR (Fig. 3.6 and 3.7) identified the compound as 1,2,3,4-tetraphenyl-1-butene. The  $^1\text{H}$ -NMR consists of one multiplet at 7.3-6.6 ppm, as expected for the presence of the phenyl ring protons. An olefinic proton  $\text{HC}=\text{C}$  appears as a singlet at 6.5 ppm. One triplet centered at 4.03 ppm  $|^3J_{\text{XA}}=9.6\text{Hz}|$ ,  $|^3J_{\text{XB}}=6.4\text{Hz}|$  and two double doublets at 3.32 ppm  $|^2J_{\text{AB}}=12.8\text{Hz}|$ ,  $|^3J_{\text{AX}}=9.6\text{Hz}|$  and 3.16 ppm  $|^3J_{\text{BX}}=6.4\text{Hz}|$  are as expected for the ABX system of  $-\text{C}^*\text{H}_\text{X}\text{Ph}-$

$\text{CH}_A\text{H}_B\text{Ph}$ . The presence of this fragment is also consistent with the fragmentation pattern of the mass spectrum. All the signals integrated satisfactorily.

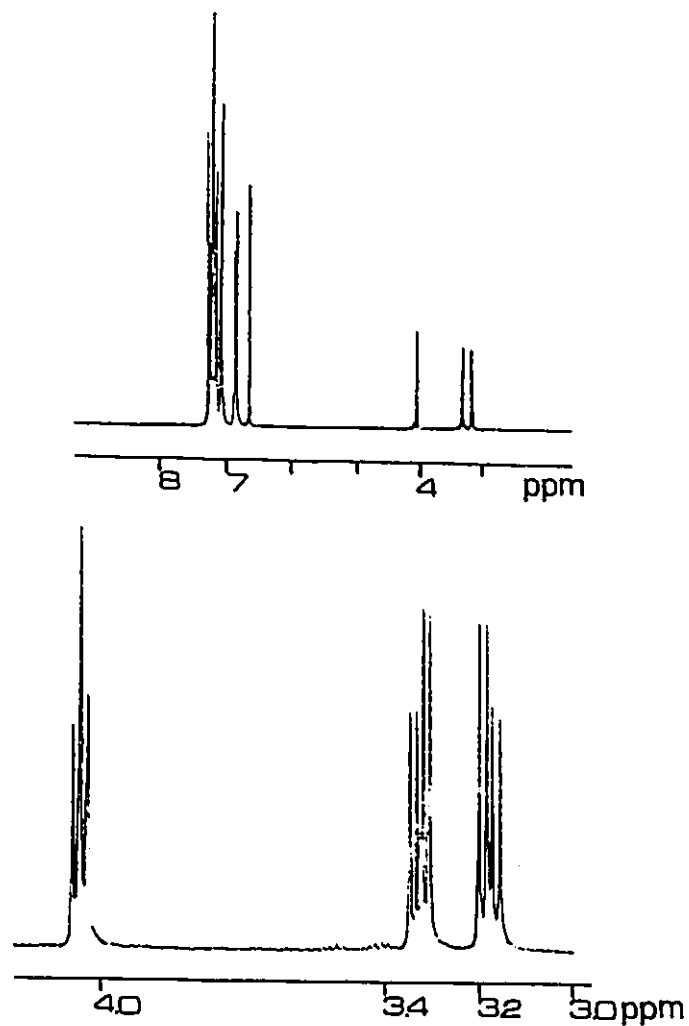


FIG. 3.6  $^1\text{H}$ -NMR Spectrum of 1,2,3,4-tetraphenyl-1-butene

The DEPT  $^{13}\text{C}$ -NMR spectrum showed the  $\text{CH}$  resonance at 55 ppm,  $\text{CH}_2$  at 39 ppm, and the multiplet of aromatic carbons and olefinic carbon  $=\text{CH}$  at 127 ppm.

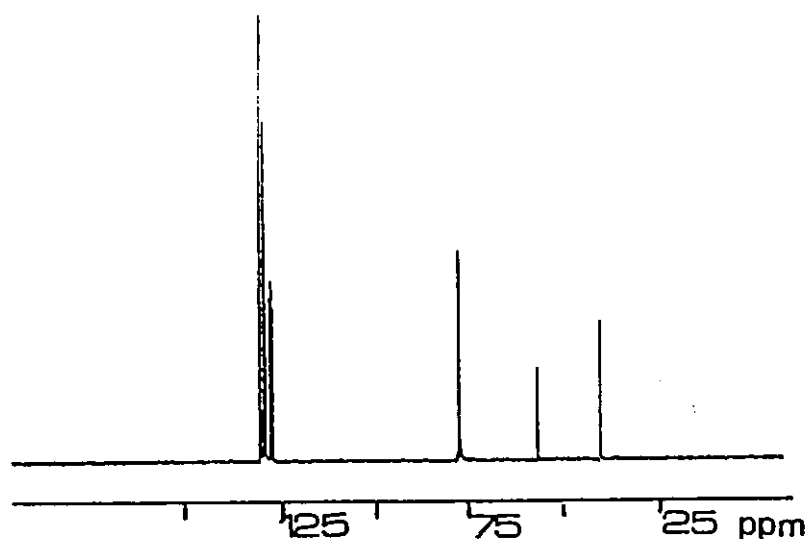


FIG. 3.7  $^{13}\text{C}$ -NMR of 1,2,3,4-tetraphenyl-1-butene

The formation of 1,2,3,4-tetraphenyl-1-butene **9**, promoted by **4** is the result of two separate processes. The formation of C-C bond indicates a two electron transfer operated by two metal centers on the two molecules of alkynes. The consequent formation of carbon radicals and subsequent coupling to form the C-C bond is in line with the finding in the case of pyridine. However, in the present case an additional transfer of two molecules of  $\text{H}_2$  occurred (Scheme 3.4).

Recent results obtained in our laboratory have shown the unprecedented ability of the  $(i\text{Pr})_2\text{N}$  moiety to eliminate three atoms of H to form metallacyclobutane ring connected to an external  $\text{C}=\text{CH}_2$  function (Fig. 3.8).<sup>99</sup> These results indicate that alkylic amido moieties have the possibility to function as hydrogen reservoir.

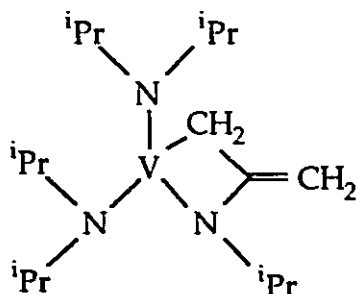
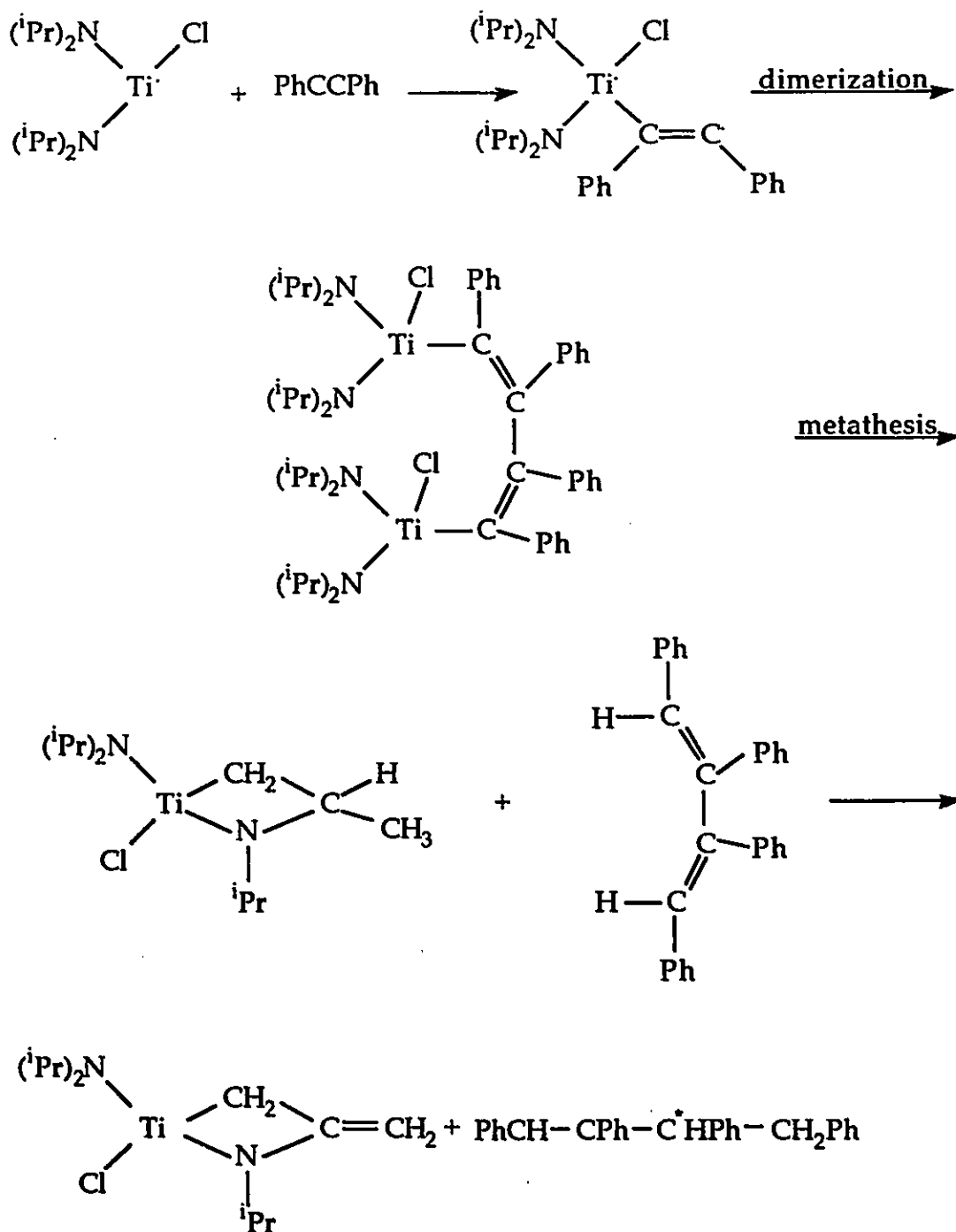


FIG. 3.8 V-metallacyclobutane Species

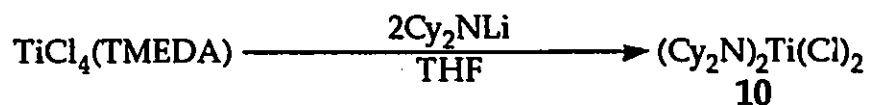
At this stage, it is difficult to demonstrate that the source of hydrogen for the formation of 9 was the amido ligand, since the fate of the titanium moiety remains unclear. Unfortunately, attempts to isolate the residual Ti complex failed. However, the NMR spectrum of the diamagnetic reaction mixture clearly showed a rather intense olefinic resonance at 6.8 ppm. Therefore, assuming that a transformation similar to that observed in V chemistry occurred in the case of titanium complex, we tentatively suggest the mechanistic pathway described in Scheme 3.4.

The electron-transfer from Ti to alkyne and consequent reductive-coupling is probably the starting point of the reaction. The reaction is expected to yield a tetraphenylbutadienyl complex, either mono- or dimetallic. The next steps possibly consist of a metathetic reaction between the Ti-C(alkyne) bond with the CH<sub>3</sub> bond of the amido function to eliminate tetraphenyl-1,4-butadiene forming the metallacyclobutenyl function. At this stage partial hydrogenation of the butadiene occurs by transferring one molecule of hydrogen from the metallacycle to the substrate forming the final organic product 9 and the metallacycle-ene Ti derivative.



SCHEME 3.4 Proposed Mechanistic Pathway for the Reaction 3.1

Although diverting from the main goal of studying the chemistry of low-valent titanium-amides, we have also examined the chemistry of similar Ti(IV) compound. The possibility to form heterometallacyclobutene rings, their analogy with the metallacyclobutane species for which a remarkable reactivity has been shown,<sup>39</sup> prompted us to test the preparation of suitable Ti(IV) amido precursors. The most convenient precursor for this purpose was obviously (iPr<sub>2</sub>N)<sub>2</sub>Ti(Cl)<sub>2</sub>. Unfortunately, repeated attempts to prepare this complex by modifying the reaction conditions gave only intractable oily materials. Conversely, the reaction of TiCl<sub>4</sub>(TMEDA) with 2 eq of Cy<sub>2</sub>NLi yielded dark orange diamagnetic crystals of (Cy<sub>2</sub>N)<sub>2</sub>Ti(Cl)<sub>2</sub> **10** (Eq. 3.2).



### 3.2

The molecular structure is shown in Fig. 3.9. The titanium metal center is placed in the center of a distorted tetrahedron (Cl1-Ti1-Cl2=110.07(4); Cl1-Ti1-N1=108.69(7); Cl1-Ti1-N2=109.08(7); Cl2-Ti1-N1=107.43(7); Cl2-Ti1-N2=115.7(1); N1-Ti1-N2=115.7(1)°). The Ti-Cl distances are as expected (Ti1-Cl1=2.2801(9); Ti1-Cl2=2.2566(9)Å). The very short titanium-nitrogen distances (Ti1-N1=1.862(2); Ti1-N2=1.865(2)Å) suggest, together with the trigonal planar coordination geometry of the nitrogen atom, the presence of a Ti-N π-bond character.

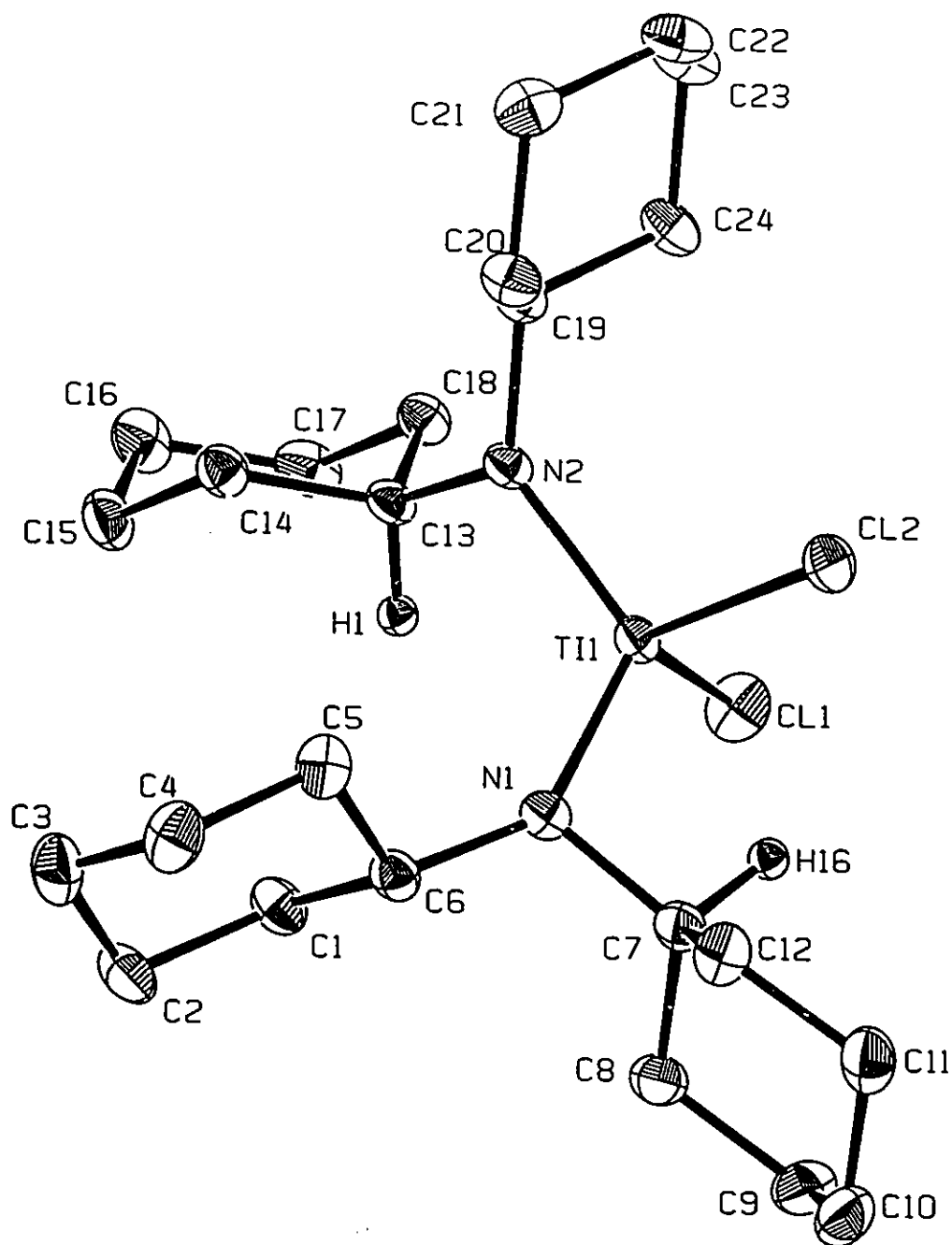
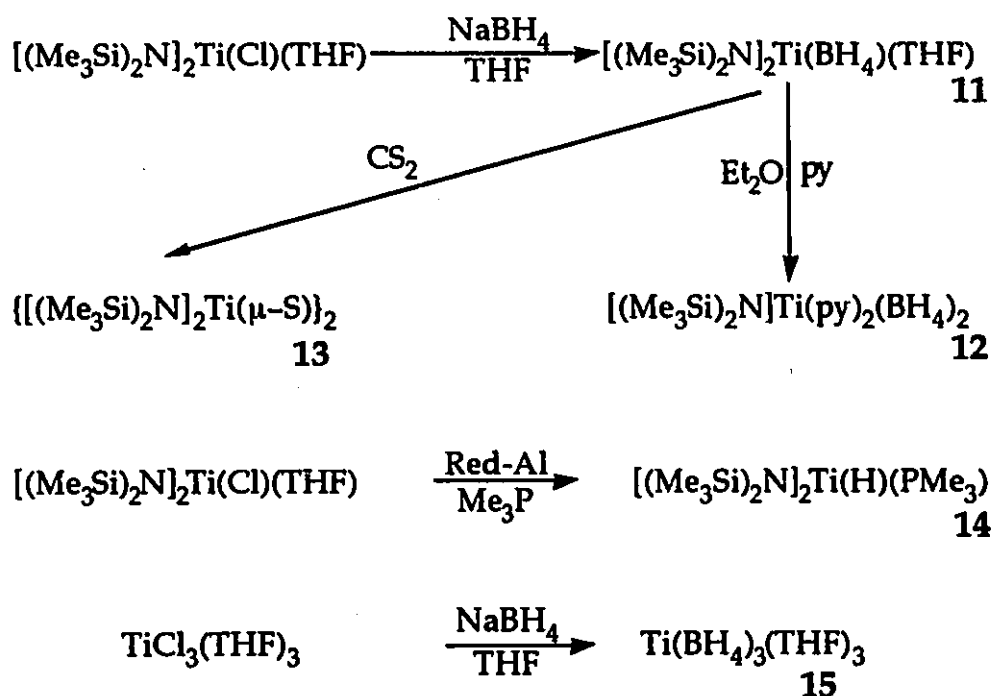


**FIG. 3.9** ORTEP drawing of 10. Bond distances (Å) and angles (deg) are as follows: Ti1-Cl1=2.2801(9), Ti1-Cl2=2.2566(9), Ti1-N1=1.862(2), Ti1-N2=1.865(2), N1-C6=1.476(3), N1-C7=1.490(3), Cl1-Ti1-Cl2=110.07(4), Cl1-Ti1-N1=108.69(7), Cl1-Ti1-N2=109.08(7), Cl2-Ti1-N1=107.43(7), Cl2-Ti1-N2=105.80(7), N1-Ti1-N2=115.7(1)

### 3.2 Titanium Hydrides and Borohydrides.

Although a considerable reactivity has been described for titanium hydride and borohydride complexes, these species remain poorly known. We have therefore attempted the preparation of these species by using Ti(III) bisamido complexes 1, 4 and 5. Their sterically demanding anionic ligands may protect and stabilize the hydride function.

The most convenient preparation of hydrides and borohydrides was achieved via chloride replacement reactions carried out using  $[(\text{Me}_3\text{Si})_2\text{N}]_2\text{Ti}(\text{Cl})(\text{THF})$  1, and  $\text{TiCl}_3\text{THF}_3$  as starting materials (Scheme 3.5).



**SCHEME 3.5** Synthesis of Ti(III) Borohydrides

The reaction of  $[(\text{Me}_3\text{Si})_2\text{N}]_2\text{Ti}(\text{Cl})(\text{THF})$  **1** with an excess of  $\text{NaBH}_4$  in THF formed a green suspension. The paramagnetic  $[(\text{Me}_3\text{Si})_2\text{N}]_2\text{Ti}(\text{BH}_4)(\text{THF})$  **11** ( $1.81\mu\text{g}$ ) was obtained after evaporation and recrystallization from hexane upon cooling to  $-30^\circ\text{C}$ . The infrared spectrum shows the absorption bands of the  $\text{BH}_4$  moiety (Fig. 3.10) as a sharp doublet at  $2440\text{-}2400\text{ cm}^{-1}$ , and two bands at  $2270$  and  $2195\text{ cm}^{-1}$ . These data are consistent with those of other titanium borohydride species reported in the literature.<sup>70</sup>

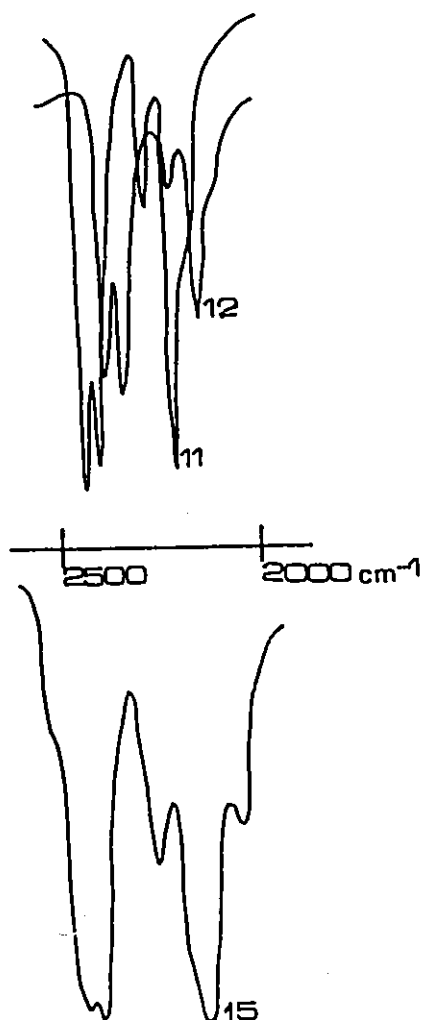
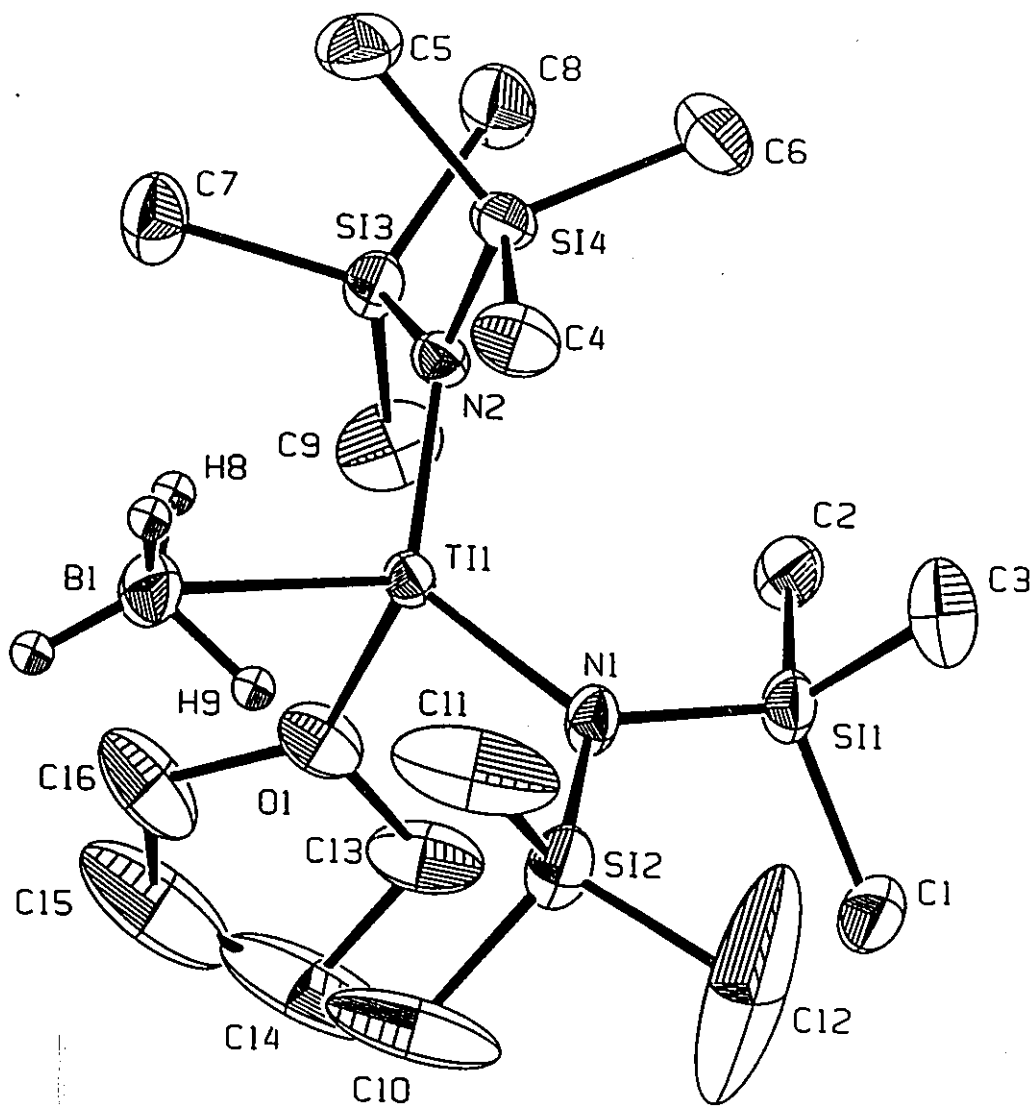


FIG. 3.10 Characteristic Absorption Bands of  $\text{BH}_4$  ligand in **11**, **12**, and **15**

The molecular structure of complex 11 was determined by X-ray analysis (Fig. 3.11). The distorted tetrahedral coordination geometry around titanium is defined by two amido groups, one  $\text{BH}_4$  ligand, and one molecule of THF ( $\text{O1-Ti1-N1}=98.0(1)$ ;  $\text{O1-Ti1-N2}=109.9(1)$ ;  $\text{O1-Ti1-B1}=91.8(1)$ ;  $\text{N1-Ti1-N2}=123.3(1)$ ;  $\text{N1-Ti1-B1}=116.9(1)$ ;  $\text{N2-Ti1-B1}=110.6(1)^\circ$ ). The distortion is likely to be caused by the large steric hindrance of the bulky amide ligands. The titanium nitrogen distances ( $\text{Ti1-N1}=1.971(3)$ ;  $\text{Ti1-N2}=1.949(3)\text{\AA}$ ) are comparable to those of the other complexes reported in this work. The quality of the crystal structure was sufficient to successfully locate and refine the H atom positions thus clarifying the bonding mode of the  $\text{BH}_4$  group. The  $\text{BH}_4$  ligand is connected to the titanium center in a  $\eta^2$  fashion by two bridged hydrogen atoms ( $\text{Ti1-H9}=2.08$ ;  $\text{Ti1-H8}=2.13\text{\AA}$ ) forming a  $\text{TiH}_2\text{B}$  planar core. These Ti-H distances are normal and compare well with those of other titanium(III)  $\text{BH}_4$  complexes.<sup>75</sup> The angles subtended by boron and titanium at the bridging hydrogen moiety are rather narrow ( $\text{Ti1-H8-B1}=54(1)$ ;  $\text{Ti1-H9-B2}=55(2)^\circ$ ).

The fact that  $\text{BH}_4$  derivatives of Ti and Zr have been successfully used for the preparation of terminal hydrides,<sup>68</sup> prompted us to attempt, by using similar reactions,  $\text{BH}_3$  abstraction from 11 to prepare amido-stabilized low-valent Ti-hydrides. A very high reactivity may be in fact anticipated for these species. Reaction of 11 with a Lewis base such as pyridine gave a surprising redistribution of ligands, forming complex 12. Deep-red crystals of  $[(\text{Me}_3\text{Si})_2\text{N}]\text{Ti}(\text{py})_2(\text{BH}_4)_2$  12, were obtained after evaporation and recrystallization from hexane at  $-30^\circ\text{C}$ .



**FIG. 3.11** ORTEP drawing of 11. Bond distances (Å) and angles (deg) are as follows: Ti1-O1=2.075(2), Ti1-N1=1.971(3), Ti1-N2=1.949(3), Ti1-B1=2.454(4), B1-H9=1.18(3), B1-H8=1.13(4), Ti1-H9=2.08, Ti1-H8=2.13, N1-Si1=1.753(3), O1-Ti1-N1=98.0(1), O1-Ti1-N2=109.9(1), O1-Ti1-B1=91.8(1), N1-Ti1-N2=123.3(1), N1-Ti1-B1=116.9(1), N2-Ti1-B1=110.6(1)

Similar reactions with TMEDA or  $\text{PMe}_3$  gave only intractable materials. The magnetic moment of 12 ( $\mu_{\text{eff}}=1.8\mu_{\text{B}}$ ) is as expected for a  $d^1$  electronic configuration of Ti(III). The presence of  $\text{BH}_4^-$  was confirmed in the IR spectrum by the absorption bands at 2380, 2340, 2220 and 2140  $\text{cm}^{-1}$ , which are characteristic of bidentate  $\text{BH}_4^-$ .<sup>70</sup> Attempts to isolate and identify other components in the reaction mixture failed.

The molecular structure of complex 12 was clarified by X-ray analysis (Fig. 3.12). The geometry around the titanium metal center is distorted trigonal bipyramidal ( $\text{N1-Ti1-N2}=162.4(1)^\circ$ ;  $\text{N1-Ti1-N3}=98.0(1)^\circ$ ;  $\text{N1-Ti1-B1}=82.1(2)^\circ$ ;  $\text{N1-Ti1-B2}=91.3(2)^\circ$ ;  $\text{N2-Ti1-N3}=99.6(1)^\circ$ ). Two  $\text{BH}_4^-$  groups and the amido ligand define the equatorial plane ( $\text{N3-Ti1-B2}=115.6(2)^\circ$ ;  $\text{B2-Ti1-B1}=125.8(2)^\circ$ ;  $\text{B1-Ti1-N3}=118.6(2)^\circ$ ). Two molecules of pyridine are placed in *trans*-position with respect to each other ( $\text{N1-Ti1-N2}=162.4(1)^\circ$ ) forming rather-normal titanium-nitrogen distances ( $\text{Ti1-N1}=2.214(3)$ ;  $\text{Ti1-N2}=2.221(3)\text{\AA}$ ). Even in this case, it was possible to locate and refine the hydrogen atoms positions, thus clarifying the bonding modes of the  $\text{BH}_4^-$  groups. Similar to the case of 11, each  $\text{BH}_4^-$  is bonded to the titanium center in a  $\eta^2$  fashion ( $\text{Ti1-H12}=1.980$ ;  $\text{Ti1-H26}=1.984$ ).

Similar attempts to prepare hydride and borohydride complexes by using diisopropyl 4 or dicyclohexyl 5 Ti(III) amides were unsuccessful.

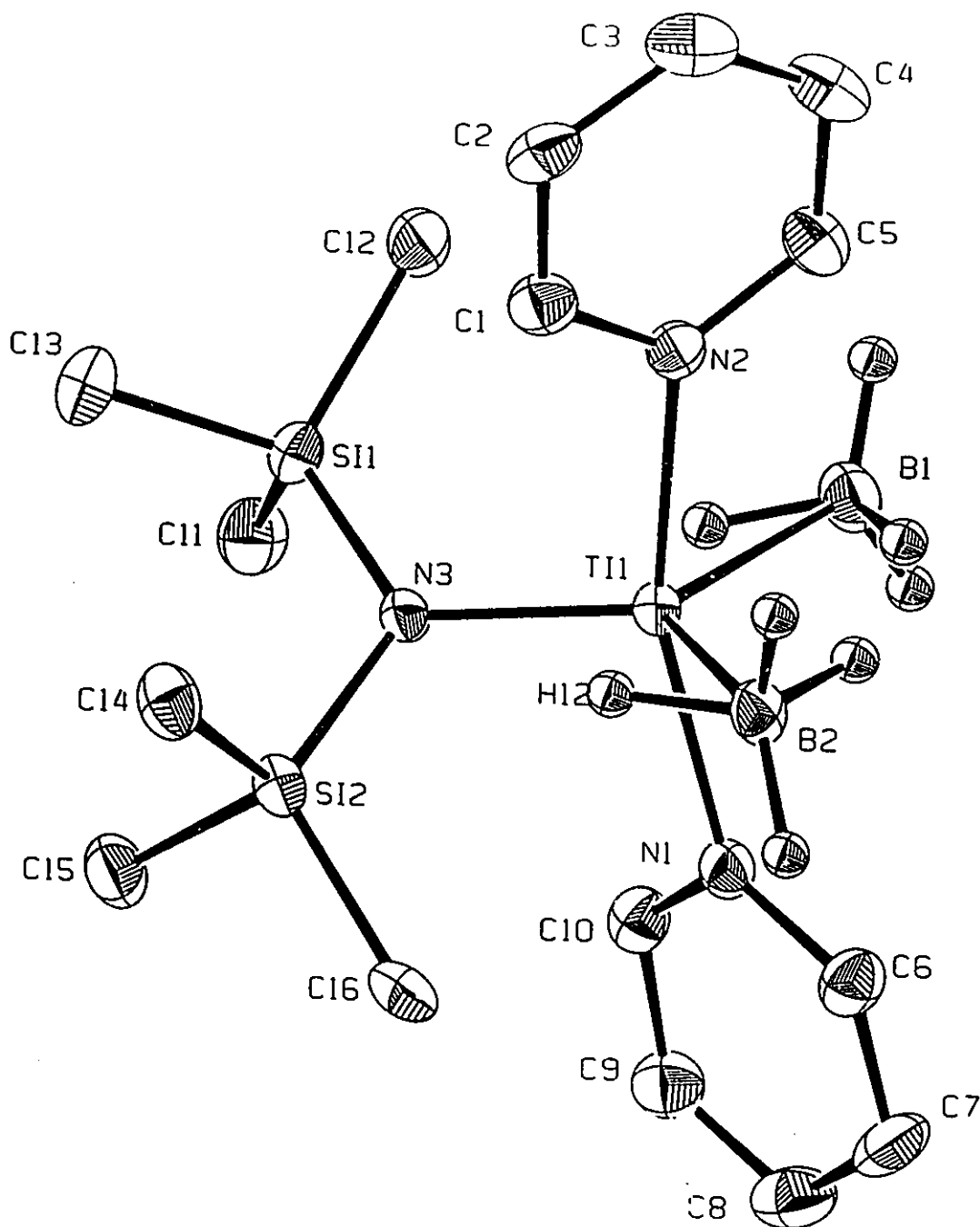


**FIG. 3.12** ORTEP drawing of 12. Bond distances (Å) and angles (deg) are as follows: Ti1-N1=2.214(3), Ti1-N2=2.221(3), Ti1-N3=1.929(3), Ti1-B1=2.476(6), Ti1-B2=2.482(5), Ti1-H26=1.989, Ti1-B25=2.059, Ti1-H12=1.982, Ti1-H13=2.033, B1-H25=1.18, B1-H26=1.11, B2-H11=1.08, N1-Ti1-N2=162.4(1), N1-Ti1-N3=98.0(1), N1-Ti1-B1=82.1(2), N1-Ti1-B2=91.3(2), N2-Ti1-N3=99.6(1), N2-Ti1-B1=90.5(2)

In order to clarify the nature of the highly reactive  $\text{Ti}(\text{BH}_4)_3$  species, Girolami used several stabilizing tertiary phosphines.<sup>75</sup> Our primary interest was to evaluate the stability of  $\text{Ti}(\text{BH}_4)_3$  in the presence of less coordinating ligands. Simple reaction of  $\text{TiCl}_3\text{THF}_3$  with  $\text{NaBH}_4$  in refluxing THF resulted into a blue-green suspension. Shiny blue crystals  $\text{Ti}(\text{BH}_4)_3(\text{THF})_3$  15, were obtained from diethylether at  $-30^\circ\text{C}$ . The magnetic measurement based on proposed formula  $\text{TiB}_3\text{O}_3\text{C}_{12}\text{H}_{36}$  showed magnetic moment of  $1.79 \mu_B$  which is in agreement with a  $d^1$  electronic configuration of  $\text{Ti}(\text{III})$ . The presence of  $\text{BH}_4$  moieties was diagnosed by the IR spectrum showing the characteristic absorption bands at 2440, 2260, 2150 and  $2050 \text{ cm}^{-1}$  (Fig. 3.10). The presence of coordinated THF is also suggested by two characteristic bands at 1130 and  $970 \text{ cm}^{-1}$ . Unfortunately, the poor crystal quality prevented X-ray structure determination.

The preparation of terminal titanium-hydrides was attempted by reacting  $[(\text{Me}_3\text{Si})_2\text{N}]_2\text{Ti}(\text{Cl})(\text{THF})$  with a variety of reagents such as  $\text{LiBH}_4$ ,  $\text{LiAlH}_4$ ,  $\text{NaHB}(\text{C}_2\text{H}_5)_3$ ,  $(n\text{Bu})_3\text{SnH}$ ,  $\text{PhSiH}_3$ ,  $\text{EtLi}$ , Red-Al, by using different stoichiometric ratios and with and without the presence of additional ligands such as TMEDA or  $\text{PMe}_3$ . The major part of these reactions gave oily intractable materials. Only the reaction with Red-Al carried out in the presence of  $\text{Me}_3\text{P}$  in toluene produced a blue microcrystalline  $[(\text{Me}_3\text{Si})_2\text{N}]_2\text{Ti}(\text{H})(\text{PMe}_3)$  14, after replacement of toluene with hexane and crystallization at  $-30^\circ\text{C}$ . The infrared spectrum showed an very intense sharp band at  $1750 \text{ cm}^{-1}$ , as expected for terminal hydrides.<sup>5c</sup> This microcrystalline product gave vigorous gas evolution when placed in contact with water. Unfortunately, the very poor yield (<5%) precluded further characterization.

Given the inability of Lewis bases to perform abstraction of  $\text{BH}_3$ , we became interested in studying the reactivity of complex 11 to see the possibility of insertion reactions. For this purpose, we examined the reactions of 11 with several cumulenes and other unsaturated molecules including trimethylsilyldiazomethane, CO, olefins and acetylenes. All these reactions yielded complicated, diamagnetic, analytically impure compounds. However, reaction of 11 with  $\text{CS}_2$  resulted in an oxidation reaction from which the diamagnetic sulfido-bridged  $\{[(\text{Me}_3\text{Si})_2\text{N}]\text{Ti}(\mu\text{-S})\}_2$  13 was the only clearly identified product. The reaction was carried out in hexane and complex 13 was isolated as red-orange crystals upon standing overnight at  $-30^\circ\text{C}$ . The  $^1\text{H-NMR}$  spectrum showed only a sharp singlet at 0.1 ppm corresponding to  $\text{Si}(\text{Me}_3)$  group. The crystal structure (Fig. 3.13) of the complex 13 has shown a dinuclear species, where two Ti atoms are bridged by two sulfur atoms forming a planar  $\text{Ti}_2\text{S}_2$  core ( $\text{S1-Ti1-S1}=94.4(1)$ ;  $\text{S1-Ti1-N1}=112.0(2)$ ;  $\text{S1-Ti2-S1}=89.7(1)$ ;  $\text{S1-Ti2-N2}=121.4(3)$ ;  $\text{Ti1-S1-Ti2}=87.99(8)^\circ$ ). The distorted tetrahedral geometry around titanium is defined by two amide and two sulfur groups. The titanium-sulfur distances are as expected ( $2.255(2)$ ;  $2.346(2)\text{\AA}$ ).

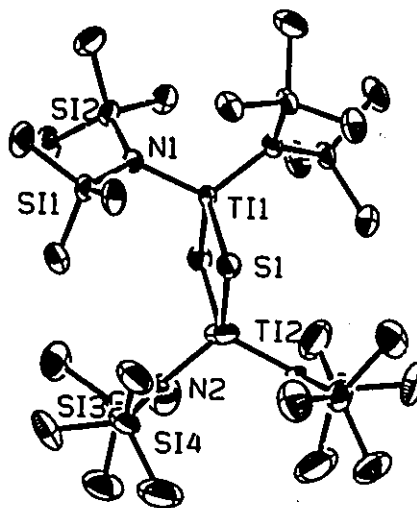


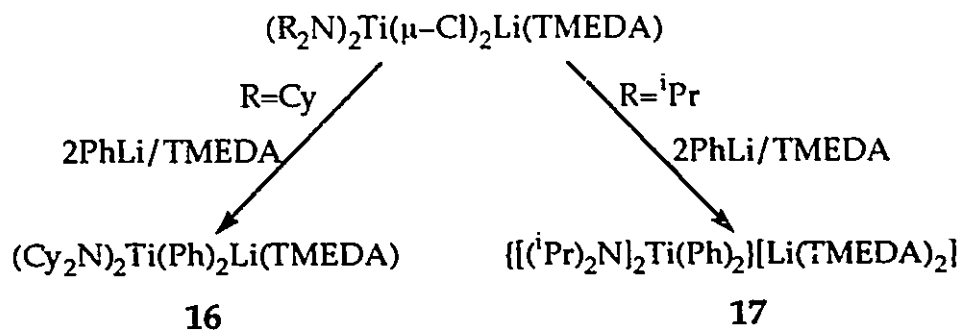
FIG. 3.13 ORTEP Drawing of 13

Although the original target to prepare and characterize terminal Ti-H hydrides has not been achieved, however, the fact that some bis(amido)titanium(III) complexes may function as a tool in the synthesis of Ti(III)-borohydrides, is a certainly significant contribution to the chemistry of this transition metal.

### 3.3 Titanium Alkyls

The electronic configuration of the amide ligands in complexes 1, 4 and 5, coupled with their large steric bulk, make these compounds promising substrates for the preparation of a novel series of low-valent Ti alkyls. Chlorine replacement reactions were attempted with different alkylating reagents such as MeLi, PhLi, NpLi, BuLi, BzLi(TMEDA), NfLi. Unfortunately, alkylation reactions carried out with 1 as the starting material were rather discouraging, since only intractable diamagnetic materials were produced in all cases. On the other hand recent results in our laboratory have shown that the methyl group of silane ligand can be easily deprotonated to form highly reactive metallacycles.<sup>100</sup> It is therefore possible that similar reactions occur in system 1, forming complicated mixtures of products.

By contrast, alkylation of  $(R_2N)_2Ti(\mu-Cl)_2Li(TMEDA)$  ( $R=iPr$  4, Cy 5) were successful. In particular the reactions with PhLi summarized in Scheme 3.6, gave good yields of crystalline compounds 16 and 17.



**SCHEME 3.6** Reactions of  $(R_2N)_2Ti(\mu-Cl)_2Li(TMEDA)$  ( $R=Cy$  5,  $iPr$  4) with PhLi

Addition of PhLi to a green solution of  $(Cy_2N)_2Ti(\mu-Cl)_2Li(TMEDA)$  in ether and in the presence of TMEDA formed a purple-red solution. Red-brown crystals of  $(Cy_2N)_2Ti(Ph)_2Li(TMEDA)$  16 separated upon standing overnight at  $-30^\circ C$ . As in the case of 4 and 5, the role of TMEDA seems rather crucial, since reactions carried out without the stoichiometric amount of TMEDA resulted only in the formation of oily intractable product, which was unsuitable for further investigation. The absorption in the IR spectrum of 16 observed at  $1551\text{ cm}^{-1}$  indicated the presence of aromatic ring, corresponding to C=C vibrational stretching. The presence of TMEDA was confirmed by absorption bands in the region  $1029-950\text{ cm}^{-1}$  and at  $788\text{ cm}^{-1}$ . In agreement with the proposed Ti(III) formulation, the magnetic susceptibility measurements gave the magnetic moment ( $\mu_{eff}=1.79\mu_B$ ), as expected for a monomeric  $d^1$  electronic configuration of Ti(III).

A similar reaction carried out with  $iPr$  derivative gave crystals of  $\{[(iPr)_2N]_2Ti(Ph)_2\}[Li(TMEDA)_2]$  17, suitable for X-ray analysis. Addition of PhLi to a forest green solution of  $[(iPr)_2N]_2Ti(\mu-Cl)_2Li(TMEDA)$  in

diethylether, rapidly turned the color to cherry-red. The color did not change upon further treatment of the solution with TMEDA. Dark red crystals of 17 were obtained upon standing at room temperature overnight. The presence of phenyl group was indicated by the IR absorptions at 1610 and 1549  $\text{cm}^{-1}$ , while the absorptions in the region 1029-946  $\text{cm}^{-1}$  and at 788  $\text{cm}^{-1}$  are assigned to the coordinated TMEDA. Complex 17 is paramagnetic with the magnetic moment ( $\mu_{\text{eff}}=1.77\mu_{\text{B}}$ ) as expected for a monomeric  $d^1$  Ti(III) species.

The molecular structure of 17 (Fig. 3.14) demonstrated by an X-ray crystal structure, showed  $\{[(i\text{Pr}_2\text{N})_2\text{Ti}(\text{Ph})_2]^-$  anion, and  $[\text{Li}(\text{TMEDA})_2]^+$  cation fragments. The titanium metal center is distorted tetrahedral with two phenyl and two amido ligands (N3-Ti1-N4=118.0(2); N3-Ti1-C1=109.6(2); N3-Ti1-C7=106.3(2); N4-Ti1-C1=105.6(2); N4-Ti1-C7=115.6(2); C1-Ti1-C7=100.2(2) $^\circ$ ). The Ti-N and Ti-C distances are normal (Ti1-N3=1.962(4); Ti-N4=1.965(4); Ti1-C1=2.173(5) and Ti1-C7=2.210(5) $\text{\AA}$ ). The tetrahedral counter cation showed a Li atom placed in the center of a regular tetrahedron defined by the four nitrogen atoms of two molecules of TMEDA.

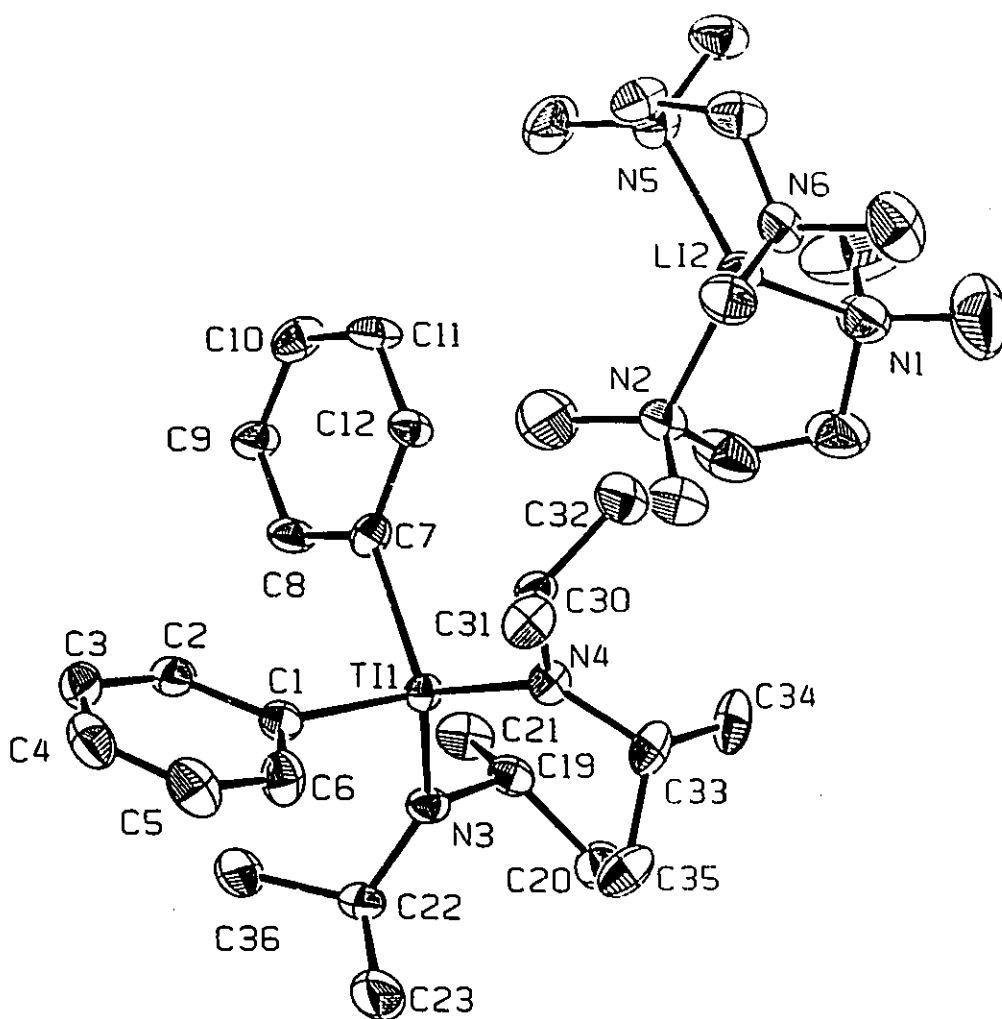
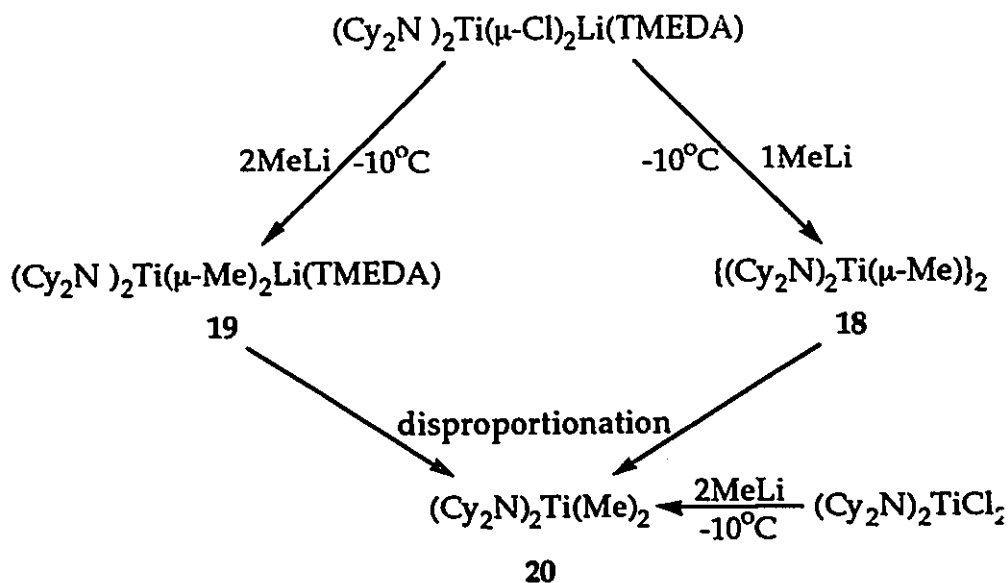


**FIG. 3.14** ORTEP drawing of 17. Bond distances (Å) and angles (deg) are as follows: Ti1-N3=1.962(4), Ti1-N4=1.965(4), Ti1-C1=2.173(5), Ti1-C7=2.210(5), N1-Li2=2.21(1), N2-Li2=2.13(1), N3-Ti1-N4=118.0(2), N3-Ti1-C1=109.6(2), N3-Ti1-C7=106.3(2), N4-Ti1-C1=105.6(2), N4-Ti1-C7=115.6(2), C1-Ti1-C7=100.2(2), C13-N1-C17=107.3(5), Ti1-N3-C19=108.8(3), Ti1-N3-C22=135.7(3), Ti1-N4-C33=134.1(3), C25-N5-Li2=101.0(4)

Depending on the stoichiometric ratio, reactions of 4 with MeLi afforded two different alkyl derivatives (Scheme 3.7).



**SCHEME 3.7**  $(\text{Cy}_2\text{N})_2\text{Ti}(\mu\text{-Cl})_2\text{Li}(\text{TMEDA})$  5 and  $(\text{Cy}_2\text{N})_2\text{TiCl}_2$  10 in the Reactions with MeLi

Addition of 1 eq of MeLi to a diethylether solution of  $(\text{Cy}_2\text{N})_2\text{Ti}(\mu\text{-Cl})_2\text{Li}(\text{TMEDA})$  at  $-10^\circ\text{C}$  led to formation of a green colored solution which turned brown at  $0^\circ\text{C}$ . Red-orange crystals of the dimeric  $\{(\text{Cy}_2\text{N})_2\text{Ti}(\mu\text{-Me})\}_2$  18 were obtained upon recrystallization from hexane, after standing a few days at room temperature.

The molecular structure of 18 was elucidated by an X-ray analysis and is shown in Fig. 3.15. The complex is dimeric with two inequivalent  $(\text{Cy}_2\text{N})_2\text{Ti}$  moieties bridged by two methyl groups. The rather short Ti-Ti distance ( $\text{Ti1-Ti2}=2.935(2)\text{\AA}$ ) of the planar  $\text{Ti}_2\text{C}_2$  core

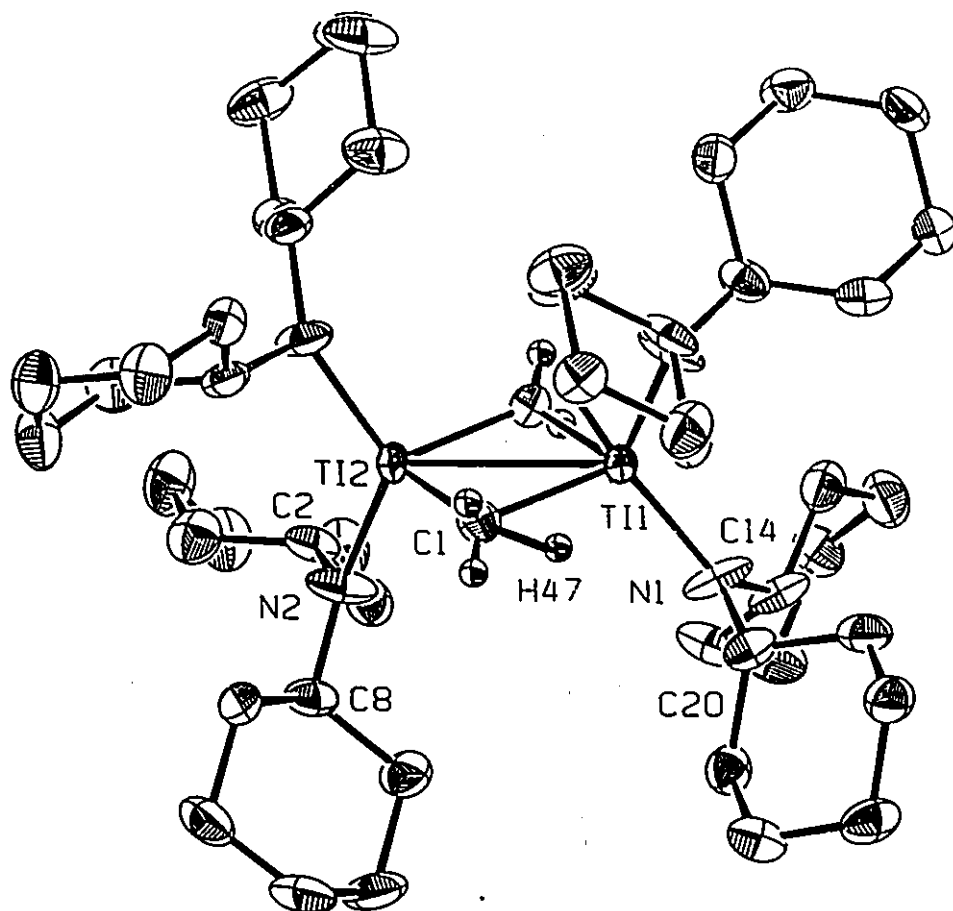


**FIG. 3.15** ORTEP drawing of 18. Bond distances ( $\text{\AA}$ ) and angles (deg) are as follows:  $\text{Ti1-Ti2}=2.935(2)$ ,  $\text{Ti1-N1}=1.937(4)$ ,  $\text{Ti1-Cl1}=2.025(6)$ ,  $\text{Ti2-N21}=1.94(4)$ ,  $\text{Ti2-C1}=2.009(6)$ ,  $\text{Ti1-H47}=1.291$ ,  $\text{C1-H45}=0.96(6)$ ,  $\text{C1-H46}=0.75(7)$ ,  $\text{C1-H47}=1.284$ ,  $\text{Ti2-Ti1-N1}=119.1(2)$ ,  $\text{Ti2-Ti1-C1}=43.1(2)$ ,  $\text{N1-Ti1-N1}'=121.8(3)$ ,  $\text{N1-Ti1-C1}=113.3(2)$ ,  $\text{Ti1-Ti2-N2}=118.1(2)$ ,  $\text{N2-Ti2-N2}'=123.7(3)$ ,  $\text{Ti1-C1-Ti2}=93.4(2)$

(Ti1-Ti2-C1=43.1(2); Ti1-C1-Ti2=93.4(2)<sup>o</sup>) suggest the presence of a Ti-Ti single bond. The tetrahedral coordination geometry of the first Ti atom is defined by two amido groups and two carbon atom (N1-Ti1-N1'=121.8(3); Ti1-N1-C20=108.6(3); C20-N1-C14=116.3(4)Å), while the second one is octahedral (N2-Ti2-N2'=123.7(3); Ti2-N2-C2=106.9(3); Ti2-N2-C8=136.0(3)Å), with the coordination polyhedron defined by two amido groups, two carbon atoms and two hydrogen atoms of two methyl groups. The crystal structure was in fact of sufficient quality to successfully locate and refine the H atom positions of the  $\mu$ -CH<sub>3</sub> group. According to the H atom positions, the two bridging-methyl groups are distorted from their regular tetrahedral geometry. One of the C-H bonds appears unusually stretched (C1-H47=1.284(6); C1-H46=0.95(7); C1-H45=0.96(6)Å), with the H atom pointing toward the metal center. The very short Ti-H distance indicates the presence of a very strong "agostic" interaction (Ti1-H47=1.291Å). The titanium-nitrogen distances (Ti1-N1=1.937(4); Ti2-N2=1.940(4)Å) are rather short indicating some  $\pi$ -bond character.<sup>42,43</sup> The *sp*<sup>2</sup> planar geometry around amido nitrogen is slightly distorted (C2-N2-C8=116.2(4); C2-N2-Ti2=106.9(3); Ti2-N2-C8=136.0(3); Ti1-N1-C14=133.6(3); Ti1-N1-C20=108.6(3); C14-N1-C20=116.3(4)<sup>o</sup>). The cyclohexyl groups were found in the typical chair conformation.

The short Ti1-Ti2 distance shown by the X-ray crystal structure might indicate the presence of a Ti-Ti single bond. However, the magnetic susceptibility measurement ( $\mu_{\text{eff}}=0.88\mu_{\text{B}}$ /per dimer) has shown the presence of small residual paramagnetism which could arise either from direct antiferromagnetic coupling between the two d<sup>1</sup> Ti centers, or superexchange through the methyl bridges.

In an attempt to better understand the nature of the Ti-Ti interaction, an extended Hückel calculation has been carried out on  $[(\text{H}_2\text{N})_2\text{Ti}(\mu\text{-H})]_2$  as a simplified model for 18. The LUMO orbital is formed by the overlap of the empty  $p_z$  orbitals. The energy of this molecular orbital (-1.632 e.v.) is 3.141 e.v. higher than the HOMO (-4.773 e.v.), which is formed by the overlap of the two  $d_{z^2}$  (Fig. 3.16). The shape of the HOMO orbital indicates that some overlap is present, and therefore a Ti-Ti bond may exist in complex 18. However, the relatively high energy of this molecular orbital and the small extent of overlap indicates that the direct Ti-Ti interaction should be weak giving only a minor contribution to the stabilization of the dimeric structure.

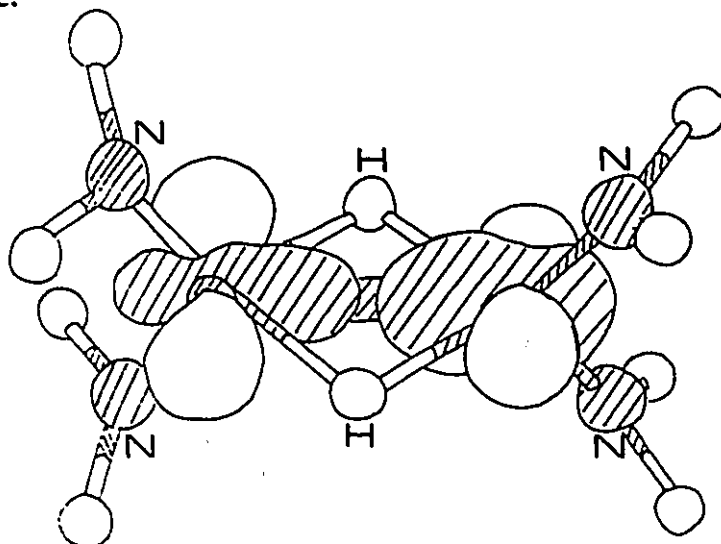


FIG. 3.16 Plot of the Highest Occupied MO

By contrast, the most significant Ti-Ti interaction is realized through the H bridges, as indicated by the molecular orbital resulting from the  $\sigma$  interaction of the titanium  $d_{xz}$  orbitals with the  $s$  orbital of bridging hydrides (-10.178 e.v.) (Fig. 3.17). Since the stabilization energy of the direct Ti-Ti interaction is considerably smaller than the Ti-H-Ti, we

suggest that superexchange or antiferromagnetic exchange contribute more significantly to the Ti-Ti coupling. The small residual paramagnetism may be explained in terms of thermal depopulation of the HOMO in favor of the LUMO.

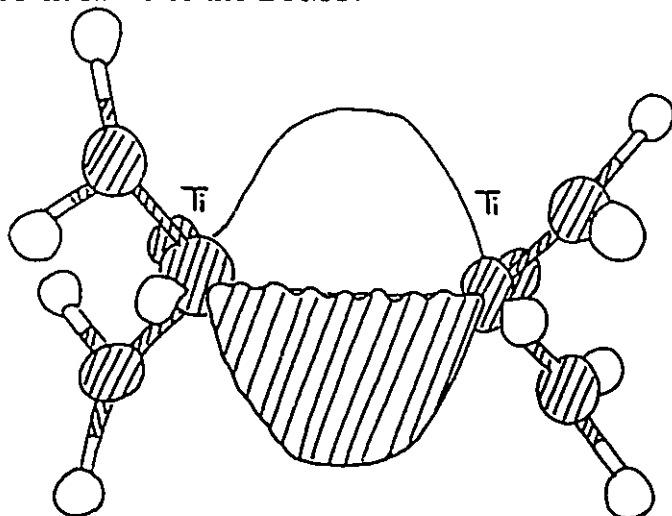


FIG. 3.17 MO Resulting from Ti-H-Ti Interaction

Fig. 3.18 shows a molecular  $\pi$  orbital resulting from the  $d_{\pi}-p_{\pi}$  overlap between  $d_{x^2-y^2}$  orbital with the  $p$  orbital of the amido nitrogen atom. This molecular orbital is found at -11.139 e.v. and its strongly stabilizing contribution is in agreement with the existence of the Ti-N  $\pi$  bond suggested by the  $sp^2$  planar arrangement around amido nitrogens observed in the crystal structure.

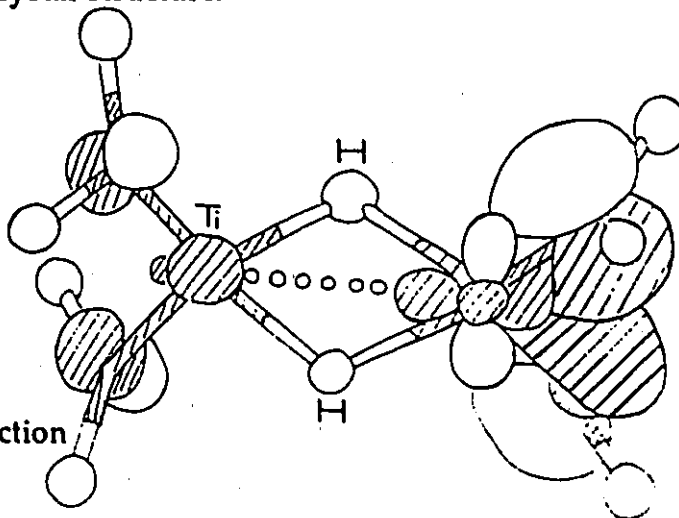
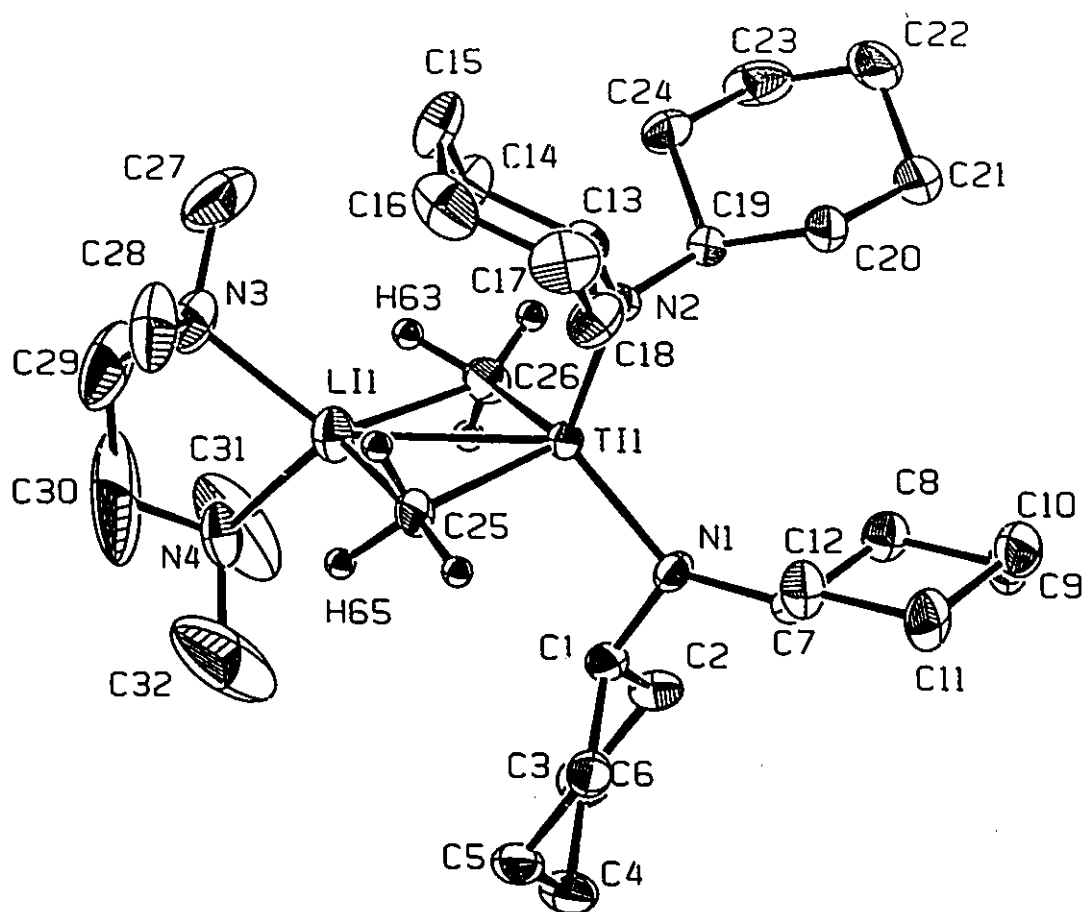


FIG. 3.18 Ti-N  $d_{\pi}p_{\pi}$  Interaction

The  $^1\text{H-NMR}$  spectrum of 18 showed the characteristic resonances of the cyclohexyl ligand as a broad multiplet in the region 2.3-1.2 ppm, and multiplet at 3.4 ppm originated by the cyclohexyl methyne proton. A singlet at 8.3 ppm was assigned to the bridging  $\text{CH}_3$  groups in the complex. Although the chemical shift is very unusual for a  $\text{Ti-CH}_3$  group, on the other hand is in agreement with the NMR resonances detected for other "agostic" metal alkyls.<sup>90</sup> In addition, the shift may be caused by the residual paramagnetism of the Ti atom. The  $^{13}\text{C-NMR}$  spectrum showed four signals which are assigned to the three methylene (37.8, 26.2, 27.5 ppm) and methyne (56.5 ppm) of the cyclohexyl ring. A signal at 2 ppm was attributed to the  $\text{CH}_3$  group.

The stoichiometric ratio between  $(\text{Cy}_2\text{N})_2\text{Ti}(\mu\text{-Cl})_2\text{Li}(\text{TMEDA})$  and  $\text{MeLi}$  controls the nuclearity of the final product. The employment of the stoichiometric ratio 1:2 between the reagents gave the mononuclear "ate" complex 19 where a  $\text{Li}(\text{TMEDA})$  counter-cation was retained in the molecular structure. The monomeric Ti-Me derivative  $(\text{Cy}_2\text{N})_2\text{Ti}(\mu\text{-Me})_2\text{Li}(\text{TMEDA})$  19 was prepared by addition of 2 eq of  $\text{MeLi}$  at  $-10^\circ\text{C}$  to a green solution of  $(\text{Cy}_2\text{N})_2\text{Ti}(\mu\text{-Cl})_2\text{Li}(\text{TMEDA})$ . After evaporation and recrystallization from hexane, pale green crystals of 19 separated at  $-30^\circ\text{C}$ . The magnetic moment at room temperature ( $\mu_{\text{eff}}=1.77\mu_{\text{B}}$ ) is in agreement with the  $d^1$  electronic configuration of  $\text{Ti(III)}$ .

The heterobimetallic nature was confirmed by X-ray crystal structure (Fig. 3.19). The crystal structure of 19 showed the titanium metal center in a distorted tetrahedral geometry linked to a lithium-



**FIG. 3.19** ORTEP drawing of 19. Bond distances (Å) and angles (deg) are as follows: Ti1-N1=1.964(4), Ti1-N2=1.941(4), Ti1-C25=2.235(5), Ti1-C26=2.229(5), Ti1-Li1=2.784(9), N1-Ti1-N2=119.9(2), N1-Ti1-C25=105.6(2), N1-Ti1-C26=112.3(2), N1-Ti1-Li1=125.5(2), N2-Ti1-C25=109.3(2), N2-Ti1-C26=106.1(2), N2-Ti1-Li1=114.6(2), C25-Ti1-C26=102.3(2), C25-Ti1-Li1=51.6(2), Ti1-N1-C1=106.7(3), Ti1-N1-C7=137.0(3).

TMEDA fragment by two bridging methyl groups (Ti1-C26=2.229(3), Ti1-C25=2.235(5); Li1-C26=2.21(1); Li1-C25=2.24(1); Li1-Ti1=2.784(9)Å). The Ti(Me)<sub>2</sub>Li core is almost planar (C25-Ti1-C26=102.3(2); C25-Ti1-Li1=51.6; C26-Ti1-Li1=51.0(2)°). The *sp*<sup>2</sup> planar arrangement around the amido nitrogen N1 and N2, and the titanium-nitrogen distances (Ti1-N1=1.946(4); Ti1-N2=1.941(4)Å) indicate the presence of some Ti-N π bond.<sup>43</sup> The crystal structure was of sufficient quality to locate and refine the H atom positions. According their positions, the Li atom was found *side-on* with respect to one of the three C-H bond of each of two bridging methyl group (Li1-C26-H63=61.24; Li1-C25-H65=66.57°), forming remarkably short lithium-hydrogen distances (Li1-H63=1.94; Li1-H65=2.07Å).

The Me-bridged Ti(III) dimer 18 is thermally unstable. After standing a few days at room temperature the mother liquor separated out the monomeric Ti(IV) (Cy<sub>2</sub>N)<sub>2</sub>Ti(Me)<sub>2</sub> 20, which was also isolated as yellow-green crystals. The dinuclear structure of 18 possibly indicates that a disproportionation may take place to form (Cy<sub>2</sub>N)<sub>2</sub>TiMe<sub>2</sub> 20 and an unidentified low-valent Ti species. Since Ti(IV) alkyl derivatives are powerful catalysts for a number of processes, including C-H bond activation, olefin metathesis, and polymerization,<sup>38,39</sup> the serendipitous isolation and formation of 20, prompted us to prepare a new class of (Cy<sub>2</sub>N)<sub>2</sub>TiR<sub>2</sub> derivatives via direct alkylation of the largely available (Cy<sub>2</sub>N)<sub>2</sub>TiCl<sub>2</sub> (Scheme 3.7).

Addition of 2 eq of MeLi to a brown-orange solution of (Cy<sub>2</sub>N)<sub>2</sub>Ti(Cl)<sub>2</sub> in diethylether at -10°C, resulted in the formation of a pale yellow-green suspension. Yellow-green crystals of 20 separated after evaporation and recrystallization from hexane at -30°C overnight.

The diamagnetism of complex 20 was confirmed by magnetic measurement in solid state and by the  $^1\text{H-NMR}$ , showing the presence of a well-resolved multiplet at 3.65 ppm, corresponding to a CH function of the cyclohexyl amido ligand, and a multiplet between 2.1-1.0 ppm, corresponding to the  $\text{CH}_2$  groups of the same cyclohexyl ring. The resonance attributable to the Ti- $\text{CH}_3$  groups is observed at 0.9 ppm.  $^{13}\text{C-NMR}$  showed the presence of CH at 57 ppm,  $\text{CH}_2$  of cyclohexyl at 36, 27, 26 ppm. The  $\text{CH}_3$  resonance was located at 4 ppm.

The crystal structure of this complex with selected bond distances and angles is shown in Fig. 3.20. The compound is monomeric with a distorted tetrahedral geometry around the titanium center ( $\text{N1-Ti1-C25}=108.7(1)$ ;  $\text{C25-Ti1-N2}=109.2(1)$ ;  $\text{N2-Ti1-C26}=107.3(1)$ ,  $\text{N1-Ti1-C26}=106.5(1)^\circ$ ). The Ti-N and Ti-C are normal and comparable to those of complexes 1 and 2 ( $\text{Ti1-N1}=1.888(3)$ ;  $\text{Ti1-N2}=1.892(3)$ ;  $\text{Ti1-C25}=2.111(4)$ ;  $\text{Ti1-C26}=2.118(3)\text{\AA}$ ). The  $sp^2$  geometry around the nitrogen atoms is significantly distorted from the planarity ( $\text{Ti1-N1-C7}=141.2(2)$ ;  $\text{Ti1-N1-C20}=103.4(2)$ ;  $\text{Ti1-N2-C13}=133.0(2)$ ;  $\text{C1-N2-C13}=115.2(2)^\circ$ ).

A unique characteristic of the neopentyl ligands, widely used in the preparation of Schrock-type carbene complexes,<sup>39</sup> is their ability to give the so called  $\alpha$ -hydrogen atom abstraction (Scheme 3.8), which consists of the migration of a hydrogen atom from the  $\alpha$ -carbon atom of one alkyl group to another.

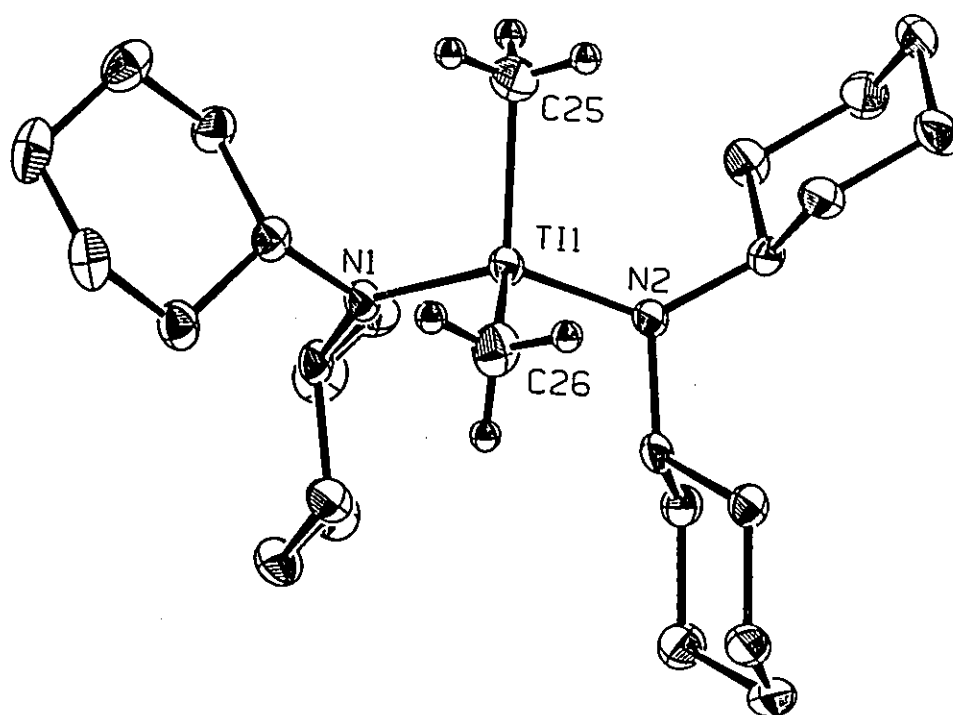
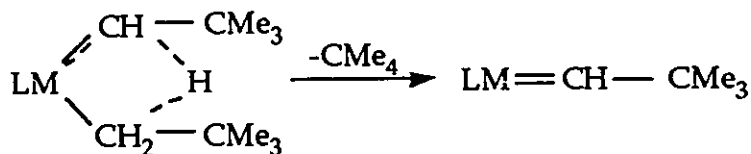
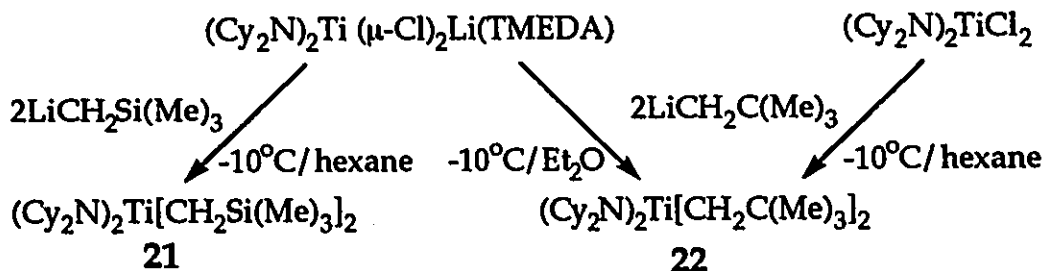


**FIG. 3.20** ORTEP drawing of 20. Bond distances (Å) and angles (deg) are as follows: Ti1-N1=1.888(3), Ti1-N2=1.892(3), Ti1-C25=2.111(4), Ti1-C26=2.118(3), N1-C7=1.477(4), N1-C20=1.478(4), N1-Ti1-N2=118.4(1), N1-Ti1-C25=108.7(1), N1-Ti1-C26=106.5(1), N2-Ti1-C25=109.2(1), N2-Ti1-C26=107.3(1), C25-Ti1-C26=105.9(1), Ti1-N1-C7=141.2(2), Ti1-N1-C20=103.4(2), Ti1-N2-C1=110.5(2)



**SCHEME 3.8** Schrock-type Carbene Formation via  $\alpha$ -Hydrogen  
Abstraction (M=metal, L=sum of the ligands)

In an attempt to further explore the stability and the chemistry of Ti alkyl amides, we have carried out alkylation reactions of  $(\text{Cy}_2\text{N})_2\text{Ti}(\mu\text{-Cl})_2\text{Li}(\text{TMEDA})$  **4** with  $\text{LiCH}_2\text{Si}(\text{Me})_3$  and  $\text{LiCH}_2\text{C}(\text{Me})_3$  (Scheme 3.9).



**SCHEME 3.9** Reaction of  $(\text{Cy}_2\text{N})_2\text{Ti}(\mu\text{-Cl})_2\text{Li}(\text{TMEDA})$  **5** and  $(\text{Cy}_2\text{N})_2\text{TiCl}_2$  **10** with  $\text{LiCH}_2\text{Si}(\text{Me})_3$  and  $\text{LiCH}_2\text{C}(\text{Me})_3$

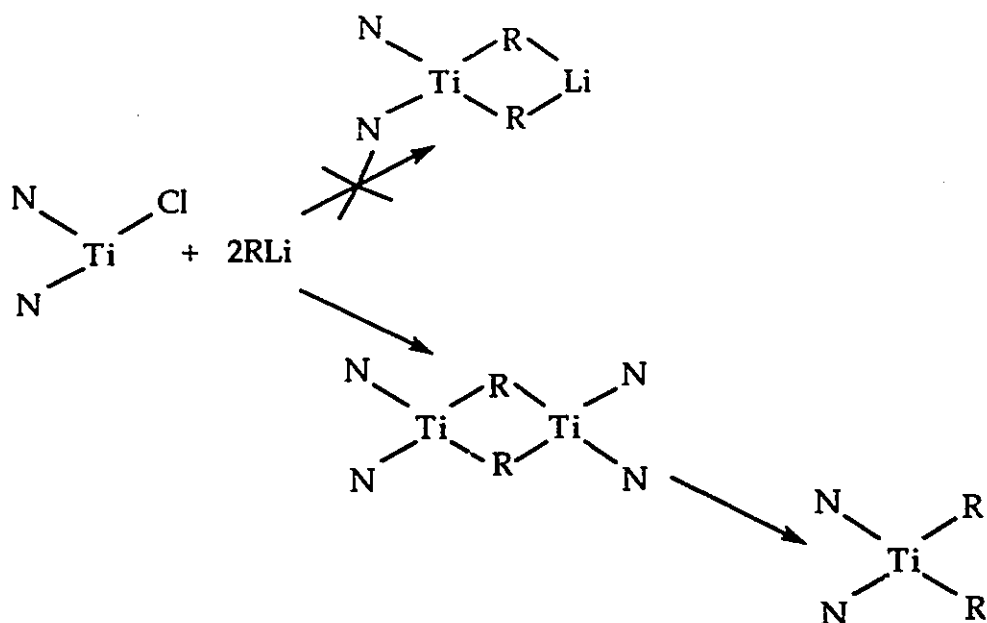
The reaction of  $(\text{Cy}_2\text{N})_2\text{Ti}(\mu\text{-Cl})_2\text{Li}(\text{TMEDA})$  with 2 eq of  $\text{LiCH}_2\text{Si}(\text{Me})_3$  or 2 eq of  $\text{LiCH}_2\text{C}(\text{Me})_3$  produced bright-yellow, diamagnetic microcrystalline Ti(IV) complexes  $(\text{Cy}_2\text{N})_2\text{Ti}[\text{CH}_2\text{Si}(\text{Me})_3]_2$  **21** and  $(\text{Cy}_2\text{N})_2\text{Ti}[\text{CH}_2\text{C}(\text{Me})_3]_2$  **22**. The formulation of these compounds as Ti(IV) derivatives is suggested by both NMR and analytical data.

The  $^1\text{H}$ -NMR spectrum of complex 21 showed the cyclohexylamido ligand as a characteristic multiplet at 3.5 ppm for CH function, and a broad multiplet in the region 2.1-1.1 ppm originated by the  $\text{CH}_2$  groups of cyclohexyl ring. A sharp singlet at 0.3 ppm is due to the  $\text{Me}_3\text{Si}$  group, while the singlet at 1.3 ppm is given by the  $\text{CH}_2$  group. All the signals integrated correctly for the proposed structure.  $^{13}\text{C}$ -NMR showed the presence of  $\text{CH}_2$  at 69 ppm, CH of cyclohexyl at 58 ppm, three different  $\text{CH}_2$  of the cyclohexyl group 37, 27, 26.3 ppm, and  $\text{CH}_3$  at 5 ppm.

While the IR spectrum of 22 did not show any significant features, the  $^1\text{H}$ -NMR confirmed the presence of cyclohexylamido ligand as a multiplet at 3.7 ppm corresponding to CH of cyclohexyl ring and broad multiplet between 2.05-1.1 ppm due to the  $\text{CH}_2$  groups. The resonance of the  $\text{C}(\text{CH}_3)_3$  was found at 0.9 ppm as a sharp singlet, while the  $\text{CH}_2$  resonance was found at 1.3 ppm.  $^{13}\text{C}$  showed the presence of CH of cyclohexyl at 58 ppm,  $\text{CH}_2$  at 36 ppm, three different  $\text{CH}_2$  of cyclohexyl at 35, 27, 25 ppm,  $\text{CH}_3$  at 4 ppm.

Complex 22 can be conveniently obtained by reaction of  $(\text{Cy}_2\text{N})_2\text{Ti}(\text{Cl})_2$  with 2 eq of  $\text{LiCH}_2\text{C}(\text{CH}_3)_3$  under the same reaction conditions.

The formation of Ti(IV) alkyl complexes 21 and 22 from Ti(III) precursor is striking. The addition of 2 eq of neopentyl ligand was probably followed by the formation of the monomeric "ate" complex. It seems that this species serves as a precursor for a rather rapid disproportionation with formation of a Ti(IV) complex in both cases (Scheme 3.10). Unfortunately, attempt to identify the other reaction products were unsuccessful.



**SCHEME 3.10** Disproportionation of Ti(III) Precursor  
(R=allyl)

The reactivity of complex 22 as a polymerization catalyst has been preliminary tested with ethylene. The reaction of 22 with excess of ethylene was followed by NMR (Fig. 3.21). The sharp singlet corresponding to free ethylene at 5.25 ppm decreased as a function of time, while the color of the solution changed from bright yellow to dark brown, and white solid formed. Meanwhile the two singlets corresponding to the neopentyl groups decreased, while a singlet corresponding to neopentane increased. After four days the transformation was complete, and no further variations of the NMR spectra were observed.

The reaction of 22 with  $\text{CH}_2=\text{CH}_2$  was carried out in toluene in a preparative scale by using 200 mg of catalyst. The reaction gave

complete gelation of the solution after 14 days yielding 1.1.g of polyethylene. Unfortunately further characterization of the polymer (molecular weight, turnover rate, kinetics studies) were not carried out due to the lack of the necessary facilities. The  $^1\text{H-NMR}$  spectra of mother solution showed only one singlet at 0.9 ppm, corresponding to neopentane.

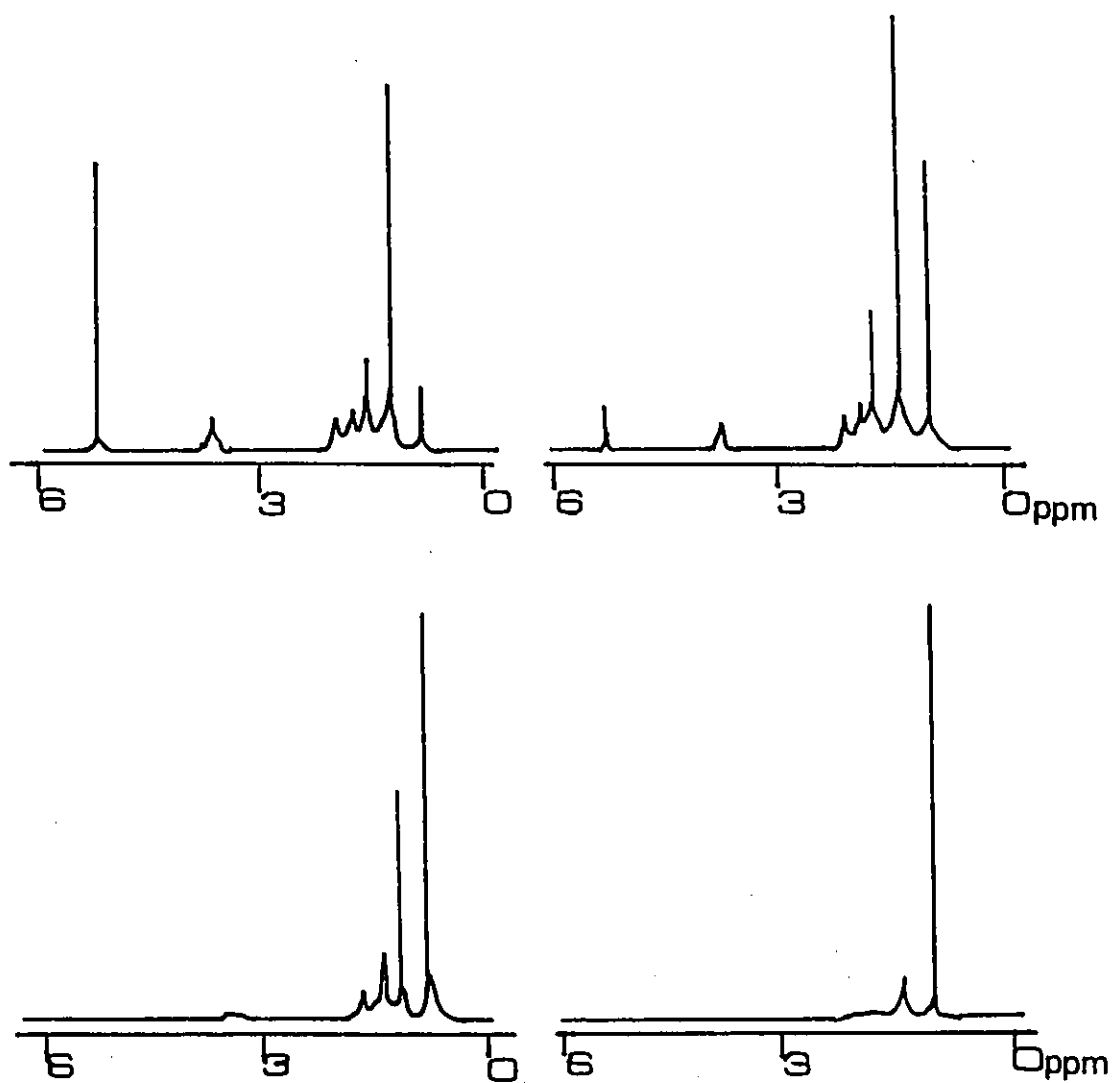


**FIG. 3.21** NMR Polymerization of Ethylene

Alkylidene complexes can easily react with olefin to form an intermediate metallacyclobutane species.<sup>39</sup> Since in the polymerization of ethylene performed by **22**, we observed elimination of neopentane, we suggest that the polymerization may proceed via initial formation of a neopentylidene titanium derivative which metathesized ethylene, forming an intermediate metallacyclobutane complex. Ring expansion via further insertion of ethylene leads to the formation of the polymer.

## CHAPTER IV

### SUMMARY

Our interest in the chemistry of low-valent titanium was focused on the use of a variety of bulky amido species as supporting ligands. These ligands were selected due to their flexible electronic and differing steric properties. As a result of this work we have successfully synthesized and crystallographically characterized a series of bis(amido) Ti(III) complexes, as well as one Ti(IV) species.

For the synthesis of bis(amido) Ti(III) complexes, transmetallation reactions of  $\text{TiCl}_3\text{THF}_3$  with  $\text{R}_2\text{NLi}$  ( $\text{R}=\text{Me}_3\text{Si}$ , Cy,  $i\text{Pr}$ ) were used. In some cases the presence of TMEDA was necessary for stabilizing the final product. Although there is no apparent interaction of TMEDA with titanium, its function is believed to involve the saturation of the coordination sphere of the metal.

Depending on the stoichiometry and the presence of TMEDA, the reaction of  $\text{TiCl}_3\text{THF}_3$  with  $(\text{Me}_3\text{Si})_2\text{NLi}$  led to the formation of three different products:  $[(\text{Me}_3\text{Si})_2\text{N}]_2\text{Ti}(\text{Cl})(\text{THF})$  1,  $[(\text{Me}_3\text{Si})_2\text{N}]\text{Ti}(\text{Cl})_2(\text{THF})_2$  2, and  $[(\text{Me}_3\text{Si})_2\text{N}]_2\text{Ti}(\text{Cl})_2[\text{Li}(\text{TMEDA})_2]$  3. X-ray crystallographic determination showed titanium-nitrogen distances in the range of 1.933-1.989Å, suggesting the presence of some Ti-N  $\pi$ -bond character.

The presence of TMEDA was necessary for the formation of  $(\text{R}_2\text{N})_2\text{Ti}(\mu\text{-Cl})_2\text{Li}(\text{TMEDA})$  ( $\text{R}=i\text{Pr}$  4, Cy 5). Further investigation of the reactivity of 4 and 5 with py showed that both complexes underwent

unprecedented tail-to-tail reversible coupling of pyridine in its *para*-position. Reaction of 4 with PhCCPh afforded 1,2,3,4,-tetraphenyl-1-butene 9. The formation of this organic product is the result of reductive coupling of two acetylene units, followed by additional hydrogen transfer from the diisopropyl moiety. The mechanistic pathway of this transfer is still under debate, although one possible mechanism may involve a Ti metallacycle-ene species.

Our new synthetic strategy for the preparation of borohydrides, hydrides, and alkyls compounds utilizes bis(amido) Ti(III) complexes as starting materials.

In the synthesis of Ti(III) borohydrides the most convenient precursor has been shown to be  $[(\text{Me}_3\text{Si})_2\text{N}]_2\text{Ti}(\text{Cl})(\text{THF})$  1 and  $\text{TiCl}_3\text{THF}_3$ . The reaction of 1 with  $\text{NaBH}_4$  resulted in  $[(\text{Me}_3\text{Si})_2\text{N}]_2\text{Ti}(\text{BH}_4)(\text{THF})$  11, which was examined as a possible tool for the preparation of Ti-H derivatives. However, reactions of 11 with Lewis bases such as pyridine proceeded unexpectedly; scrambling of ligands was followed by the formation of  $[(\text{Me}_3\text{Si})_2\text{N}]\text{Ti}(\text{BH}_4)_2(\text{py})_2$  12. Several attempts to prepare the titanium-hydride species were performed by reacting of  $[(\text{Me}_3\text{Si})_2\text{N}]_2\text{Ti}(\text{Cl})(\text{THF})$  1 with a variety of reagents. Only the reaction with Red-Al, carried out in the presence of  $\text{Me}_3\text{P}$ , formed a microcrystalline product, suggested by IR characterization to be the compound  $[(\text{Me}_3\text{Si})_2\text{N}]_2\text{Ti}(\text{H})(\text{PMe}_3)$  14. Further investigation of the reactivity of 11 was carried out using different substrates, such as diazo, cumulenes, olefins, and acetylenes. The only productive result being the reaction with  $\text{CS}_2$  to form a dimeric Ti(IV) species containing a  $\text{Ti}(\mu\text{-S})_2\text{Ti}$  core. The reaction

between  $\text{TiCl}_3\text{THF}_3$  and  $\text{NaBH}_4$  produced a paramagnetic Ti(III) complex  $\text{Ti}(\text{BH}_4)_3(\text{THF})_3$  15.

Alkylation reactions of  $[(\text{Me}_3\text{Si})_2\text{N}]_2\text{Ti}(\text{Cl})(\text{THF})$  1,  $[(i\text{Pr})_2\text{N}]_2\text{Ti}(\mu\text{-Cl})_2\text{Li}(\text{TMEDA})$  4, and  $(\text{Cy}_2\text{N})_2\text{Ti}(\mu\text{-Cl})_2\text{Li}(\text{TMEDA})$  5 were performed with a series of alkylating reagents. While the attempted alkylation reactions of 1 were unsuccessful, 4 and 5 showed different reactivities towards alkyl functionalities.

Specifically, the reactions of 5 and 4 with  $\text{PhLi}$ , carried out in the presence of  $\text{TMEDA}$ , produced  $(\text{Cy}_2\text{N})_2\text{Ti}(\text{Ph})_2\text{Li}(\text{TMEDA})$  16, and  $\{[(i\text{Pr})_2\text{N}]_2\text{Ti}(\text{Ph})_2\}[\text{Li}(\text{TMEDA})_2]$  17.

Depending on the stoichiometric ratio, the treatment of 5 with  $\text{MeLi}$  proceeded in two different pathways. When the reaction was carried out in the ratio 1:1, an exclusive Ti-Ti dimer  $\{(\text{Cy}_2\text{N})_2\text{Ti}(\mu\text{-Me})\}_2$  18 was formed. By employing the 1:2 ratio, the reaction yielded a mononuclear "ate" complex  $(\text{Cy}_2\text{N})_2\text{Ti}(\mu\text{-Cl})_2\text{Li}(\text{TMEDA})$  19. The crystal structure of 18 showed a very short Ti-H distance ( $\text{Ti1-H47}=1.291\text{\AA}$ ) suggesting a strong "agostic" interaction. The Ti-Ti distance ( $\text{Ti1-Ti2}=2.935\text{\AA}$ ) is at the limit of what may be considered a Ti-Ti bond. An extended Huckel calculation carried out on  $[(\text{H}_2\text{N})_2\text{Ti}(\mu\text{-H})]_2$  as a simplified model for 18 showed that the shape of HOMO indicates some overlap and therefore a Ti-Ti bond may exist, although very weak, since there is a rather high energy (-4.773 e.v.).

The Ti(IV) alkyl species  $(\text{Cy}_2\text{N})_2\text{TiMe}_2$  20 was synthesized in the reaction of  $(\text{Cy}_2\text{N})_2\text{TiCl}_2$  10 with 2 eq of  $\text{MeLi}$ .

The methylation of  $[(i\text{Pr})_2\text{N}]_2\text{Ti}(\mu\text{-Cl})_2\text{Li}(\text{TMEDA})$  4 afforded only intractable products, possibly due to the complicated hydrogen transfer from the diisopropyl group into the coordination periphery of titanium,

followed by the elimination of methane and the formation of a Ti-metallacycle species.

The reaction of  $(\text{Cy}_2\text{N})_2\text{Ti}(\mu\text{-Cl})_2\text{Li}(\text{TMEDA})$  **5** with 2 eq of  $\text{LiCH}_2\text{Si}(\text{Me})_3$  or  $\text{LiCH}_2\text{C}(\text{Me})_3$  in the first step probably afforded the monomeric "ate" complex. However, a rapid disproportionation yielded Ti(IV) complexes  $(\text{Cy}_2\text{N})_2\text{Ti}[\text{CH}_2\text{Si}(\text{Me})_3]_2$  **21**, and  $(\text{Cy}_2\text{N})_2\text{Ti}[\text{CH}_2\text{C}(\text{Me})_3]_2$  **22**, respectively. Preliminary results showed that complex **22** has catalytic activity towards ethylene.

## CHAPTER V

### EXPERIMENTAL SECTION

#### 5.1 General Procedures

All manipulation of air and moisture-sensitive compounds were carried out with use of standard Schlenk-type glassware on a vacuum-nitrogen line or inside a N<sub>2</sub> filled glove box.

THF and hexane were distilled from potassium metal, toluene from sodium metal and diethyl ether from sodium-potassium alloy.

TiCl<sub>3</sub>THF<sub>3</sub> and TiCl<sub>4</sub>(TMEDA) was prepared according to procedures reported in the literature.<sup>101</sup>

Dicyclohexylamine, diisopropylamine, (Me<sub>3</sub>Si)<sub>2</sub>NLi, CS<sub>2</sub>, Red-Al, Me<sub>3</sub>P, pyridine, <sup>t</sup>Bu-pyridine, neopentylalcohol, (trimethylsilyl)methanol, TMEDA, NaBH<sub>4</sub>, LiBH<sub>4</sub>, NaHB(C<sub>2</sub>H<sub>5</sub>)<sub>3</sub>, (Bu)<sub>3</sub>SnH, PhSiH<sub>3</sub>, LiAlH<sub>4</sub>, MeLi, <sup>n</sup>BuLi, C<sub>6</sub>D<sub>6</sub>, C<sub>5</sub>D<sub>5</sub>N and CDCl<sub>3</sub> were purchased from Aldrich Chemical Co.

Pyridine and <sup>t</sup>Bu-pyridine were refluxed over calcium hydride, TMEDA over sodium metal, distilled prior to use and stored under N<sub>2</sub>.

Dicyclohexylamine, and diisopropylamine were refluxed over potassium metal and distilled prior to use. Dried reagents were stored under N<sub>2</sub>.

(Me<sub>3</sub>Si)<sub>2</sub>NLi was purified by recrystallization from hexane before use.

Deuterated benzene  $C_6D_6$  was dried over sodium-potassium alloy,  $C_5D_5N$  was dried over calcium hydride, vacuum transferred to the appropriate container and stored in the glove box.

PhLi, NpLi,  $LiCH_2SiMe_3$ , NfLi, BzLi(TMEDA) and BzK were prepared according to published procedures.<sup>102</sup>

Infrared spectra were recorded on a Perkin-Elmer 283, and on a Michelson Bomem Spectrometer as a Nujol mulls, prepared in the dry box using KBr plates.

NMR spectra were recorded on a Varian Gemini 200-MHz and Bruker 500-MHz spectrophotometer.

Elemental analysis were carried out at the Microanalytical Department of the Chemistry Department at the Rijksuniversiteit Groningen, Netherlands.

Mass spectra were recorded on a VG 7070E spectrometer.

Melting point temperature was measured on a Mel. Temp. II. apparatus.

Magnetic susceptibility measurements were carried out in sealed tubes at room temperature using a Johnson Matthey balance. Magnetic moments were calculated following standard methods.<sup>103</sup>

EPR measurements were carried out at National Research Council of Canada's Chemistry Department in Ottawa.

### X-ray Crystal Diffraction Analysis

All measurements were made on a Rigaku AFC6S diffractometer with graphite monochromated  $Mo-K\alpha$  radiation and a 12KW anode generator. Cell constants and an orientation matrix for data collection

were obtained from a least-squares refinement using the setting angles of 25 carefully centered reflections. The intensities of three standard reflections, measured every 150 scans remained constant for all three data collections. All calculations were performed using the TEXAN crystallographic software package of Molecular Structure Corporation. The data were corrected for Lorentz and polarization effects. The structures were solved by direct methods and the non-hydrogen atoms were refined anisotropically. The refinement was carried out by using full-matrix, least-squares techniques on  $F$  minimizing the function  $w(|F_o| - |F_c|)^2$  where the weight  $w$ , is defined as  $4F_o^2/2\sigma(F_o^2)$  and  $F_o$  and  $F_c$  are the observed and calculated structure factor amplitudes.

### Preparation of $Cy_2NLi$

A solution of  $nBuLi$  in hexane (1.6 M, 63 mL, 10% excess) was slowly added to a colorless solution of  $Cy_2NH$  (20 mL, 100.4 mmol) in hexane at room temperature. After 20 minutes standing at room temperature, the reaction mixture was heated to the boiling point and then slowly cooled. White microcrystals of  $Cy_2NLi$  (15 g, 79.48%) were obtained upon standing overnight at room temperature. IR (KBr plates, Nujol mull  $cm^{-1}$ )  $\nu$ : 2892(s), 2756(w), 1452(s), 1377(m), 1339(m), 1299(w), 1261(w), 1236(w), 1174(m), 1140(s), 1085(s), 1025(m), 984(m), 948(s), 918(m), 885(s), 844(w), 794(w), 778(w), 635(s), 606(s).  $^1H$ -NMR (200 MHz,  $C_6D_6$ ,  $\delta$ (ppm)): 3.5(m, 4H cyclohexyl), 2.0-1.0(bd m, 40H cyclohexyl).  $^{13}C$ -NMR (200 MHz,  $C_6D_6$ ,  $\delta$ (ppm)): 61, 59(CH cyclohexyl), 41, 40( $CH_2$  cyclohexyl)

### Preparation of (iPr)<sub>2</sub>NLi

A solution of <sup>n</sup>BuLi in hexane (1.6 M, 89.2 mL, 10% excess) was slowly added to a colorless solution of (iPr)<sub>2</sub>NH (20 mL, 142.6 mmol) in hexane at -10°C. The reaction mixture was allowed to warm to room temperature and after 1 hour standing at room temperature was frozen to -30°C. White microcrystalline (iPr)<sub>2</sub>NLi (13.1 g, 85.85%) was obtained upon standing at -30°C overnight. IR (KBr plates, Nujol mull cm<sup>-1</sup>): 2880(s), 2583(s), 1455(s), 1369(s), 1332(m), 1301(s), 1153(s), 1167(s), 1059(s), 999(s), 931(s), 898(s), 825(m), 805(s), 723(m), 631(s). <sup>1</sup>H-NMR (500 MHz, C<sub>6</sub>D<sub>6</sub>, δ(ppm)): 3.1(m, H isopropyl), 3.0(m, H isopropyl), 1.05(two s, 24H isopropyl). <sup>13</sup>C-NMR (500 MHz, C<sub>6</sub>D<sub>6</sub>, δ(ppm)): 50, 53(CH isopropyl), 26,25(CH<sub>3</sub> isopropyl)

## 5.2 Synthesis and Characterization of Titanium Amides

### Preparation of [(Me<sub>3</sub>Si)<sub>2</sub>N]<sub>2</sub>Ti(Cl)(THF) 1

Crystalline ((Me)<sub>3</sub>Si)<sub>2</sub>NLi (3.6 g, 20 mmol) was added to a green suspension of TiCl<sub>3</sub>THF<sub>3</sub> (4.0 g, 10 mmol) in toluene under a nitrogen atmosphere at -10°C. The reaction mixture was allowed to warm up and stirred for two hours at room temperature. The dark green-blue solution was evaporated to dryness and the residual solid redissolved in hexane. The white precipitate of LiCl was removed by filtration and green crystals of 1 (5.7 mmol, 68%) were obtained upon cooling to -30°C. Anal. Calcd (found) for C<sub>16</sub>H<sub>44</sub>Si<sub>4</sub>N<sub>2</sub>OCITi: C, 40.38 (39.87); H,

9.25 (9.4); N, 5.9 (6.01). IR (KBr plates, Nujol mull  $\text{cm}^{-1}$ )  $\nu$ : 2870(s), 1440(s), 1360(s), 1235(s), 1160(w), 1105(s), 985(m), 830(v bd), 790(w), 770(w), 750(w), 620(w), 590(w), 430(w), 400(w), 365(w).  $\mu_{\text{eff}}=1.71\mu\text{B}$

### Preparation of $(\text{Me}_3\text{Si})_2\text{NTi}(\text{Cl})_2(\text{THF})_2$ 2

A solution of  $(\text{Me}_3\text{Si})_2\text{NLi}$  (2.51 g, 15 mmol) in toluene (50 mL) was added dropwise to a green suspension of  $\text{TiCl}_3\text{THF}_3$  (5.57 g, 15 mmol) in toluene. The color turned blue. The reaction mixture was evaporated to dryness and the residual solid redissolved in hexane. LiCl was removed by filtration and a blue crystals of 2 (mixture with 1) were obtained upon cooling to  $-30^\circ\text{C}$ .

### Preparation of $\{[(\text{Me}_3\text{Si})_2\text{N}]_2\text{TiCl}_2\}[\text{Li}(\text{TMEDA})_2]$ 3

A suspension of  $\text{TiCl}_3\text{THF}_3$  (20 g, 54 mmol) in THF (200 mL) was treated with TMEDA (17 mL). The addition of  $\text{LiN}(\text{SiMe}_3)_2$  (18 g, 108 mmol) to the resulting light blue solution turned the color light green. After standing 30 minutes. at room temperature the solvent was evaporated *in vacuo*. The residual solid was redissolved in diethylether and the insoluble material eliminated by filtration. Colorless crystals of 3 (21.9 g, 59 %) separated upon concentration and standing at  $-30^\circ\text{C}$  overnight. Anal. Calcd (found) for  $\text{C}_{24}\text{H}_{68}\text{N}_6\text{Si}_4\text{Cl}_2\text{TiLi}$ : C, 42.46 (42.38); H, 10.10 (10.00); N, 12.38 (12.33), Ti, 7.05 (7.01). IR (KBr, Nujol mull  $\text{cm}^{-1}$ )  $\nu$ : 2900(s), 2800(m), 1460(s), 1380(m), 1290(s), 1260(sh), 1240(s), 1190(m),

1170(m), 1140(m), 1105(m), 1070(m), 1030(s), 1015(s), 930(s), 890(s), 835(s), 785(s), 760(m), 720(s), 695(s), 670(s), 630(m), 615(w), 500(m), 450(w), 410(m), 390(m).  $\mu_{\text{eff}}=1.75\mu\text{B}$

#### Preparation of [(iPr)<sub>2</sub>N]<sub>2</sub>Ti(μ-Cl)<sub>2</sub>Li(TMEDA) 4

(iPr)<sub>2</sub>NLi (1.11 g, 10.36 mmol) was added to a blue solution of TiCl<sub>3</sub>THF<sub>3</sub> (1.93 g, 5.2 mmol) in THF at -10°C followed by addition of 2 eq of anhydrous TMEDA (1.6 mL, 10.6 mmol). The forest green solution was warmed to room temperature, stirred for two hours, and then evaporated to dryness. The oily residue was redissolved in hexane, and LiCl removed by filtration. Green needles of 4 (1.24 mmol, 24%) were obtained upon cooling to -30°C. Anal. Calcd (found) for TiLiCl<sub>2</sub>N<sub>4</sub>C<sub>18</sub>H<sub>42</sub>: Cl, 16.1 (15.88); N, 12.72 (12.69); C, 49.24 (50.08); H, 9.61 (9.44). IR (KBr plates, Nujol mull cm<sup>-1</sup>) v: 2899(s), 1457(s), 1369(s), 1292(m), 1251(w), 1166(s), 1132(w), 1102(m), 1064(w), 1036(m), 1010(m), 934(s), 853(m), 813(m), 790(m), 770(w), 724(w), 606(m), 526(w), 491(w), 439(w).  $\mu_{\text{eff}}=1.8\mu\text{B}$

#### Preparation of (Cy<sub>2</sub>N)<sub>2</sub>Ti(μ-Cl)<sub>2</sub>Li(TMEDA) 5

Cy<sub>2</sub>NLi (2.0 g, 10.68 mmol) was added to a blue solution of TiCl<sub>3</sub>THF<sub>3</sub> (1.98 g, 5.3 mmol) in THF at -10°C, followed by the addition of 1.5 eq of dry TMEDA (1.2 mL, 7.9 mmol). The emerald green mixture was allowed to warm up and stirred for two hours at room temperature.

The solution was evaporated to dryness and the crystalline residue was redissolved in hexane. The LiCl was removed by filtration and emerald green crystals of 5 (2.1 mmol, 41 %) were obtained upon cooling to -30°C. IR (KBr plates, Nujol mull  $\text{cm}^{-1}$ )  $\nu$ : 2900(s), 1440(s), 1365(s), 1287(s), 1249(s), 1154(s), 1222(s), 1063(s), 1028(s), 982(s), 950(s), 888(s), 842(s), 803(m), 789(s), 773(m), 723(w), 690(s), 585(s), 489(s), 449(m), 419(m).  $\mu_{\text{eff}}=1.76\mu_{\text{B}}$

#### Preparation of $[(i\text{Pr})_2\text{N}]_2\text{TiCl}_2[\mu-(\text{NC}_5\text{H}_5-\text{C}_5\text{H}_5\text{N})]$ 6

Freshly distilled pyridine (0.19 mL, 2.35 mmol) was added to a forest green solution of  $[(i\text{Pr})_2\text{N}]_2\text{Ti}(\mu\text{-Cl})_2\text{Li}(\text{TMEDA})$  (1.08 g, 2.4 mmol) in hexane. The color changed rapidly to ink-blue and then to emerald green with formation of white precipitate, which was removed by filtration. The color of the solution changed from greenish to brown upon cooling to -30°C and red-orange crystals of 6 (0.76 mmol, 32 %) separated after two days standing at this temperature. IR (KBr plates, Nujol mull  $\text{cm}^{-1}$ )  $\nu$ : 2900(s), 1655(s), 1591(s), 1457(s), 1417(m), 1377(m), 1360(m), 1263(s), 1188(s), 1163(s), 1122(m), 1099(s), 1065(m), 1044(s), 993(s), 960(s), 922(s), 864(s), 817(m), 793(s), 752(w), 733(w), 701(m), 647(m), 625(m), 612(s), 540(s), 509(s), 462(m). EPR (toluene, RT):  $g=1.9660$ .  $\mu_{\text{eff}}=0.0\mu_{\text{B}}$  (solid state)

### Preparation of $\{(Cy_2N)_2TiCl\}_2[\mu-(NC_5H_5-C_5H_5N)]$ 7

The addition of anhydrous pyridine (0.2 mL, 2.25 mmol) to an emerald green solution of  $(Cy_2N)_2Ti(\mu-Cl)_2Li(TMEDA)$  (1.34 g, 2.22 mmol) in hexane rapidly deepened the color. A white precipitate, which separated after one hour of standing at room temperature was removed by filtration. The color of the solution turned brown upon cooling at  $-30^\circ C$  and red-orange crystals of 7 (0.5 g, 37%) separated after standing two days at low temperature. Anal. Cald (found) for  $C_{58}H_{98}N_6Ti_2Cl_2$ : Cl, 6.78 (6.31); Ti, 9.15 (8.52); N, 8.03 (7.31); H, 9.44 (9.88); C, 66.59 (67.01). IR (KBr plates, Nujol mull  $cm^{-1}$ )  $\nu$ : 2900(s), 1375(s), 1295(m), 1260(s), 1160(s), 1145(m), 1120(s), 1075(w), 1030(s), 980(m), 950(m), 890(m), 840(m), 800(w), 785(w), 770(w), 750(s), 675(w), 640(s). EPR (toluene, RT):  $g=1.9677$ .  $\mu_{eff}=0.00\mu_B$  (solid state)

### Preparation of $(Cy_2N)_2Ti(Cl)(^tBu-py)$ 8

The addition of anhydrous  $^tBu$ -pyridine (0.34 mL, 2.3 mmol) to an emerald green solution of  $(Cy_2N)_2Ti(\mu-Cl)_2Li(TMEDA)$  (1.31 g, 2.3 mmol) in hexane rapidly changed the color to blue with formation of white precipitate, which was removed by filtration. Dark blue crystals of 8 (0.52 g, 37.4 %) were obtained upon cooling to  $-30^\circ C$ . Anal. Cald (found) for  $C_{33}H_{57}N_3TiCl$ : Cl, 6.12 (6.23); Ti, 8.27 (8.16); N, 7.26 (7.29); H, 9.92 (9.93); C, 68.44 (68.31). IR (KBr plates, Nujol mull  $cm^{-1}$ )  $\nu$ : 2906(s), 1606(m), 1532(w), 1492(m), 1454(m), 1415(m), 1375(m), 1343(m), 1272(m), 1249(m), 1161(s), 1144(s), 1065(w), 1033(s), 983(s), 952(s), 887(s), 842(s),

829(s), 802(m), 779(m), 744(w), 689(s), 583(s), 567(s), 498(s), 450(m), 421(m).  $\mu_{\text{eff}}=1.82\mu_{\text{B}}$

#### Reaction of $[(i\text{Pr})_2\text{N}]_2\text{Ti}(\mu\text{-Cl})_2\text{Li}(\text{TMEDA})$ with PhCCP 9

The addition of PhCCPh (0.4 g, 2.25 mmol) to a forest green solution of  $[(i\text{Pr})_2\text{N}]_2\text{Ti}(\mu\text{-Cl})_2\text{Li}(\text{TMEDA})$  (1.2 g, 26 mmol) in hexane, rapidly turned the color brown-red. The reaction mixture was allowed to stand at room temperature overnight, after which time a small amount of solid separate. After filtration, concentration and further standing at room temperature colorless needles of PhCH=CPh-CHPh-CH<sub>2</sub>Ph (0.3 g, 30%), were obtained. IR (KBr plates, Nujol, mull  $\text{cm}^{-1}$ ): 2900(s), 1596(m), 1456(s), 1377(s), 1069(m), 1027(m), 912(m), 865(m), 789(m), 764(w), 751(w), 738(s), 697(s), 644(w), 582(m), 529(m), 516(m), 479(w). <sup>1</sup>H-NMR (500 MHz, CDCl<sub>3</sub>,  $\delta$ (ppm)): 7.3-6.6(m, 24H aromatic), 6.5(s, 1H CH olefinic), 4(t, 1H<sub>X</sub>), 3.0-3.1(two q, 2H CH<sub>2</sub>),  $|^3J_{\text{XA}}=9.6\text{Hz}|$ ,  $|^3J_{\text{XB}}=6.4\text{Hz}|$ ,  $|^2J_{\text{AB}}=12.8\text{Hz}|$ ,  $|^3J_{\text{AX}}=9.6\text{Hz}|$ ,  $|^3J_{\text{BX}}=6.4\text{Hz}|$ . <sup>13</sup>C-NMR (500 MHz, CDCl<sub>3</sub>,  $\delta$ (ppm)): 127(m, CH, aromatic), 55(CH), 39(CH<sub>2</sub>); MS. m/z 360, 269, 252, 191, 189, 165, 152, 115, 91, 86, 65, 44. m.p: 146°C

#### Preparation of $(\text{Cy}_2\text{N})_2\text{Ti}(\text{Cl})_2$ 10

Lithium dicyclohexylamido (2.36 g, 12.6 mmol) was added to a solution of TiCl<sub>4</sub>(TMEDA) (1.93 g, 6.3 mmol) in THF at -10°C. The reaction mixture was slowly warmed to room temperature and stirred for one

hour. The volume was reduced by evaporation of the solvent *in vacuo*, hexane was added and the colorless precipitate of LiCl(TMEDA) was removed by filtration. Dark orange crystals of 10 (2.5 mmol, 40 %), were obtained upon cooling to -30°C overnight. IR (KBr, Nujol mull  $\text{cm}^{-1}$ )  $\nu$ : 2900(s), 1455(s), 1375(m), 1253(m), 1160(s), 1142(s), 1111(s), 1092(s), 1021(s), 978(m), 948(s), 890(s), 843(s), 806(m), 780(s), 723(w), 707(s), 601(m), 580(m), 522(s), 485(s), 432(s), 409(s).  $^1\text{H-NMR}$  (200 MHz,  $\text{C}_6\text{D}_6$ ,  $\delta$ (ppm)): 3.7(m, 4H cyclohexyl), 2.1-0.9(bd m, 40H cyclohexyl).  $\mu_{\text{eff}}=0.0\mu\text{B}$

### 5.3 Synthesis and Characterization of Titanium Hydrides and Borohydrides

#### Preparation of $[(\text{Me}_3\text{Si})_2\text{N}]_2\text{Ti}(\text{BH}_4)(\text{THF})$ 11

A green-blue solution of  $[(\text{Me}_3\text{Si})_2\text{N}]_2\text{Ti}(\text{Cl})(\text{THF})$  (3.0 g, 6 mmol) in THF was stirred with  $\text{NaBH}_4$  (1.92 g, 50 mmol) at room temperature for four days. The resultant green suspension was evaporated to dryness and the residual solid redissolved in hexane. After removal of the insoluble residue by filtration, crystals of 11 (30 mmol, 46 %) were obtained upon cooling to -30°C. Anal. Calcd (found) for  $\text{TiN}_2\text{Si}_4\text{OBC}_{16}\text{H}_{48}$ : N, 6.15 (6.01); C, 42.18 (42.9); H, 10.62 (10.09); Si, 24.45 (24.57). IR (KBr plates, Nujol mull  $\text{cm}^{-1}$ )  $\nu$ : 2900(s), 2440(s), 2400(s), 2270(m), 2195(s), 1465(s), 1385(s), 1260(s), 1440(s), 1050(w), 1015(s), 850(v bd), 790(m), 770(w), 670(s), 645(s), 620(w), 520(m), 440(m), 420(m), 420(w), 395(s), 380(w).  $\mu_{\text{eff}}=1.81\mu\text{B}$

### Preparation of $[(\text{Me}_3\text{Si})_2\text{N}]\text{Ti}(\text{py})_2(\text{BH}_4)_2$ 12

Anhydrous pyridine (0.26 mL, 3.28 mmol) was added to a violet solution of  $[(\text{Me}_3\text{Si})_2\text{N}]_2\text{Ti}(\text{BH}_4)(\text{THF})$  (1.00 g, 2.19 mmol) in diethylether. Upon standing at room temperature overnight, the color changed to dark-red. The solution was evaporated to dryness and the residual dark-red solid was redissolved in hexane. Deep-red crystals of 12 (1.01 mmol, 46%) were obtained upon cooling to  $-30^\circ\text{C}$ . Anal. Calcd (found) for  $\text{TiN}_3\text{Si}_2\text{B}_2\text{C}_{16}\text{H}_{28}$ : N, 10.82 (10.22); C, 49.58 (49.74); H, 7.27 (7.55); Si, 14.47 (14.21). IR (KBr plates, Nujol mull  $\text{cm}^{-1}$ )  $\nu$ : 2900(s), 2860(m), 2380(m), 2340(s), 2220(w), 2140(m), 1580(m), 1465(sh), 1430(sh), 1420(s), 1355(m), 1225(s), 1195(s), 1110(m), 1045(w), 1020(w), 990(w), 875(v bd), 760(w), 730(w), 690(w), 660(s), 610(m), 585(w), 480(w), 415(w), 400(w), 365(w).  $\mu_{\text{eff}} = 1.8\mu\text{B}$

### Preparation of $\{[(\text{Me}_3\text{Si})_2\text{N}]_2\text{Ti}(\mu\text{-S})\}_2$ 13

The addition of  $\text{CS}_2$  (0.1 mL, 1.66 mmol) to a violet solution of  $[(\text{Me}_3\text{Si})_2\text{N}]_2\text{Ti}(\text{BH}_4)(\text{THF})$  (0.52 g, 1.1 mmol) in hexane rapidly changed color to dark brown-orange. Dark orange crystals of 13 (0.25 mmol, 22.7 %) were obtained upon cooling to  $-30^\circ\text{C}$  overnight. IR (KBr plates, Nujol mull  $\text{cm}^{-1}$ )  $\nu$ : 2900(s), 1560(w), 1450(s), 1370(s), 1240(s), 850(v bd), 785(w), 705(w), 690(m), 655(m), 450(m), 430(w), 415(w).  $^1\text{H-NMR}$  (200 MHz,  $\text{C}_5\text{D}_5\text{N}$ ,  $\delta(\text{ppm})$ ): 0.9(s, 18H SiMe<sub>3</sub>).  $\mu_{\text{eff}} = 0.0\mu\text{B}$

### Preparation of $[(\text{Me}_3\text{Si})_2\text{N}]_2\text{Ti}(\text{H})(\text{PMe}_3)$ 14

$\text{Me}_3\text{P}$  (1.1 mL, 0.65 mmol) was added to a green suspension of  $(\text{Me}_3\text{Si})_2\text{N})_2\text{Ti}(\text{Cl})(\text{THF})$  (1.69 g, 3.55 mmol) in toluene. The reaction mixture then changed color to blue. The addition of Red-Al (0.5 mL, 1.77 mmol) turned the color to dark green. The solution, after half hour standing at room temperature, was evaporated to dryness and a residual oily solid was redissolved in hexane and cleaned by filtration. Blue microcrystals of 14 (0.08 g, 4.8 %) were obtained upon cooling to  $-30^\circ\text{C}$ . IR (KBr plates, Nujol mull  $\text{cm}^{-1}$ )  $\nu$ : 2900(s), 1755(s), 1450(s), 1365(s), 1240(s), 1090(m), 1060(w), 1030(m), 1000(m), 860(v bd), 750(w), 710(w), 660(m), 625(w), 605(w), 530(m), 490(w), 460(w), 435(w), 405(w).

### Preparation of $\text{Ti}(\text{BH}_4)_3(\text{THF})_3$ 15

An large excess of  $\text{NaBH}_4$  (3.84 g, 101.6 mmol), in a blue solution of  $\text{TiCl}_3\text{THF}_3$  (5.35 g, 15 mmol) in THF was refluxed for 2 days. The resulting blue-green suspension was filtered and evaporated to dryness and the crystalline residue redissolved in diethylether. The solution was filtered and cooled to  $-30^\circ\text{C}$ , upon which shiny blue crystals of 15 (9.72 mmol, 64.8 %) were obtained. IR (KBr plates, Nujol mull  $\text{cm}^{-1}$ )  $\nu$ : 2900(s), 2740(w), 2440(s), 2260(m), 2150(s), 2050(m), 1465(s), 1370(s), 1250(s), 1180(w), 1130(s), 1050(s), 1025(s), 970(m), 935(m), 850(s), 785(w), 730(w), 690(s), 585(m), 430(m), 365(w).  $\mu_{\text{eff}}=1.79\mu\text{B}$

#### 5.4 Synthesis and Characterization of Titanium Alkyls

##### Preparation of $[(\text{Cy}_2\text{N})_2\text{Ti}(\text{Ph})_2]\text{Li}(\text{TMEDA})$ 16

PhLi 1.5Et<sub>2</sub>O (1.15 g, 5.9mmol) was added to an emerald green solution of  $(\text{Cy}_2\text{N})_2\text{Ti}(\mu\text{-Cl})_2\text{Li}(\text{TMEDA})$  (1.78 g, 2.95 mmol) in diethylether. The color changed rapidly to purple-red and no color change was observed after the addition of TMEDA (0.9 mL, 5.9 mmol). The reaction mixture was stirred at room temperature for two hours, filtered, concentrated and cooled. Red-brown plates of 16 (0.95 g, 53.4 %) were obtained upon standing overnight at -30°C. Anal. Calcd (found) for  $\text{TiN}_4\text{LiC}_4\text{H}_{70}$ : C, 73.5 (71.41); H, 10.29 (10.29); N, 8.16 (10.25). IR (KBr plates, Nujol mull  $\text{cm}^{-1}$ )  $\nu$ : 2905(s), 1551(m), 1458(s), 1378(m), 1288(m), 1245(m), 1159(m), 1146(m), 1118(m), 1029(s), 980(m), 950(s), 887(m), 842(m), 788(m), 699(s), 679(s), 580(m), 495(m), 449(w).  $\mu_{\text{eff}}=1.79\mu\text{B}$

##### Preparation of $\{[(i\text{Pr})_2\text{N}]_2\text{Ti}(\text{Ph})_2\}[\text{Li}(\text{TMEDA})_2]$ 17

Addition of PhLi 1.5Et<sub>2</sub>O (1.6 g, 8.2 mmol) to a forest green solution of  $[(i\text{Pr})_2\text{N}]_2\text{Ti}(\mu\text{-Cl})_2\text{Li}(\text{TMEDA})$  (1.81 g, 4.1 mmol) in diethylether, turned the color cherry-red. No apparent color change was observed after further addition of TMEDA (1.21 mL, 8.02 mmol). The reaction mixture was stirred at room temperature for 1.5 hours and the resulting precipitate removed by filtration. Dark red crystals of 17 (2.65 mmol, 64.8 %) were obtained upon standing overnight at room temperature. IR (KBr plates, Nujol mull  $\text{cm}^{-1}$ )  $\nu$ : 2900(s), 1610(w), 1549(s), 1457(s),

1407(m), 1381(s), 1346(s), 1287(s), 1245(m), 1228(m), 1169(s), 1126(m), 1099(s), 1068(s), 1043(m), 1029(s), 1009(s), 978(s), 946(s), 921(s), 848(s), 806(s), 788(s), 714(m), 705(s), 633(w), 596(m), 492(s), 443(s).  $\mu_{\text{eff}}=1.77\mu_{\text{B}}$

### Preparation of $\{(\text{Cy}_2\text{N})_2\text{Ti}(\mu\text{-Me})_2\}_2$ 18

A solution of MeLi (2.4 mL, 1.7 M solution in Et<sub>2</sub>O, 4.1 mmol) was added to a green solution of  $(\text{Cy}_2\text{N})_2\text{Ti}(\mu\text{-Cl})_2\text{Li}(\text{TMEDA})$  (2.49 g, 4.1 mmol) in diethylether at -10°C. The color was changed to brown at 0°C. The mixture was kept at this temperature for 15 minutes. and then warmed up to room temperature. Stirring was continued for additional 20 minutes. After filtration, the solution was evaporated to dryness and the residual oily solid was redissolved in hexane. This was concentrated to a 15 mL volume and allowed to stand a few days at room temperature upon which red prisms of 18 (<5%) separated. IR (KBr plates, Nujol mull  $\text{cm}^{-1}$ )  $\nu$ : 2895(s), 1454(s), 1381(s), 1343(s), 1248(s), 1160(s), 1143(s), 1110(s), 1066(w), 1032(s), 982(m), 949(s), 888(s), 842(s), 802(s), 777(s), 696(s), 649(s), 579(s), 502(s), 448(w), 419(w). <sup>1</sup>H-NMR (200 MHz, C<sub>6</sub>D<sub>6</sub>,  $\delta$ (ppm)): 8.38 (s,  $\mu\text{-CH}_3$ ), 3.4 (m, 4H cyclohexyl), 2.3-1.2 (bd m, 40H cyclohexyl). <sup>13</sup>C-NMR (200 MHz, C<sub>6</sub>D<sub>6</sub>,  $\delta$ (ppm)): 56.5(CH cyclohexyl), 37.8, 26.2, 27.5(CH<sub>2</sub> cyclohexyl), 2( $\mu\text{-CH}_3$ ).  $\mu_{\text{eff}}=0.88\mu_{\text{B}}$  per dimer

### Preparation of $(\text{Cy}_2\text{N})_2\text{Ti}(\mu\text{-Me})_2\text{Li}(\text{TMEDA})$ 19

A solution of MeLi (3.6 mL, 1.7 M solution in  $\text{Et}_2\text{O}$ , 6.0 mmol) was added at  $-10^\circ\text{C}$  to an emerald green solution of  $(\text{Cy}_2\text{N})_2\text{Ti}(\mu\text{-Cl})_2\text{Li}(\text{TMEDA})$  (1.8 g, 3.0 mmol) in diethylether. The reaction mixture was allowed to warm to room temperature, during which time LiCl precipitated. After 30 minutes this precipitate was removed by filtration and the solution was concentrated to dryness. The residual solid was redissolved in hexane and pale green crystals of 19 (0.65 g, 41 %) were obtained upon cooling at  $-30^\circ\text{C}$  overnight. IR (KBr plates, Nujol mull  $\text{cm}^{-1}$ )  $\nu$ : 2900(s), 1450(s), 1341(s), 1287(s), 1247(s), 1152(s), 1120(s), 1064(m), 1029(s), 982(s), 949(s), 887(s), 842(s), 800(m), 790(m), 723(w), 682(s), 583(s), 534(s), 4965(w), 447(w).  $\mu_{\text{eff}}=1.77\mu\text{B}$

### Preparation of $(\text{Cy}_2\text{N})_2\text{TiMe}_2$ 20

Addition of MeLi (3.64 mL, 1.84 M solution in  $\text{Et}_2\text{O}$ , 6.6 mmol) to a brown-orange solution of  $(\text{Cy}_2\text{N})_2\text{TiCl}_2$  (1.5 g, 3.3 mmol) in diethylether at  $-10^\circ\text{C}$  originated a pale yellow-green suspension. The reaction mixture was warmed up to room temperature, and the insoluble colorless solid was removed by filtration. The solvent was evaporated *in vacuo*. and the oily residue was redissolved in hexane. Yellow-green crystals of 20 (0.7 g, 48%) separated upon cooling to  $-30^\circ\text{C}$  overnight. IR (KBr plates, Nujol mull  $\text{cm}^{-1}$ )  $\nu$ : 2900(s), 1440(s), 1410(w), 1380(s), 1340(m), 1300(w), 1250(m), 1160(s), 1145(m), 1115(m), 1100(s), 1065(w), 1020(s), 980(m), 950(s), 890(s), 840(s), 800(s), 775(s), 705(s),

685(m), 595(w), 580(m), 550(w), 520(s), 500(w), 490(w), 450(w), 420(w).  $^1\text{H}$ -NMR (200 MHz,  $\text{C}_6\text{D}_6$ ,  $\delta(\text{ppm})$ ): 3.65(m, 4H cyclohexyl), 2.1-1.0 (bd m, 40H cyclohexyl), 0.9(s, 6H  $\text{CH}_3$ ).  $^{13}\text{C}$ -NMR (200 MHz,  $\text{C}_6\text{D}_6$ ,  $\delta(\text{ppm})$ ): 57(CH cyclohexyl), 36, 27, 26( $\text{CH}_2$  cyclohexyl), 4( $\text{CH}_3$ )

#### Preparation of $(\text{Cy}_2\text{N})_2\text{Ti}[\text{CH}_2\text{Si}(\text{Me})_3]_2$ 21

Addition of  $\text{LiCH}_2\text{Si}(\text{CH}_3)_3$  (0.49 g, 5.21 mmol) to an emerald green solution of  $(\text{Cy}_2\text{N})_2\text{Ti}(\mu\text{-Cl})_2\text{Li}(\text{TMEDA})$  (1.576 g, 2.6 mmol) in hexane at  $-10^\circ\text{C}$  resulted in the formation of a brown solution. The reaction mixture was warmed to room temperature and stirred overnight. The resulting solution was filtered, concentrated and cooled to  $-30^\circ\text{C}$ . Bright-yellow microcrystalline 21 (0.9 g, 57 %) was obtained upon standing overnight at  $-30^\circ\text{C}$ . Anal. Calcd (found) for  $\text{TiN}_2\text{Si}_2\text{C}_{32}\text{H}_{66}$ : C, 66 (65.76); H, 11.3 (11.48); N, 4.8 (4.62). IR (KBr plates, Nujol mull  $\text{cm}^{-1}$ )  $\nu$ : 2900(s), 1452(s), 1376(s), 1344(m), 1245(s), 1159(m), 1143(w), 1103(s), 1068(w), 1027(s), 980(m), 952(s), 897(s), 836(s), 779(w), 747(m), 718(s), 682(m), 614(m), 591(m), 580(m), 510(m), 493(m), 427(m).  $^1\text{H}$ -NMR (200 MHz,  $\text{C}_6\text{D}_6$ ,  $\delta(\text{ppm})$ ): 3.5(m, 4H cyclohexyl), 2.1-1.1(bd m, 40H cyclohexyl), 1.3(s, 4H  $\text{CH}_2$ ), 0.3(s, 18H  $\text{SiMe}_3$ ).  $^{13}\text{C}$ -NMR (200 MHz,  $\text{C}_6\text{D}_6$ ,  $\delta(\text{ppm})$ ): 69( $\text{CH}_2$ ), 58(CH cyclohexyl), 37,27,26.3( $\text{CH}_2$  cyclohexyl), 5( $\text{CH}_3$   $\text{SiMe}_3$ ).  $\mu_{\text{eff}}=0.0\mu\text{B}$

## Preparation of $(\text{Cy}_2\text{N})_2\text{Ti}[\text{CH}_2\text{C}(\text{Me})_3]_2$ 22

### method a,

Addition of  $\text{LiCH}_2\text{C}(\text{CH}_3)_3$  (0.4 g, 5.1 mmol) to a emerald green solution of  $(\text{Cy}_2\text{N})_2\text{Ti}(\mu\text{-Cl})_2\text{Li}(\text{TMEDA})$  (1.54 g, 2.5 mmol) in diethylether at  $-10^\circ\text{C}$  resulted in the formation of a brown-orange color. The reaction mixture was warmed to room temperature and stirred for three hours, after which the solution was filtered, concentrated and cooled to  $-30^\circ\text{C}$ . Yellow microcrystalline 22 (0.5 g, 32.5%) was obtained upon standing overnight at  $-30^\circ\text{C}$ . Anal. Calcd (found) for  $\text{TiN}_2\text{C}_{34}\text{H}_{66}$ : C, 74.2 (73.8); H, 12 (11.82); N, 5.1 (5.3). IR (KBr plates, Nujol mull  $\text{cm}^{-1}$ )  $\nu$ : 2900(s), 1455(s), 1366(s), 1252(m), 1225(s), 1158(s), 1143(m), 1107(s), 1092(s), 1025(s), 978(m), 944(s), 887(s), 842(s), 803(m), 778(m), 751(m), 696(s), 681(m), 589(m), 579(m), 546(w), 506(s), 489(s), 423(m), 420(m).  $^1\text{H-NMR}$  (200 MHz,  $\text{C}_6\text{D}_6$ ,  $\delta(\text{ppm})$ ): 3.7(m, 4H cyclohexyl), 2.05-1.1(bd m, 40H cyclohexyl), 1.3 (s, 4H  $\text{CH}_2$ ), 0.9(s, 18H  $\text{CMe}_3$ ).  $^{13}\text{C-NMR}$  (200 MHz,  $\text{C}_6\text{D}_6$ ,  $\delta(\text{ppm})$ ): 58(CH cyclohexyl), 36( $\text{CH}_2$  cyclohexyl), 35,27,25( $\text{CH}_2$  cyclohexyl), 4( $\text{CH}_3$   $\text{CMe}_3$ ).  $\mu_{\text{eff}}=0.0\mu\text{B}$

### method b,

$\text{LiCH}_2\text{C}(\text{CH}_3)_3$  (0.3 g, 3.8 mmol) was added to an orange-brown solution of  $(\text{Cy}_2\text{N})_2\text{TiCl}_2$  (0.74 g, 1.5 mmol) in hexane at  $-10^\circ\text{C}$ . The reaction mixture was warmed to room temperature and stirred for three hours. During this reaction time the color becomes darker and white

precipitate formed. The solution was filtered, concentrated and cooled to  $-30^{\circ}\text{C}$ . Yellow microcrystalline 22 (0.3 g, 40.5%) was obtained upon standing overnight at  $-30^{\circ}\text{C}$ .

#### **Polymerization of $\text{CH}_2=\text{CH}_2$**

$(\text{C}_2\text{N})_2\text{Ti}[\text{CH}_2\text{C}(\text{Me})_3]_2$  (0.2 g, 0.36 mmol) was regularly saturated with ethylene giving complete gelation after 14 days. Polyethylene (1.1 g) was filtered and washed with HCl,  $\text{H}_2\text{O}$  and EtOH. The IR was identical to that of an analytically pure sample.

**APPENDIX**

TABLE 1: Crystallographic Parameters for  $(\text{Me}_3\text{Si})_2\text{NTi}(\text{Cl})_2(\text{THF})_2$  2  
 $[(\text{Me}_3\text{Si})_2\text{N}]_2\text{Ti}(\text{Cl})(\text{THF})$  1

	2	1
Formula	$\text{C}_{14}\text{H}_{34}\text{Si}_2\text{NO}_2\text{TiCl}_2$	$\text{C}_{16}\text{H}_{44}\text{Si}_4\text{TiN}_2\text{ClO}$
Formula Weight	423.41	476.23
Crystal Color, Habit	blue, block	green, prism
Crystal Sizes, $\text{mm}^3$	0.3x0.3x0.2	0.5x0.4x0.4
Crystal System	monoclinic	triclinic
Space Group	$P2_1/c$	$P\bar{1}$
Lattice Parameters	$a=12.846(2)\text{\AA}$ $b=13.548(2)\text{\AA}$ $c=12.871(3)\text{\AA}$ $\beta=100.66(1)^\circ$	$a=11.682(2)\text{\AA}$ $b=15.991(3)\text{\AA}$ $c=8.501(2)\text{\AA}$ $\alpha=94.25(2)^\circ$ $\beta=108.42(2)^\circ$ $\gamma=106.19(2)^\circ$
Z value	4	2
$D_{\text{calc}}$	1.278 $\text{g}/\text{cm}^3$	1.111 $\text{g}/\text{cm}^3$
F(000)	900	514
$\mu(\text{MoK}\alpha)$	7.41 $\text{cm}^{-1}$	5.64 $\text{cm}^{-1}$
Radiation	$\text{MoK}\alpha(\lambda=0.71069\text{\AA})$	$\text{MoK}\alpha(\lambda=0.71069\text{\AA})$
Temperature	-160°C	23°C
Take-off Angle	6.0°	6.0°
Detector Aperture	6.0 mm horizontal 6.0 mm vertical	6.0 mm 6.0 mm
Scan Type	$\omega$ -2 $\theta$	$\omega$ -2 $\theta$
Scan Rate	4.0°/min	4.0°/min
Scan Range	$(0.89 + 0.3 \tan\theta)^\circ$	$(1.78 + 0.2 \tan\theta)^\circ$
$2\theta_{\text{max}}$	50.0°	45°
No. Ref. Meas.	total: 4250 unique: 4062	3256 3035
$R_{\text{int}}$	0.028	0.037
No. Observation	3320	2170
No. Variables	309	222
R	0.050	0.054
Rw	0.063	0.045
GoF	2.72	3.36
Max Shift/Fin. Cycle	0.03	0.02
Residual Density $e^-/\text{\AA}^3$	-2.68 to 1.27	-0.35 to 0.57

TABLE 2: Crystallographic Parameters for (Cy<sub>2</sub>N)<sub>2</sub>Ti(μ-Cl)<sub>2</sub>Li(TMEDA) 5  
(Cy<sub>2</sub>N)<sub>2</sub>Ti(Cl)<sub>2</sub> 10

	5	10
Formula	C <sub>30</sub> H <sub>60</sub> TiCl <sub>2</sub> LiN <sub>4</sub>	C <sub>24</sub> H <sub>44</sub> Cl <sub>2</sub> TiN <sub>2</sub>
Formula Weight	602.58	479.43
Crystal Color, Habit	green, prism	orange, cube
Crystal Sizes, mm <sup>3</sup>	0.5x0.4x0.3	0.6x0.6x0.6
Crystal System	monoclinic	monoclinic
Space Group	P2 <sub>1</sub> /n	P2 <sub>1</sub> /n
Lattice Parameters	a=12.361(5)Å b=19.616(4)Å c=15.357(3)Å β=109.39(2)° V=3512(2)Å <sup>3</sup>	a= 9.860(2)Å b=18.291 (2)Å c=14.117 (3)Å β=95.52 (2)° V=2536.1(8)Å <sup>3</sup>
Z value	4	4
D <sub>calc</sub>	1.139 g/cm <sup>3</sup>	1.255 g/cm <sup>3</sup>
F(000)	1308	1032
μ (MoKα)	4.16 cm <sup>-1</sup>	5.58 cm <sup>-1</sup>
Radiation	MoKα (λ=0.71069Å)	MoKα(λ=0.71069Å)
Temperature	-160°C	-160°C
Take -off Angle	6.0	6.0
Detector Aperture	6.0 mm horizontal 6.0 mm vertical	6.0 mm 6.0 mm
Scan Type	ω-2θ	ω-2θ
Scan Rate	4.0°/min	4.0°/min
Scan Range	(1.00+0.3 tanθ)°	(1.15+0.3 tanθ)°
2θ <sub>max</sub>	50.1°	49.9°
No. Ref. Meas	total: 6706 unique: 6397	4900 4618
R <sub>int</sub>	0.144	0.122
No. Observations	4601	3839
No. Variables	519	263
R	0.077	0.036
R <sub>w</sub>	0.091	0.045
GoF	3.35	3.85
Max Shift/Fin. Cycle	0.11	0.00
Residual Density e <sup>-</sup> /Å <sup>3</sup>	-1.04 to 1.02	-0.36 to 0.40

**TABLE 3: Crystallographic Parameters for**  
**[[(*i*Pr)<sub>2</sub>N]TiCl]<sub>2</sub>[ $\mu$ (NC<sub>5</sub>H<sub>5</sub>C<sub>5</sub>H<sub>5</sub>N)] 6**

Formula	6 C <sub>34</sub> H <sub>66</sub> Ti <sub>2</sub> N <sub>6</sub> Cl <sub>2</sub>
Formula Weight	725.64
Crystal Color, Habit	orange, cube
Crystal Dimension mm <sup>3</sup>	0.4x0.3x0.2
Crystal System	monoclinic
Space Group	C <sub>2</sub> /c
Lattice Parameters	a=31.360(6)Å b=10.891(2)Å c=25.584(3)Å β=110.96(1)° V=8160(4)Å <sup>3</sup>
Z value	8
D <sub>calc</sub>	1.181 g/cm <sup>-3</sup>
F(000)	3120
α(MoKα)	5.47 cm <sup>-1</sup>
Radiation	MoKα(λ=1.71069Å)
Temperature	-153°C
Take -off Angle	6.0°
Detector Aperture	6.0 mm horizontal 6.0 mm vertical
Scan Type	ω-2θ
Scan Rate	4.0 °/min
Scan Range	(1.15+0.3tanθ)°
2θmax	50.0°
No. Ref. Meas.	total:7733 unique:7577
R <sub>int</sub>	0.069
No. Observation	4750
No. Variables	398
R	0.050
R <sub>w</sub>	0.061
GoF	1.96
Max Shift/Fin. Cycle	0.06
Residual Density e <sup>-</sup> /Å <sup>3</sup>	-0.56 to 0.44

**TABLE 4: Crystallographic Parameters for [(Me<sub>3</sub>Si)<sub>2</sub>N]<sub>2</sub>Ti(BH<sub>4</sub>)(THF)<sub>11</sub>  
[(Me<sub>3</sub>Si)<sub>2</sub>N]Ti(py)<sub>2</sub>(BH<sub>4</sub>)<sub>2</sub> 12**

	11	12
Formula	C <sub>16</sub> H <sub>48</sub> Si <sub>4</sub> TiN <sub>2</sub> BO	C <sub>16</sub> H <sub>36</sub> Si <sub>2</sub> TiN <sub>3</sub> B <sub>2</sub>
Formula Weight	439.62	398.17
Crystal Color, Habit	green, cube	orange, prism
Crystal Sizes, mm <sup>3</sup>	0.4x0.4x0.4	0.3 x 0.1 x 0.1
Crystal System	triclinic	monoclinic
Space Group	P $\bar{1}$	P2 <sub>1</sub> /c
Lattice Parameters	a= 9.920(1)Å b=17.847(2)Å c= 8.442(1)Å $\alpha$ =90.283(9)° $\beta$ =108.552(9)° $\gamma$ =100.540(9)° V=1389.8(3)Å <sup>3</sup>	a=11.569(2)Å b=15.299(3)Å c=13.486(4)Å $\beta$ =103.02(2)° V=2325.6(9)Å <sup>3</sup>
Zvalue	2	4
D <sub>calc</sub>	1.050 g/cm <sup>3</sup>	1.131 g/cm <sup>3</sup>
F(000)	482	852
$\alpha$ (MoK $\alpha$ )	4.76 cm <sup>-1</sup>	4.68 cm <sup>-1</sup>
Radiation	MoK $\alpha$ ( $\lambda$ =0.71069Å)	MoK $\alpha$ ( $\lambda$ =0.71069Å)
Temperature	-160°C	-160°C
Take - off Angle	6.0°	6.0°
Detector Aperture	6.0 mm horizontal 6.0 mm vertical	6.0 mm 6.0 mm
Scan Type	$\omega$ -2 $\theta$	$\omega$ -2 $\theta$
Scan Rate	4.0°/min	4.0°/min
Scan Range	(1.37 + 0.3tan $\theta$ )°	(1.0 + 0.3tan $\theta$ )°
2 $\theta$ <sub>max</sub>	50.0°	47.0°
No. Ref. Meas.	total: 5260 unique: 4875	3784 3588
R <sub>int</sub>	0.055	0.048
No. Observation	3761	2305
No. Variables	375	249
R	0.042	0.042
R <sub>w</sub>	0.053	0.046
GoF	2.02	1.29
Max Shift/Fin. Cycle	0.34	0.10
Residual Density e <sup>-</sup> /Å <sup>3</sup>	-3.26 to 0.99	-0.26 to 0.32

TABLE 5: Crystallographic Parameters for  $\{[(\text{Me}_3\text{Si})_2\text{N}]_2\text{Ti}(\mu\text{-S})_2\}$  13

	13
Formula	$\text{C}_{24}\text{H}_{72}\text{S}_2\text{Ti}_2\text{N}_4\text{Si}_8$
Formula Weight	443.82
Crystal Color, Habit	red, plate
Crystal Sizes, $\text{mm}^3$	0.5x0.5x0.2
Crystal System	monoclinic
Space Group	$C2/c$
Lattice Parameters	$a=16.895(6)\text{\AA}$ $b=27.20(1)\text{\AA}$ $c=11.694(2)\text{\AA}$ $\beta=105.46(2)^\circ$ $V=5274(2)\text{\AA}^3$
Z value	8
$D_{\text{calc}}$	1.118 $\text{g}/\text{cm}^3$
$F(000)$	1928
$\mu(\text{MoK}\alpha)$	5.77 $\text{cm}^{-1}$
Radiation	$\text{MoK}\alpha$ ( $\lambda=0.71069\text{\AA}$ )
Temperature	$-160^\circ\text{C}$
Take-off Angle	6.0
Detector Aperture	6.0 mm horizontal 6.0 mm vertical
Scan Type	$\omega$ -2 $\theta$
Scan Rate	4.0 $^\circ$ /min
$2\theta_{\text{max}}$	47.0 $^\circ$
No. Ref. Meas.	total: 4141 unique: 3985
$R_{\text{int}}$	0.070
No. Observation	3233
No. Variables	208
R	0.085
$R_w$	0.107
GoF	4.27
Max Shift/Fin. Cycle	0.09
Residual Density $e^-/\text{\AA}^3$	-1.18 to 1.72

TABLE 6: Crystallographic Parameters for  $(\text{Cy}_2\text{N})_2\text{TiMe}_2$  20  
 $\{[(\text{iPr})_2\text{Ti}(\text{Ph})_2][\text{Li}(\text{TMEDA})_2]\}$  17

	20	17
Formula	$\text{C}_{26}\text{H}_{50}\text{TiN}_2$	$\text{C}_{36}\text{H}_{70}\text{TiN}_6\text{Li}$
Formula Weight	438.59	641.83
Crystal Color, Habit	red. prism	red, cube
Crystal Sizes, $\text{mm}^3$	0.5x0.3x0.2	0.5x0.5x0.5
Crystal System	monoclinic	monoclinic
Space Group	$P2_1/n$	$P2_1/n$
Lattice Parameters	$a=9.906(4)\text{\AA}$ $b=18.520(6)\text{\AA}$ $c=14.271(3)\text{\AA}$ $\beta=96.87(3)^\circ$ $V=2599(3)\text{\AA}^3$	$a=9.528(2)\text{\AA}$ $b=21.675(5)\text{\AA}$ $c=19.867(9)\text{\AA}$ $\beta=97.86(2)^\circ$ $V=4065(4)\text{\AA}^3$
Z value	4	4
$D_{\text{calc}}$	1.121 $\text{g}/\text{cm}^3$	1.049 $\text{g}/\text{cm}^3$
F(000)	968	1412
$\mu(\text{MoK}\alpha)$	3.38 $\text{cm}^{-1}$	2.35 $\text{cm}^{-1}$
Radiation	$\text{MoK}\alpha(\lambda=0.71069\text{\AA})$	$\text{MoK}\alpha(\lambda=0.71069\text{\AA})$
Take-off Angle	$6.0^\circ$	$6.0^\circ$
Detector Aperture	6.0 mm horizontal 6.0mm vertical	6.0 mm 6.0 mm
Scan Type	$\omega$ -2 $\theta$	$\omega$ -2 $\theta$
Scan Rate	$4.0^\circ/\text{min}$	$4.0^\circ/\text{min}$
Scan Range	$(1.05+0.3 \tan\theta)^\circ$	$(1.00+0.3 \tan\theta)^\circ$
$2\theta_{\text{max}}$	$50.0^\circ$	$50.0^\circ$
No. Ref. Meas.	total: 4279 unique: 3994	6199 6804
$R_{\text{int}}$	0.139	0.357
No. Observation	3132	4235
No. Variables	263	399
R	0.053	0.067
Rw	0.065	0.081
GoF	2.82	2.66
Max Shift/Fin. Cycle	0.01	0.06
Residual Density $e^-/\text{\AA}^3$	0.00	-0.88 to 0.7

TABLE 7: Crystallographic Parameters for  
 $(\text{Cy}_2\text{N})_2\text{Ti}(\mu\text{-Me})_2\text{Li}(\text{TMEDA})$  19  $\{(\text{Cy}_2\text{N})_2\text{Ti}(\mu\text{-Me})\}_2$  18

	19	18
Formula	$\text{C}_{32}\text{H}_{66}\text{LiTiN}_4$	$\text{C}_{50}\text{H}_{94}\text{Ti}_2\text{N}_4$
Formula Weight	561.74	847.12
Crystal Color, Habit	green, cube	red, plate
Crystal Sizes, $\text{mm}^3$	0.4x0.4x0.4	0.4x0.3x0.1
Crysta System	monoclinic	monoclinic
Space Group	$P2_1/n$	$P2/n$
Lattice Parameters	$a=12.505(5)\text{\AA}$ $b=19.333(9)\text{\AA}$ $c=15.359(5)\text{\AA}$ $\beta=109.10(2)^\circ$ $V=3517(3)\text{\AA}^3$	$a=13.619(4)\text{\AA}$ $b=12.484(6)\text{\AA}$ $c=14.811(3)\text{\AA}$ $\beta=96.51(7)^\circ$ $V=2502(3)\text{\AA}^3$
Z value	4	2
$D_{\text{calc}}$	1.061 $\text{g}/\text{cm}^3$	1.124 $\text{g}/\text{cm}^3$
$F(000)$	1244	932
$\mu(\text{MoK}\alpha)$	2.62 $\text{cm}^{-1}$	3.49 $\text{cm}^{-1}$
Radiation	$\text{MoK}\alpha(\lambda=0.71069\text{\AA})$	$\text{MoK}\alpha(\lambda=0.71069\text{\AA})$
Temperature	$-160^\circ\text{C}$	$160^\circ\text{C}$
Take-off Angle	$6.0^\circ$	$6.0^\circ$
Detector Aperture	6.0 mm horizontal 6.0mm vertical	6.0 mm 6.0 mm
Scan Type	$\omega$ -2 $\theta$	$\omega$ -2 $\theta$
Scan Rate	$4.0^\circ/\text{min}$	$4.0^\circ/\text{min}$
Scan Range	$(1.57+0.3\tan\theta)^\circ$	$(1.78+0.3\tan\theta)^\circ$
$2\theta_{\text{max}}$	$49.9^\circ$	$50.1^\circ$
No. Ref. Meas.	total: 6526 unique:6219	4407 4205
$R_{\text{int}}$	0.104	0.104
No. Observation	3644	2560
No. Variables	343	263
R	0.066	0.058
Rw	0.061	0.068
Max Shift/Fin. Cycle	0.68	0.55
Residual Density $e^-/\text{\AA}^3$	-0.43 to 0.87	-0.62 to 0.9

## SUGGESTIONS FOR FURTHER RESEARCH

The properties of  $(R_2N)_2Ti(\mu-Cl)_2Li(TMEDA)$  ( $R=iPr$  4,  $Cy$  5) have interesting prospects for further research involving reductive coupling and hydrogen transfer reactions. Since the mechanism of hydrogen transfer remain unknown, further study is necessary. For example, modification of the coordination environment of 4, and the isolation and characterization of the organic and organometallic species at the same time, could answer this question.

The problem remaining in the synthesis of the Ti-H single bond is the finding of both a suitable starting material and a hydride source.

The industrial importance of titanium alkyls in polymerization processes is very well known. Since polymerization of ethylene has been achieved in this work, the full physical characterization of the polymer is essential to the advancement of this chemistry.

## REFERENCES

1. Y. Dank, H. J. Geise, *J. Organomet. Chem.*, 1991, 405, 1
2. G. P. Pez, P. Apgar, R. K. Crissey. *J. Am. Chem. Soc.*, 1982, 104, 482
3. L. B. Kool, M. D. Rausch, *Angew. Chem. Int. Ed. Engl.*, 1985, 24, 394
4. J. Boor, *Ziegler-Natta Catalysts and Polymerization*, Academic Press New York, 1979
5. a, G. Wilkinson, F. G. A. Stone, E. W. Abel, *Comprehensive Organometallic Chemistry* Vol. 3., Pergamon 1982  
b, P. C. Wailes, R. S. P. Coutts, H. Weigold, *Organometallic Chemistry of Titanium, Zirconium, and Hafnium*, Academic Press, New York, 1974  
c, G. Wilkinson, R. D. Gillard, *Comprehensive Coordination Chemistry* Vol. 1 and 2., Pergamon 1987
6. F. Pruchnik, *Organometallic Chemistry of the Transition Elements*, Plenum Press, New York and London, 1992
7. a, G. A. Luinstra, *Investigation in Organotitanium Chemistry*, Drukkerij Van Denderen B. V. Groningen, 1991  
b, for review see also 1
8. M. T. Reetz, *Organotitanium Reagents in Organic Synthesis*, Springer-Verlag, 1986
9. J. E. McMurry, *Acc. Chem. Res.*, 1983, 16, 405
10. J. E. McMurry, K. L. Kees, *J. Org. Chem.*, 1977, 42, 2665

11. L. D. Durfee, P. E. Fanwick, I. P. Rothwell, *J. Am. Chem. Soc.*, 1987, 109, 4720
12. J. E. Hill, P. E. Fanwick, I. P. Rothwell, *Organometallics*, 1992, 11, 1771
13. R. L. Richards, in *Biology and Biochemistry of Dinitrogen Fixation*, Elsevier, Amsterdam, 1991, p. 58
14. a, E. G. Berkovich, V. B. Shur, M. E. Volpin, *Fundamental Research in Homogenous Catalysis*, Science Publisher Inc., New York, 1986  
b, M. E. Volpin, V. B. Shur, R. V. Kudryavtsev, L. A. Prodayko, *Chem. Comm.*, 1968, 1038  
c, E. E. Van Tamelen, *Acc. Chem. Res.*, 1970, 3, 361
15. M. E. Volpin, V. B. Shur, *Akad. Nauk SSSR*, 1964, 156, 1102
16. M. E. Volpin, *J. Organomet. Chem.*, 1980, 200, 319
17. M. D. Fryzuk, T. S. Haddad, M. Mylvaganam, D. H. McConville, S. J. Rettig, *J. Am. Chem. Soc.*, 1993, 115, 2782
18. J. Jeffry, M. F. Lappert, P. I. Riley, *J. Organomet. Chem.*, 1979, 181, 25
19. W. J. Evans, T. A. Ulibarri, J. W. Ziller, *J. Am. Chem. Soc.*, 1988, 110, 6877
20. R. Duchateau, S. Gambarotta, N. Beydoun, C. Bensimon, *J. Am. Chem. Soc.*, 1991, 113, 8986
21. D. H. Berry, L. J. Procopio, P. J. Carroll, *Organometallics*, 1988, 7, 570
22. a, F. V. van der Weij, J. H. Teuben, *J. Organomet. Chem.*, 1976, 120, 223

- b, Yu. G. Borodko, I. N. Ivleva, L. M. Kachapina, E. F. Kvashina, A. K. Shilova, A. E. Shilov, *J. Chem. Soc., Chem. Comm.*, 1973, 169
- c, J. E. Bercaw, *J. Am. Chem. Soc.*, 1974, 96, 5087
23. P. Sobota, Z. Janas, *Inorg. Chim. Acta*, 1981, 53, 111
24. a, N. Beydoun, R. Duchateau, S. Gambarotta, *J. Am. Chem. Soc.*, 1992, 244
- b, for review see also 20
25. J. D. Zeinstra, J. H. Teuben, F. Jellinek, *J. Organomet. Chem.*, 1979, 170, 39
26. G. Fachinetti, G. Fochi, C. Floriani, *J. Chem. Soc. Chem. Comm.*, 1976, 230
27. G. Fachinetti, C. Floriani, *Chem. Comm.*, 1974, 66
28. a, L. B. Kool, M. D. Rausch, *J. Organomet. Chem.*, 1985, 297, 159
29. a, H. G. Alt, M. D. Rauch, *J. Organomet. Chem.*, 1988, 356, C50
- b, H. G. Alt, M. D. Rauch, *J. Organomet. Chem.*, 1988, 356, C53
30. L. B. Kool, M. D. Rausch, *J. Organomet. Chem.*, 1986, 310, 27
31. J. Ellis, B. A. Kelsey, *J. Am. Chem. Soc.*, 1986, 108, 1344
32. K. M. Chi, S. R. Frerichs, S. B. Philson, J. E. Ellis, *J. Am. Chem. Soc.*, 1988, 110, 303
33. S. R. Frerichs, B. K. Stein, J. E. Ellis, *J. Am. Chem. Soc.*, 1987, 109, 5558
34. K. M. Chi, S. R. Frerichs, B. K. Stein, D. W. Blackburn, J. E. Ellis, *J. Am. Chem. Soc.*, 1988, 110, 163
35. J. E. Ellis, A. J. DiMaio, A. L. Rheingold, B. S. Haggetry, *J. Am. Chem. Soc.*, 1992, 114, 10676
36. J. E. Ellis, *Polyhedron*, 1989, 8, 1611

37. J. E. Ellis, P. Yuen, *Inorg. Chem.*, 1993, 32, 4998
38. a, R. H. Grubbs, W. Tumas, *Science*, 1989, 243, 908  
b, K. J. Ivin, *Olefin Metathesis*, Academic Press, London, 1983
39. R. R. Schrock, *Science*, 1983, 219, 13
40. H. Sinn, W. Kaminsky, *Adv. Organomet. Chem.*, 1980, 18, 99
41. D. C. Bradley, M. H. Chisholm, *Acc. Chem. Res.*, 1976, 9, 273
42. D. M. Giolando, K. Kirschbaum, L. J. Graves, U. Bolle, *Inorg. Chem.*, 1992, 31, 3887
43. M. F. Lappert, P. P. Power, A. R. Sanger, R. C. Srivastava, *Metal and Metalloid Amides*, Ellis Howood: Chichester, England, 1980
44. R. A. Anderson, D. B. Beach, W. L. Jolly, *Inorg. Chem.*, 1985, 24, 4741
45. M. H. Chisholm, M. W. Extine, *J. Am. Chem. Soc.*, 1977, 99, 782
46. W. Petz, *J. Organomet. Chem.*, 1993, 465, 85
47. D. C. Bradley, M. B. Hursthouse, *Chem. Comm.*, 1970, 672
48. a, M. Lynam, in *Coord. Chem. Rev.*, 1993, 127, 39  
b, for review see also 41, 43
49. C. Airoidi, D. C. Bradley, H. Chudzynska, M. B. Hursthouse, K. M. A. Malik, P. Raithby, *J. Chem. Soc., Dalton Trans.*, 1980, 2010
50. D. C. Bradley, H. Chudzynska, J. D. J. Backer-Dirks, M. B. Hursthouse, A. A. Ibrahim, M. Motevalli, A. C. Sullivan, *Polyhedron*, 1990, 11, 1423
51. R. P. Planalp, R. A. Anderson, *Organometallics*, 1983, 2, 16
52. Ch. R. Bennett, D. C. Bradley, *J. Chem. Soc., Chem. Comm.*, 1974, 29
53. S. Friedrich, L. H. Gade, A. J. Edwards, M. McPartlin, *J. Chem. Soc., Dalton Trans.*, 1993, 2861

54. Ch. C. Cummins, R. R. Schrock, W. M. Davis, *Organometallics*, 1992, 11, 1452
55. Ch. T. Vroegop, J. H. Teuben, F. van Bolhuis, J. G. M. van der Linden, *J. Chem. Soc., Chem. Comm.*, 1983, 550
56. J. Feldman, J. C. Calabrese, *J. Chem. Soc., Chem. Comm.*, 1991, 1043
57. a, E. C. Alyea, D. C. Bradley, M. F. Lappert, A. R. Sanger, *J. Chem. Soc., Chem. Comm.*, 1969, 1064  
b, D. S. Bradley, R. G. Copperthwaite, *J. Chem. Soc., Chem. Comm.*, 1971, 764  
c, for review see also 43
58. M. F. Lappert, A. R. Sanger, *J. Chem. Soc. (A)*, 1971, 878
59. a, G. A. Nesterov, V. A. Zakharov, V. V. Volkov, K. G. Myakishev, *J. Mol. Catal.*, 1986, 36, 253  
b, V. A. Zakharov, V. K. Duchenko, E. A. Paukshtis, L. G. Karakchiev, Yu. I. Yermakov, *J. Mol. Catal.*, 1977, 2, 241  
c, J. Schwartz, M. D. Ward, *J. Mol. Catal.*, 1980, 8, 465
60. H. S. Lee, K. Isagava, H. Toyoda, Y. Otsuji, *Chem. Lett.*, 1984, 673
61. S. I. Troynov, K. Mach, V. Varga, *Organometallics*, 1993, 12, 3387
62. S. I. Troynov, H. Antropiusova, K. Mach, *J. Organomet. Chem.*, 1992, 492, 49
63. F. Gauvin, J. Britten, E. Samuel, J. F. Harrod, *J. Am. Chem. Soc., Chem. Comm.*, 1992, 114, 1489
64. E. Samuel, J. F. Harrod, *J. Am. Chem. Soc.*, 1984, 106, 1859
65. T. Yu. Sokolova, A. I. Sizov, B. M. Bulchev, E. A. Rozova, V. K. Belsky, G. L. Soloveichik, *J. Organomet. Chem.*, 1990, 288, 11

66. A. I. Sizov, I. V. Molodnitskaya, B. M. Bulchev, V. K. Belskii, G. L. Soloveichik, *J. Organomet. Chem.*, 1988, 344, 185
67. S. I. Troynov, V. Varga, K. Mach, *J. Chem. Soc., Chem. Comm.*, 1993, 1174
68. J. E. Gozum, J. E. Girolami, *J. Am. Chem. Soc.*, 1991, 113, 3830
69. a, D. G. Dick, R. Duchateau, J. J. H. Edama, S. Gambarotta, *Inorg. Chem.*, 1993, 32, 1959  
b, for review see also 5c
70. T. J. Marks, W. J. Kennely, J. R. Kolb, L. A. Shimp, *Inorg. Chem.*, 1972, 11, 2540
71. J. A. Jensen, S. R. Wilson, A. J. Schultz, G. S. Girolami, *J. Am. Chem. Soc.*, 1987, 109, 8094
72. R. J. Morris, G. S. Girolami, *Inorg. Chem.*, 1990, 29, 4167
73. C. R. Lucas, *Inorganic Syntheses*, 1977, 17, 91
74. J. H. Teuben, *Organometallics*, 1987, 6, 1004
75. J. A. Jensen, S. R. Wilson, G. S. Girolami, *J. Am. Chem. Soc.*, 1988, 110, 4977
76. J. A. Jensen, G. A. Girolami, *J. Am. Chem. Soc.*, 1986, 1160
77. C. J. Dain, A. J. Downs, M. J. Goode, D. G. Evans, K. T. Nicholls, D. W. H. Rankin, H. E. Robertson, *J. Chem. Soc., Dalton Trans.*, 1991, 967
78. A. Jarid, A. Lledos, Y. Jean, F. Volatron, *Inorg. Chem.*, 1993, 32, 4695
79. F. Volatron, M. Duran, A. Lledos, Y. Jean, *Inorg. Chem.*, 1993, 32, 951
80. a, H. A. Alt, H. E. Engelhardt, *J. Organomet. Chem.*, 1987, 329, 61  
b, E. Samuel, *J. Organomet. Chem.*, 1980, 198, C65

- c, P. J. Davison, M. F. Lappert, R. Pearce, *Acc. Chem. Res.*, 1974, 7, 209
81. E. Samuel, *J. Organomet. Chem.*, 1980, 198, C65
82. P. Courtois, R. Pichon, Y. Raoult, J. Y. Salaun, *J. Organomet. Chem.*, 1987, 327, C1
83. R. F. Johnston, J. C. Cooper, *Organometallics*, 1987, 6, 2448
84. a, R. R. Schrock, G. W. Parshall, *Chem. Rev.*, 1976, 76, 243  
b, P. J. Davidson, M. F. Lappert, R. Pearce, *Acc. Chem. Res.*, 1974, 7, 209  
c, Yu. Sh. Guzman, O. I. Adrov, G. N. Bondarenko, E. I. Tinyakova, B. A. Dolgoplosk, *Organomet. Chem. in the USSR*, 1990, 3, 694  
d, M. Mena, P. Royo, R. Serrano, M. A. Pellinghelli, A. Tiripichio, *Organometallics*, 1989, 8, 476  
e, for review see also 5
85. M. Yu. Antipin, Yu. T. Struchkov, I. Sh. Guzman, O. I. Adrov, *Organomet. Chem. in the USSR*, 1990, 3, 697
86. Z. Dawoodi, M. L. H. Green, V. S. B. Mtetwa, K. Prout, *J. Chem. Soc., Chem. Comm.*, 1982, 1410
87. S. G. Blanco, M. P. Gomez-Sal, S. M. Carreras, M. Mena, P. Royo, R. Serrano, *J. Chem. Soc., Chem. Comm.*, 1986, 1572
88. P. Gomez-Sal, M. Mena, F. Palacios, P. Royo, R. Serrano, S. M. Carreras, *J. Organomet. Chem.*, 1989, 375, 59
89. R. Serrano, J. C. Flores, P. Royo, M. Mena, M. A. Pellinghelli, A. Tiripichio, *Organometallics*, 1989, 8, 1404
90. P. B. Mackenzie, R. J. Coots, R. H. Grubbs, *Organometallics*, 1989, 8, 8

91. J. W. Park, L. M. Henling, W. P. Schaefer, R. H. Grubbs,  
*Organometallics*, 1991, 10, 171
92. G. S. Girolami, G. Wilkinson, A. M. R. Galas, M. Thorthon-Pett,  
M. B. Hursthouse, *J. Chem. Soc. Dalton Trans.*, 1985, 1339
93. a, G. A. Luinstra, J. H. Teuben, *J. Am. Chem. Soc.*, 1992, 114, 3361  
b, G. A. Luinstra, J. H. Teuben, *Organometallics*, 1992, 11, 2273  
c, for review see also 5
94. a, E. Klei, J. H. Teuben, *J. Organomet. Chem.*, 1980, 188, 97  
b, E. Klei, J. H. Telgen, J. H. Teuben, *J. Organomet. Chem.*, 1981,  
209, 297
95. a, G. A. Luinstra, J. H. Teuben, *Organometallics*, 1992, 11, 2273  
b, for review see also 7a
96. G. A. Luinstra, J. A. Teuben, *J. Am. Chem. Soc.*, 1992, 114, 3361
97. R. Fandos, A. Meetsma, J. H. Teuben, *Organometallics*, 1991, 10,  
1637
98. a, F. Calderazzo, G. Pampaloni, *J. Organomet. Chem.*, 1985  
296, 1  
b, F. Calderazzo, G. Pampaloni, *Organometallics*, 1988,  
7, 1083
99. S. Gambarotta, J. Song, *J. Am. Chem. Soc.*, in press
100. P. Berno, S. Gambarotta, *Organometallics*, in press
101. L. E. Manzer, *Inorganic Syntheses*, 1982, 21, 135
102. S. P. Patterman, I. L. Karle, *J. Am. Chem. Soc.*, 1970, 92, 1150
103. M. B. Mabbs, D. J. Machin, *Magnetism and Transition Metal  
Complexes*, Chapman and Hall: London 1973